



Fall 1982

Quaternary Chronology of the Palouse Loess near Washtucna, Eastern Washington

Lucy L. (Lucy Louglin) Foley
Western Washington University

Follow this and additional works at: <https://cedar.wwu.edu/wwuet>



Part of the [Geology Commons](#)

Recommended Citation

Foley, Lucy L. (Lucy Louglin), "Quaternary Chronology of the Palouse Loess near Washtucna, Eastern Washington" (1982). *WWU Graduate School Collection*. 782.
<https://cedar.wwu.edu/wwuet/782>

This Masters Thesis is brought to you for free and open access by the WWU Graduate and Undergraduate Scholarship at Western CEDAR. It has been accepted for inclusion in WWU Graduate School Collection by an authorized administrator of Western CEDAR. For more information, please contact westerncedar@wwu.edu.

QUATERNARY CHRONOLOGY OF THE
PALOUSE LOESS NEAR WASHTUCNA,
EASTERN WASHINGTON

A Thesis
Presented to
The Faculty of
Western Washington University

In Partial Fulfillment
Of the Requirements for the Degree
Master of Science

by
Lucy L. Foley
December, 1982

MASTER'S THESIS

In presenting this thesis in partial fulfillment of the requirements for a master's degree at Western Washington University, I grant to Western Washington University the non-exclusive royalty-free right to archive, reproduce, distribute, and display the thesis in any and all forms, including electronic format, via any digital library mechanisms maintained by WWU.

I represent and warrant this is my original work and does not infringe or violate any rights of others. I warrant that I have obtained written permissions from the owner of any third party copyrighted material included in these files.

I acknowledge that I retain ownership rights to the copyright of this work, including but not limited to the right to use all or part of this work in future works, such as articles or books.

Library users are granted permission for individual, research and non-commercial reproduction of this work for educational purposes only. Any further digital posting of this document requires specific permission from the author.

Any copying or publication of this thesis for commercial purposes, or for financial gain, is not allowed without my written permission.

Name: Lucy L. Foley LUCY L. FOLEY

Signature: [Handwritten Signature]

Date: 20 June 2018

QUATERNARY CHRONOLOGY OF THE
PALOUSE LOESS NEAR WASHTUCNA,
EASTERN WASHINGTON

by


Lucy L. Foley


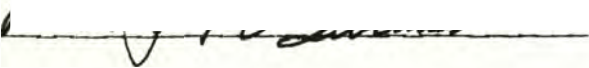


Accepted in Partial Completion
of the Requirements for the Degree
Master of Science

December, 1982

Dean, Graduate School

ADVISORY COMMITTEE


Chairman

ABSTRACT

Four roadcuts in the Palouse loess near Washtucna, southeastern Washington, expose a thick sequence of buried calcic soils and tephra layers which span more than the last 730,000 years. The identification of four tephra layers of known age in the upper part of the loess sequence (Mazama, Mt. St. Helens Set S, and two separate layers of Mt. St. Helens Set C) allow the formulation of a soil chronology for the last 40,000 years. Paleomagnetic stratigraphy resulted in the identification of the Brunhes Normal-Matuyama Reversed polarity epoch boundary in one roadcut, thereby establishing an age of at least 730,000 years for the lower part of the loess section.

The soils are described in terms of field characteristics and clay mineralogy. Three broad groupings of soils are distinguished on the basis of carbonate stage of development, stratigraphic position, and age: soils younger than about 30,000 years have stage I and II carbonate; soils which formed between 30,000 and at least 40,000 years B.P. have stage III carbonate; and soils which formed prior to at least 40,000 years ago have stage III and IV carbonate. The clay mineral assemblage of the Palouse loess consists of chlorite and mica with minor amounts of smectite, vermiculite and mixed layer clays. The buried soils do not appear to have clay mineral assemblages which can distinguish among them, although three samples from buried soils contained kaolinite.

The stratigraphy exposed in the Washtucna roadcuts and the chronology of loess deposition and soil formation developed herein could provide a framework for the Pleistocene chronology of loess deposits on the Columbia Plateau.

ACKNOWLEDGEMENTS

This project would not have been possible without the participation and support of numerous individuals. Don Easterbrook, my committee chairman, suggested the use of paleomagnetism as a chronologic tool, and provided continual encouragement and support.

This study actually began in 1975 when Henry Smith, of Washington State University, hired me to collect tephra samples and stratigraphic information throughout the Palouse region. I later chose to return to the Washtucna roadcuts to gather more detailed stratigraphic and chronologic information. Henry Smith has served on my committee and has very generously shared his unpublished microprobe data for tephra layers in the Palouse region and for reference samples from Mount St. Helens.

I am very grateful to Russ Burmester for his endless patience while instructing me in the use of paleomagnetism and for scrutinizing many drafts of the Paleomagnetism chapter. Chris Suczek has been very helpful by editing several drafts of the thesis. David Pevear instructed me in x-ray diffraction and clay mineralogy, helped me to interpret numerous x-ray patterns, and edited the Clay Mineralogy chapter.

Peter Birkeland, of the University of Colorado, advised me on the scope of the thesis during its initial stages, suggested soil horizon terminology, and edited the Soils portion of this thesis.

Rose Okazaki, of Washington State University, is responsible for the petrographic and electron microprobe analyses of the tephra layers described here.

I would like to thank George Mustoe for helping me with the scanning electron microscope and for fixing the x-ray machine when it broke down.

I am grateful to Kurt Othberg who helped collect paleomagnetic samples and who suggested that the field work be supported by the Department of Natural Resources. Discussions of Quaternary chronology with Alan Nelson have proved invaluable to the interpretation of the Washtucna stratigraphy.

Patty Combs has been exceedingly helpful by typing and editing the final draft of this thesis.

I am especially appreciative of the support that my parents have provided through yet another degree program, and the undying patience of my husband, Jeffrey.

Funding for this research came from several sources: Washington State Department of Natural Resources; Penrose Grant and J. Hoover Mackin Grant, Geological Society of America; and the paleomagnetic analyses were supported by a National Science Foundation grant to Don Easterbrook.

TABLE OF CONTENTS

	Page
ABSTRACT	i
ACKNOWLEDGEMENTS	ii
LIST OF TABLES	vi
LIST OF FIGURES	vii
INTRODUCTION	1
Objectives	1
Field Methods	3
Laboratory Methods	10
GEOLOGY OF THE PALOUSE REGION	11
Columbia River Basalt	11
Ringold Formation	11
Palouse Loess	12
Scabland Floods	14
Holocene Stratigraphy	16
Summary of Pleistocene Chronologic Problems	16
PLEISTOCENE GEOLOGY OF THE WASHTUCNA AREA	18
The Washtucna Locality	18
Climate and Vegetation	18
Geomorphic Setting	18
Soils	19
Soil Stratigraphy	21
Roadcut #3	26
Roadcut #4	29
Roadcut #5	30
Roadcut #9	30
Discussion	31
CLAY MINERALOGY	36
Methods	36
Identification of Clay Minerals	37
Results	45
Origin of Clay Minerals	48
TEPHRA	52
Introduction	52
Source of Tephra	52
Tephra Analysis	53
The Washtucna Tephra	53

	Page
PALEOMAGNETISM	69
Sampling Procedure	71
Magnetic Cleaning and Measurements	72
Results	72
Discussion	84
QUATERNARY CHRONOLOGY	90
Age of the Washtucna Loess	90
Loess younger than 40,000 years B.P.	90
Loess 40,000 to ~50-100,000 years old	93
Loess 40,000 to 730,000 years old	93
Loess older than 730,000 years B.P.	94
Soil Development	95
Comparison with Columbia Plateau Loess Chronology	100
Evidence for Scabland Floods	102
Regional Correlations	104
Summary	106
CONCLUSIONS	107
REFERENCES	109
APPENDIX	124

List of Tables

Table		Page
1	Relative abundance of clay minerals in Washtucna soil samples.	40
2	Correlation of Washtucna tephra layers with tephra of known source and age.	57
3	Petrographic data for Washtucna tephra samples.	58
4	Electron microprobe data for reference samples of Mount St. Helens tephra Sets S, M, and C.	60
5	Electron microprobe data for Washtucna tephra samples.	62
6	Magnetic directions for samples from roadcut #3 at selected demagnetization levels.	76
7	Mean magnetic directions for sample pairs listed in Table 6.	80

List of Figures

Figure		Page
1	Location of the area studied.	2
2	Location of Washtucna roadcuts.	4
3	Stratigraphy of roadcut #3, facing north, with vertical exaggeration.	5
4	Stratigraphy of roadcut #4, facing north, with vertical exaggeration.	6
5	Stratigraphy of roadcut #5, facing north, with vertical exaggeration.	7
6	Stratigraphy of roadcut #9, north side of Highway 26, facing north, with vertical exaggeration.	8
7	Stratigraphy of roadcut #9, south side of Highway 26, facing south, with vertical exaggeration.	9
8	Location of Rattlesnake Flat and Collier Coulee relative to roadcut #9.	20
9	Stratigraphic column for roadcut #3.	22
10	Stratigraphic column for roadcut #4.	23
11	Stratigraphic column for roadcut #5.	24
12	Stratigraphic column for roadcut #9, north.	25
13	Calcareous root casts in buried soil #6, roadcut #3.	28
14	X-ray diffraction patterns for sample 5-2, from the modern soil profile.	38
15	X-ray diffraction patterns for sample 9-9, from the K horizon in the 7th buried soil.	39
16	X-ray diffraction patterns for sample 5-7, from the K horizon in the 3rd buried soil.	43
17	X-ray diffraction patterns for sample 3-1, from the modern soil profile.	44

Figure		Page
18	X-ray diffraction patterns for sample 9-14, from the K horizon in the oldest buried soil (#11) in roadcut #9.	46
19	Correlation of tephra layers in the Washtucna roadcuts.	56
20	Refractive indices of glass from the Washtucna tephra samples.	59
21	Graph of Ca:K:Fe ratios in glass shards from cummingtonite-bearing tephra from Washtucna, and from reference samples of Mount St. Helens Tephra Sets S, M, and C.	61
22	Graph of Ca:K:Fe ratios in glass shards from non-cummingtonite-bearing tephra layers from Washtucna.	67
23	Graph of paleomagnetic direction versus depth for samples from roadcut #3, at 90 meters west of the datum, at selected demagnetization levels.	73
24	Graph of paleomagnetic direction versus depth for samples from roadcut #3, at 130 and 180 meters west of the datum, at selected demagnetization levels.	74
25	Graph of the mean paleomagnetic direction versus depth from each pair of samples in roadcut #3.	79
26	Orthogonal projection of magnetization vectors in sample 90-01-02.	82
27	Orthogonal projection of magnetization vectors in sample 90-34-02.	83
28	Stereographic projection of the mean paleomagnetic direction from each pair of samples in roadcut #3.	85
29	Orthogonal projection of magnetization vectors in sample 90-32-01.	86
30	Stratigraphic columns from the Washtucna roadcuts: possible correlations and ages.	91
31	Graph of depth below surface versus carbonate stage of buried soils in roadcuts #4 and #5.	96

Figure		Page
32	Graph of depth below surface versus carbonate stage of buried soils in roadcut #9.	97
33	Graph of depth below surface versus carbonate stage of buried soils in roadcut #3.	98
34	Comparison of the Washtucna chronology with the loess chronology of Fryxell.	101

INTRODUCTION

The Quaternary geologic history of central and eastern Washington is characterized by repeated episodes of catastrophic flooding and by intermittent periods of loess deposition and soil formation. Buried soils (paleosols) in the loess represent intervals of time when deposition was minimal and climatic conditions were suitable for the existence of a stable vegetation cover and the development of a soil profile. The sequence and chronology of geologic events on the Columbia Plateau is difficult to establish due to the complex nature of the erosion-deposition cycles and the lack of dateable materials in the deposits. A dated sequence of paleosols and loess deposits is needed to establish a basis for Pleistocene chronology of the region.

Objectives

This project is an investigation of the loess and soil stratigraphy in five exposures near Washtucna, Washington (Fig. 1). The objectives are: (1) to determine the age of these buried soils and loess deposits, and (2) to establish criteria for distinguishing soil stratigraphic units. Determination of the age of the deposits and soils is based on the correlation of tephra found in the loess with tephra of known age, and by magnetostratigraphy.

Characterization of the soils, based on field descriptions and clay mineralogy, combined with the interpretation of the stratigraphic and chronologic data, may allow the formulation of a loess chronology for the area investigated, and perhaps the correlation of loess deposits in other areas in the future. The loess chronology could then be used as a basis

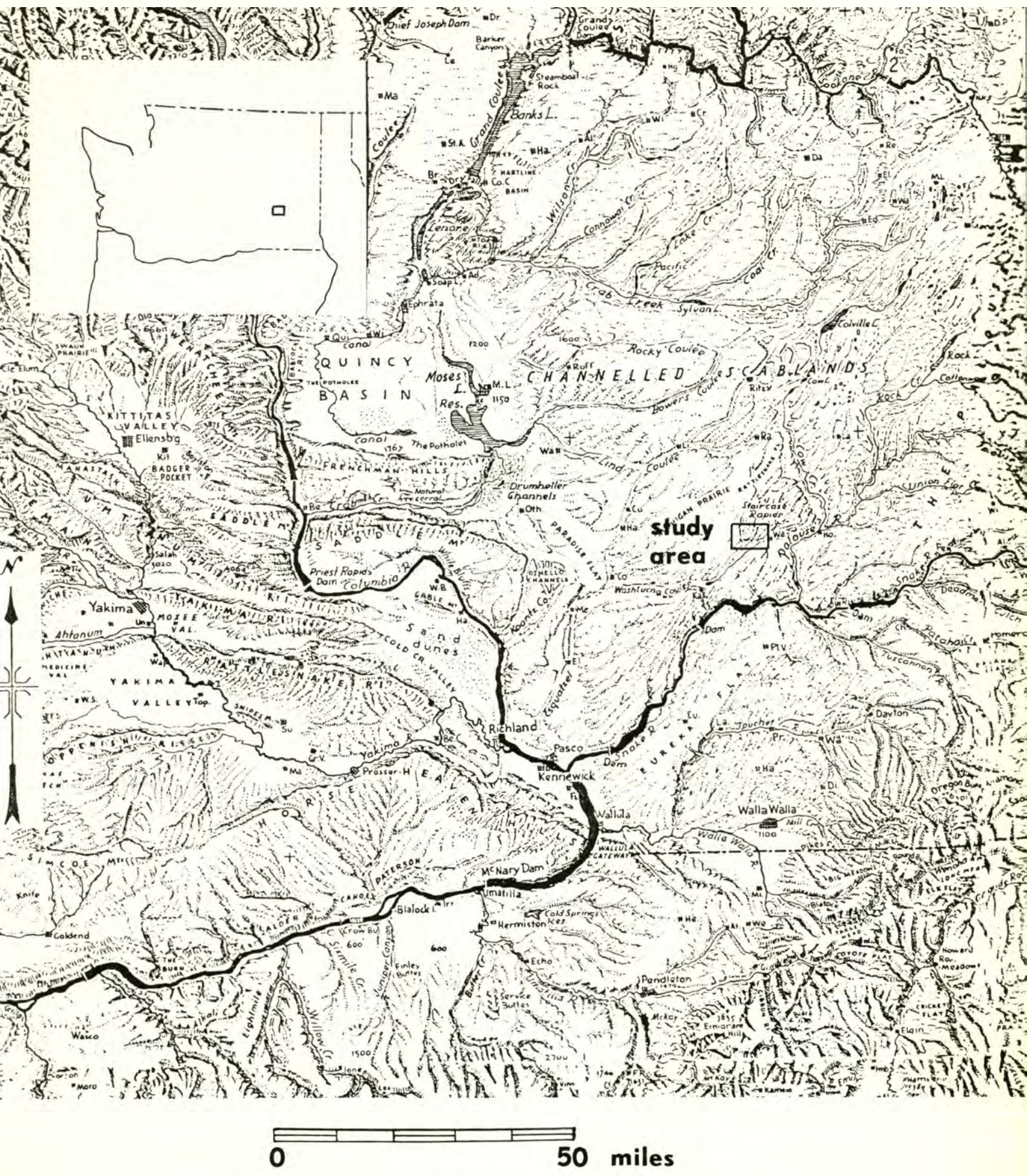


Figure 1: Location of the area studied. Map is from Erwin Raisz, Landforms of the Northwestern States, 1965.

for establishing the sequence of Pleistocene geologic events on the Columbia Plateau.

Field Methods

Investigation of the loess stratigraphy was conducted along State Highway 26, between 3.2 and 7.2 kilometers west of Washtucna (Fig. 2). Construction of the highway about fifteen years ago resulted in nine roadcuts up to 21 meters (69 feet) high where the road bisects the southwest-northeast trending hills (Fig. 2). The highway cuts through each loess hill at approximately right angles to the hill axis, creating exposures on the north and south sides of the road. Scale drawings were made of five of these roadcuts (#3, 4, 5, 9 north, 9 south; Figs. 3 to 7), and stratigraphic sections with soil descriptions were made of all of them except #9 south (Appendix).

The datum point for the scale drawing was established in a convenient place for each roadcut, and measurements were made along a line to the east and west of the datum. Stratigraphic sections were compiled, and soil descriptions were recorded for four of the exposures, usually near the center of the roadcut where the stratigraphy is well exposed and complete. The descriptions of roadcut #9 were made where each stratigraphic unit was best exposed.

The loess in the Washtucna roadcuts consists of massive pale brown silt and silt loam (Soil Survey Staff, 1951). Because no bedding is visible in the loess, stratigraphic units were distinguished by soils that have formed in the top of each loess sheet. Soil samples were obtained from each buried soil in the four exposures described, as well as from relatively unweathered loess and from the modern soil profile at the top of each section.

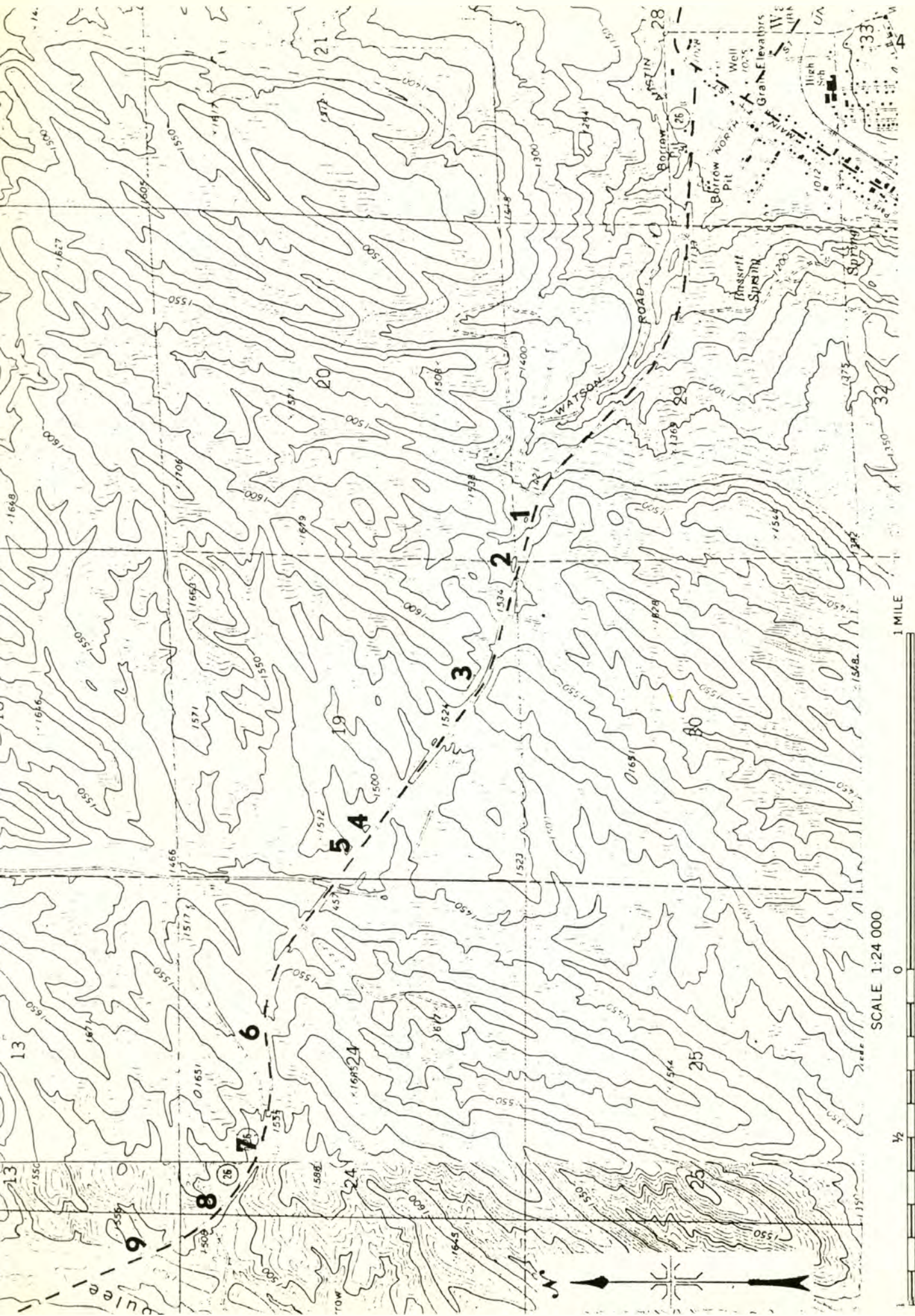


Figure 2: Location of Washtucna roadcuts. Topography is from the Washtucna Southwest and Washtucna Northwest, Washington, 7.5-minute quadrangles. Contour interval is 10 feet.

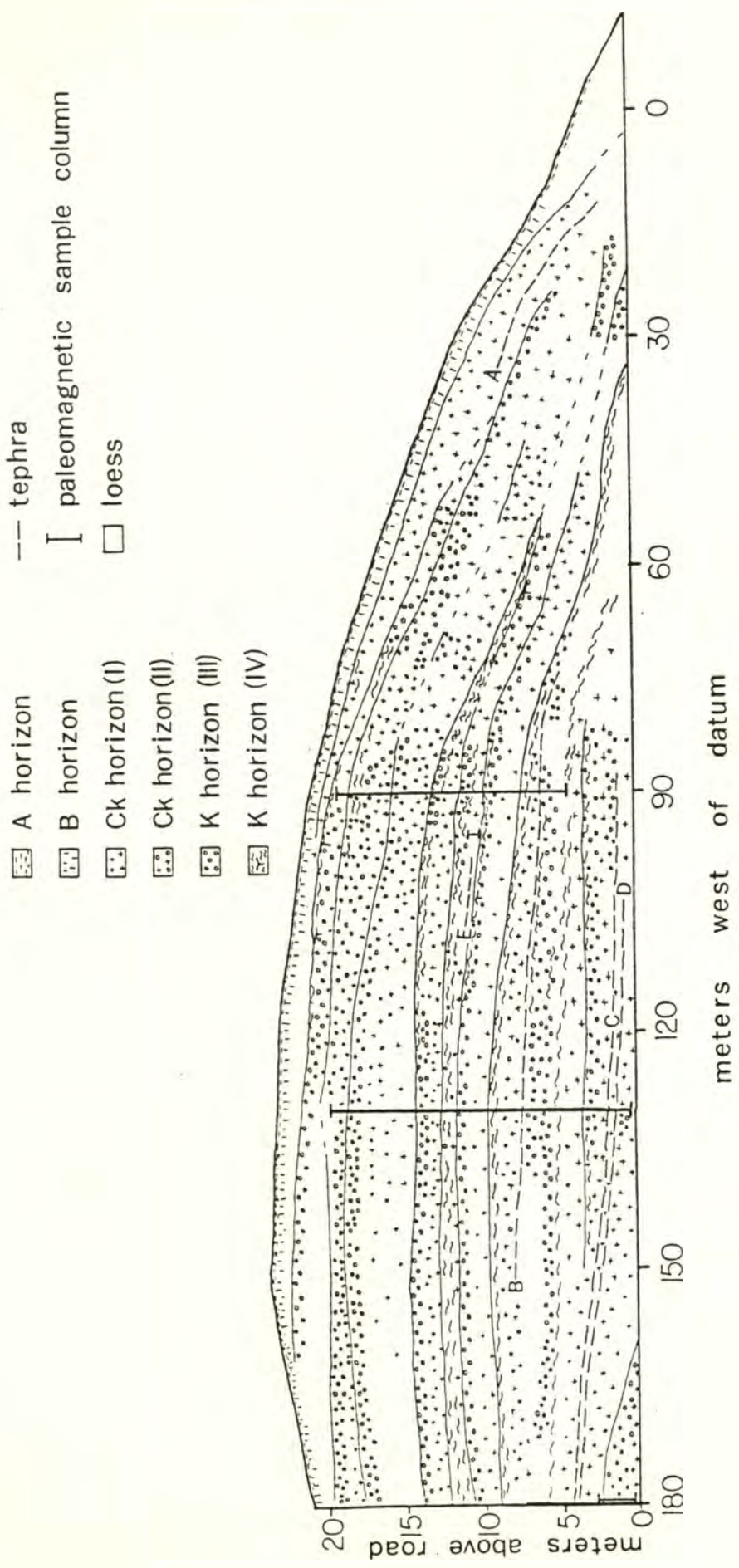


Figure 3: Stratigraphy of roadcut #3, facing North, with vertical exaggeration. Roman numerals in parentheses are carbonate stages (Gile et al., 1966).

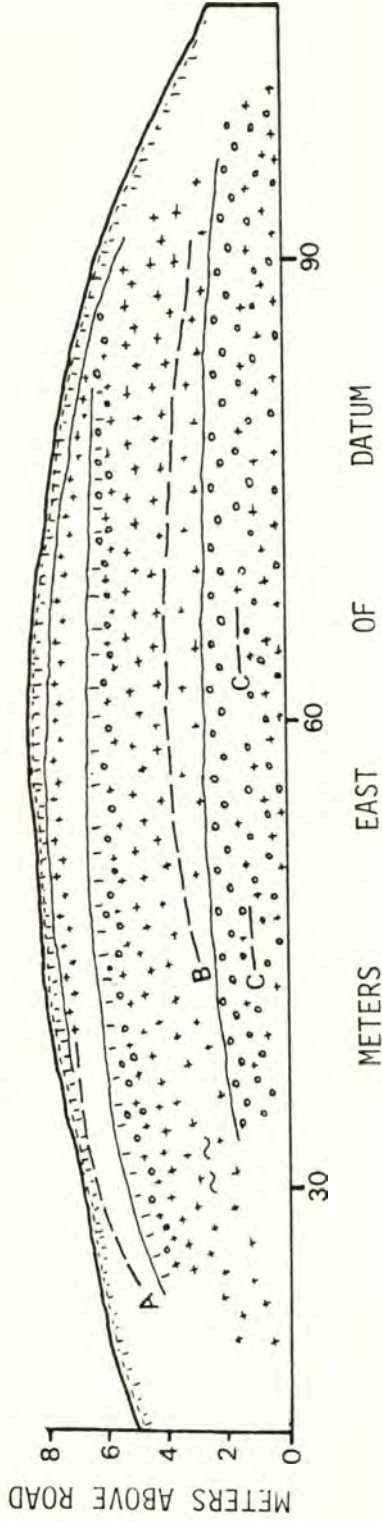
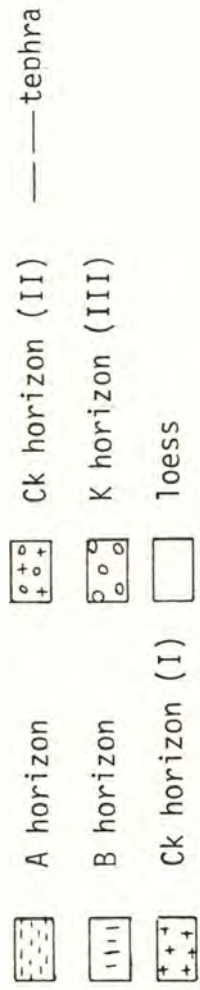


Figure 4: Stratigraphy of roadcut #4, facing North, with vertical exaggeration. Roman numerals in parentheses are carbonate stages (Gile et al., 1966).

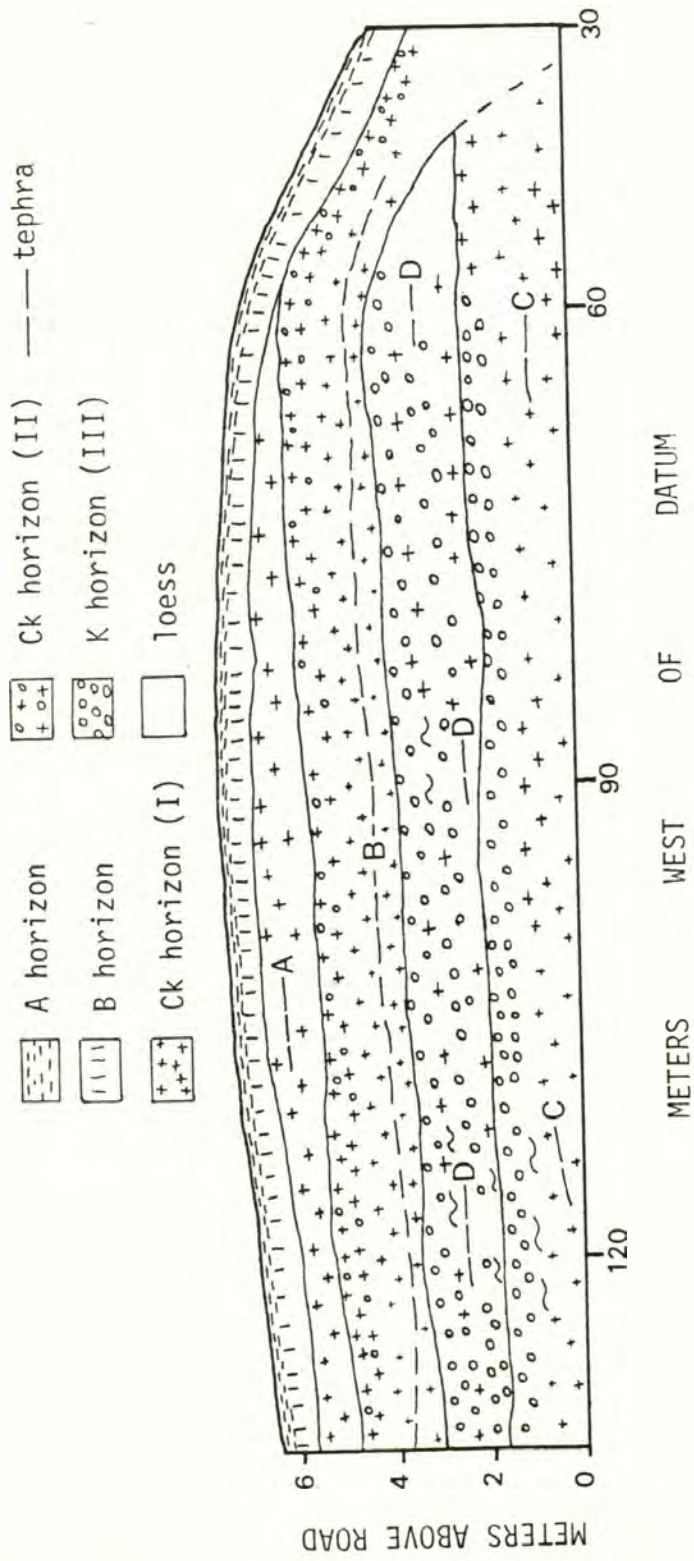


Figure 5: Stratigraphy of roadcut #5, facing North, with vertical exaggeration. Roman numerals in parentheses are carbonate stages (Gile *et al.*, 1966).

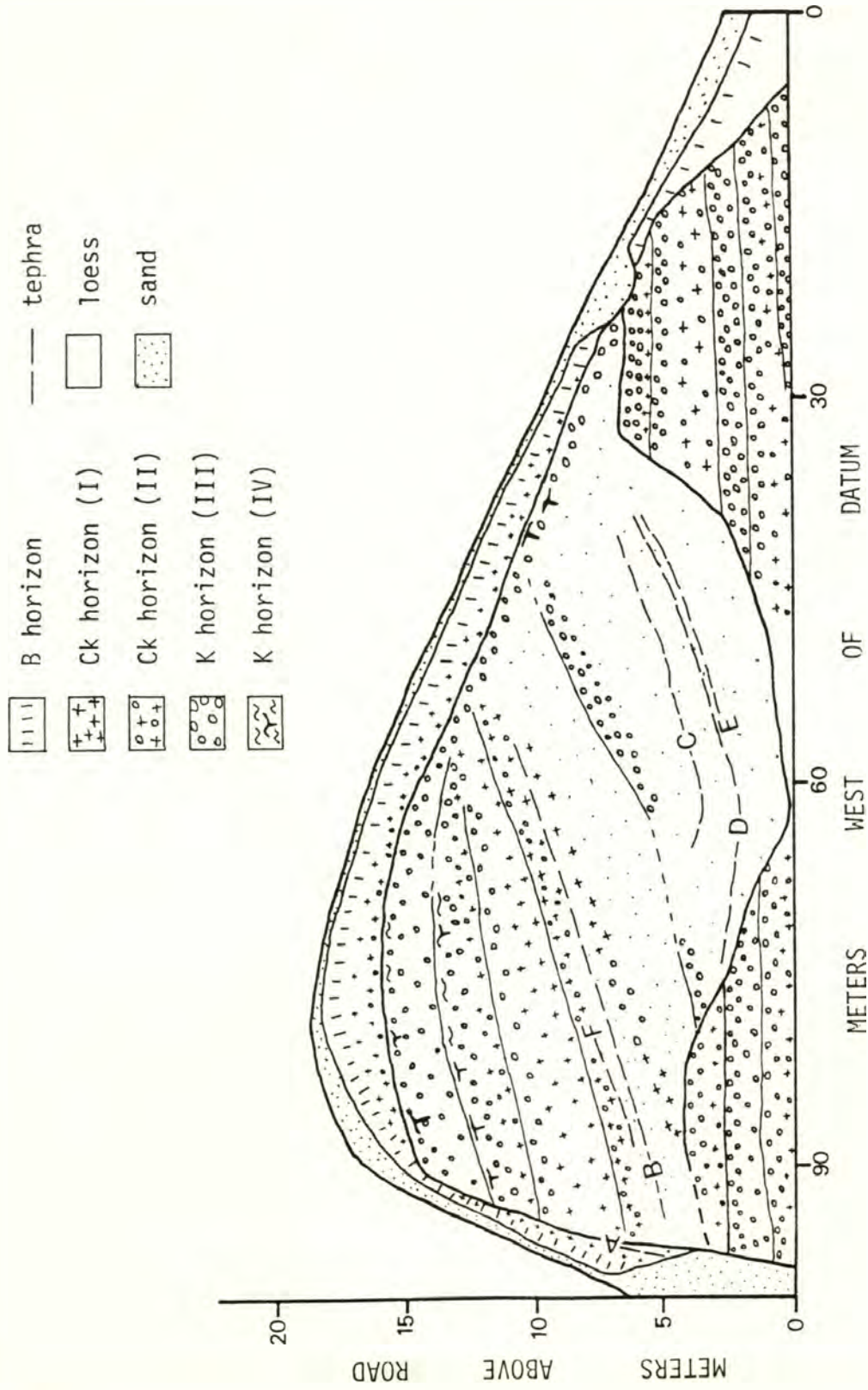


Figure 6: Stratigraphy of roadcut #9, north side of highway, facing North, with vertical exaggeration. Roman numerals in parentheses are carbonate stages (Gile et al., 1966).

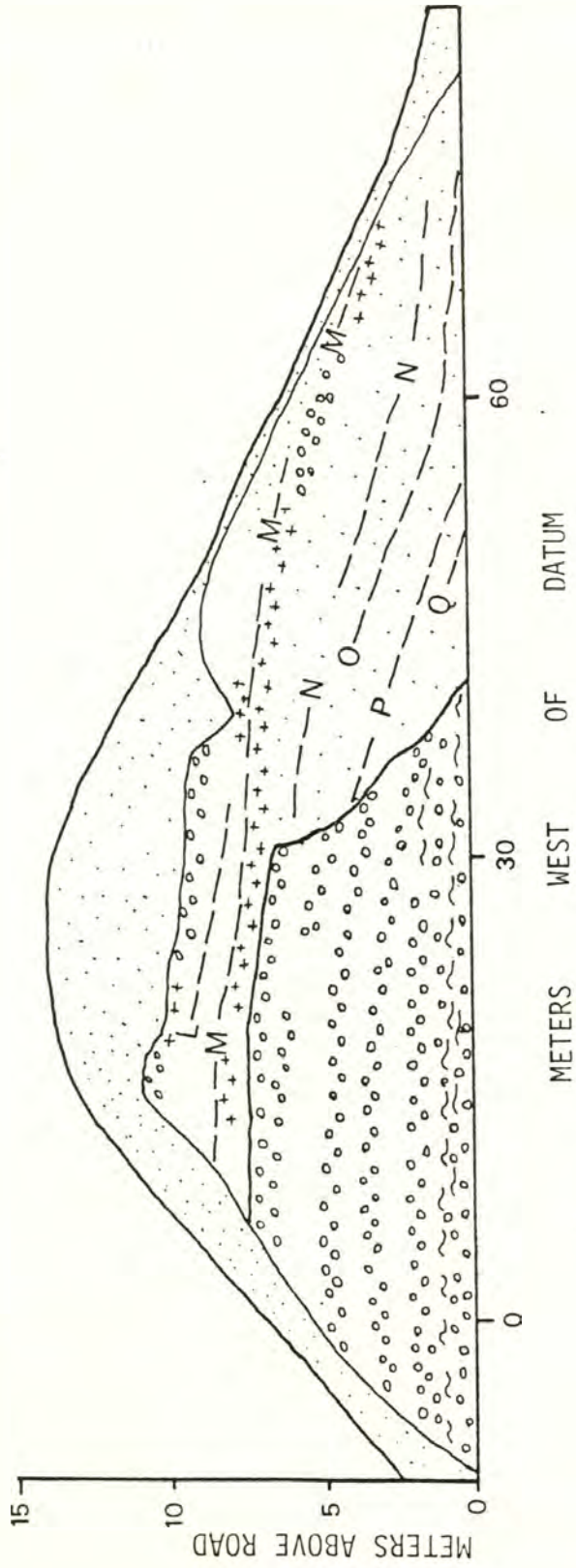


Figure 7: Stratigraphy of roadcut #9, south side of highway, facing South, with vertical exaggeration. Legend is the same as for roadcut #9, north side of highway.

Tephra is exposed in a total of twenty-four discrete layers in the six Washtucna roadcuts. These layers are the only depositional units which can be traced laterally across an outcrop, and they provide information on bedding attitude and paleoslope. Each layer was sampled for petrographic and electron microprobe analysis.

Fifty-two pairs of loess samples were collected from roadcut #3 for paleomagnetic measurement. The sampling procedure is described in the Paleomagnetism section.

Laboratory Methods

Clay-size particles ($<2\mu\text{m}$) were extracted from the soil samples and the species of clay minerals were identified by x-ray diffraction. These data are discussed in the Clay Mineralogy section. Samples of tephra were analyzed petrographically and with an electron microprobe. These data are discussed in the Tephra section. Paleomagnetic measurements of 104 samples (52 pairs) were made in order to determine the polarity of the stratigraphic units for chronologic purposes. The magnetostratigraphic information is presented in the Paleomagnetism section.

GEOLOGY OF THE PALOUSE REGION

Columbia River Basalt

The Palouse region is underlain by horizontal flows of the Columbia River Basalt Group. During the Miocene Epoch, successive flows of tholeiitic lava were extruded from fissures in southeastern Washington and neighboring parts of Idaho and Oregon. These basalts spread westward and covered the pre-existing terrain of metamorphic and granitic rocks over an area of about 200,000 square kilometers (Mackin, 1961; Waters, 1962; Swanson and Wright, 1978). Regional subsidence concurrent with extrusion formed a structural basin centered in south-central Washington, where the basalt reaches thicknesses of more than 3,000 meters (Mackin, 1961). Uplift of the Cascade Range to the west, which began during the Pliocene, had a profound and permanent effect on the climate and vegetation of the Columbia Plateau. The rain shadow created by the mountains, which reached heights of 2,500 meters, caused the previously warm, moist climate to become dry, producing the present arid and semi-arid steppe environment. Several east-west-trending anticlinal basalt ridges at the western margin of the plateau (Newcomb, 1970) may have formed due to stresses associated with the Plio-Pleistocene uplift of the Cascades (Mackin, 1961; Swanson and Wright, 1978).

Ringold Formation

The structural basin formed in the basalt filled with late Pliocene and early Pleistocene (Gustafson, 1976) sediment called the Ringold Formation (Merriam and Buwalda, 1917). It consists of fossiliferous fluvial and lacustrine clayey silt, sand and gravel, which contain white tuff and

petrocalcic horizons and is capped by a thick petrocalcic horizon. Newcomb (1958) found the thickness of these deposits to be 189 meters in the White Bluffs area along the Columbia River near Pasco, Washington. Magnetostratigraphy, coupled with paleontology, of the upper part of the Ringold Formation suggests that it was partially deposited during the Gilbert Reversed Epoch, between 3.3 and 5.1 million years ago (Rigby and Othberg, 1979).

Palouse Loess

Overlying the Columbia River Basalt and the Ringold sediments are the thick (more than 75 meters in places; Ringe, 1970) loess deposits which form the Palouse hills of eastern Washington. Originally, these sediments were thought to be the weathering products of the underlying basalt (Russell, 1897, 1901), but subsequent studies have provided overwhelming evidence for a primarily eolian origin. The first to postulate an eolian origin was Salisbury (1901), but Calkins (1905) provided the first evidence to support this idea. He cited particle size, mineralogy, and abruptness of the contact with the basalt to show an eolian origin for the loess. In 1925, Treasher proposed the term "Palouse Formation" for the sediments, and the U. S. Geological Survey later adopted it (Keroher, 1966), although no type locality has ever been designated.

Once an eolian mode of transport was accepted as the origin for the sediments, the question of source area was raised. The most likely sources are the Ringold Formation, the Touchet beds, fine waterlaid sediments of Pleistocene age (Flint, 1938), and alluvium along the Snake and Columbia Rivers. Rieger (1952) suggested that the Ringold Formation was the main source of the loess, and McCreery (1954) supported this theory with

mineralogical evidence from the two formations. The dominant heavy mineral in both the Palouse loess and the Ringold sediments is hornblende, and both have minor amounts of epidote, hypersthene and opaque minerals. The light mineral assemblage is dominated by quartz, feldspar and mica. Volcanic glass is also a constituent of the loess (Cunningham, 1964; Rieger and Smith, 1955; McCreery, 1954; Lotspeich and Smith, 1953) and originates from eruptions of volcanoes in the Cascades, which have occurred frequently during the past 40,000 years and probably during the entire Quaternary.

Another possible source for the loess is glacial flour blown southward from the southern margins of the Cordilleran Ice Sheet by "glacial winds" (Hobbs, 1947). However, two lines of evidence support a west-to-east direction of transport; the particle size of the loess decreases from the central basin to the eastern margin (Lewis, 1960), and paleosols formed in the loess overlap from west to east showing progressive easterly movement of the dunelike loess hills (Fryxell and Cook, 1964). This direction of transport is consistent with a source from Ringold and Touchet sediments, which are thickest in the central Pasco basin.

The loess of eastern Washington is younger than the Ringold Formation which it overlies in the central basin and from which it was partly derived. Hence, it is known to be mainly Pleistocene in age. The chronology of loess deposition, as proposed by Richmond et al. (1965), is based on correlation of loess sheets with glacial deposits in the Rocky Mountains and correlation of intervening paleosols with interglacial episodes. They distinguish four stratigraphic units based on the correlation of paleosols formed within the top of each unit. The degree of development exhibited by the paleosols is used to estimate the age of the loess sheets. Two pre-Bull Lake (pre-Wisconsin) loess units are distinguished by strongly

weathered paleosols containing "indurated concretions of manganese dioxide" (Richmond et al., 1965) and thick petrocalcic layers. The older of the pre-Bull Lake soils has a pinkish color possibly due to tuffaceous composition. Three Bull Lake (early Wisconsin) paleosols have well developed B horizons, but are not as thick as the pre-Bull Lake soils and have less indurated petrocalcic horizons. The Palouse Formation was informally redefined by Richmond et al. (1965) as consisting only of the Bull Lake (early Wisconsin) loess units. Pinedale (late Wisconsin) loess is lighter in color than the older loess and lacks the petrocalcic horizons associated with them according to Richmond et al. (1965).

Holocene loess blankets the older loess sheets throughout the Palouse region. This loess, referred to as the "Altithermal Loess" (Fryxell and Cook, 1964), contains Mazama ash dated elsewhere at 6,700 years B.P.

The argument for the Palouse loess being deposited during advances of the Cordilleran Ice Sheet and for soils forming during interglaciations is based on the supposition that loess is formed from glacial flour and is, therefore, directly related to the glacier's regimen. The Palouse loess differs from loesses in midwestern North America and in Europe because the Palouse loess is probably not derived directly from glacial flour but from pre-glacial Ringold beds and Scabland flood Touchet sediments which were most susceptible to wind erosion and redeposition after each Scabland flood had scoured the landscape.

Scabland Floods

During the Pleistocene, glacial lobes of the Cordilleran Ice Sheet advanced across valleys along the northeastern margin of the Columbia Plateau and impounded large lakes. The most prominent lake, Glacial Lake

Missoula, formed when the Pend Oreille glacial lobe dammed the Clark Fork River in northern Idaho. The lake filled valleys to an elevation of 1340 meters (Pardee, 1942).

Ice dams failed repeatedly during the Pleistocene, releasing catastrophic floods which drained to the southwest across the Columbia Plateau to the Pasco Basin and down the Columbia River. Each flood stripped the existing loess cover from the basalt and carved enormous channels into the bedrock, generating a system of anastomosing channels and cataracts known as the Channeled Scablands (Bretz, 1923). Evidence of catastrophic flooding cited by Bretz includes enormous gravel bars, giant current ripples, divide crossings, large scale dry cataracts, and deep anastomosing channels which resulted from extremely high velocity discharges.

The number of Pleistocene floods and their chronology remain in question. Bretz (1969) suggested that eight floods affected the Channeled Scablands and considered the floods in the Cheney-Palouse tract, at the eastern end of the Channeled Scablands, to be older than those in the western part of the Scablands because gravel bars formed by water flowing down the western channels have blocked the mouths of the eastern channels. Baker (1978) suggested that there have been only four floods because some of Bretz's gravels could have been formed during different phases of the same flood.

The only flood for which there is chronologic information is one that deposited sediments in the Columbia River valley near Vantage and Touchet sediments in the Pasco Basin about 13,000 years ago. The age is based on the presence of Mt. St. Helens Set S tephra in the deposits and was confirmed by a radiocarbon date from peat overlying flood gravels near Portland, Oregon (Mullineaux *et al.*, 1978).

Holocene Stratigraphy

After the retreat of the Cordilleran Ice Sheet, the climate in eastern Washington changed, reaching a warm, dry maximum between about 7,000 and 5,000 years ago (Hansen, 1947; Fryxell et al., 1968). Alluvial deposits in the Snake River canyon record a period of aggradation from 10,000 to 8,000 years B.P. and then soil development prior to the deposition of Mazama ash (6,700 years B.P.). Renewed aggradation occurred from 4,000 to 2,500 B.P., which was followed by eolian activity and soil formation (Hammatt, 1976).

Summary of Pleistocene Chronologic Problems

The chronology of Pleistocene geologic events on the Columbia Plateau is presently based on stratigraphic correlation of flood gravels, loess deposits, and tephra layers. The only part of the sequence which has been dated is the late Pleistocene. The pre-late Pleistocene glacial chronology is based on the correlation of glacial deposits at the northern margin of the Columbia Plateau with glacial deposits in the Rocky Mountains (Richmond et al., 1965) and in the Puget Lowland (Easterbrook, 1975, 1976). The use of stratigraphic terms from these two separate glacial sequences for non-glacial deposits on the Columbia Plateau is confusing and implies correlations for the pre-late Pleistocene deposits which have not been substantiated by radiometric dates. The conditions which caused the deposition of the Palouse loess and the development of soils within it may not be related to the conditions which caused the advance and retreat of alpine glaciers in the Rocky Mountains, and the correlation of loess sheets on the Columbia Plateau with a particular set of alpine moraines in an isolated range in Wyoming (the Wind River Range) is even more uncertain.

Correlations with the Puget Lowland sequence are preferable to the Rocky Mountain sequence, since the Puget Lobe was part of the Cordilleran Ice Sheet and was connected with the Okanogan Lobe (Easterbrook, 1976). However, a sequence of paleosols in Pleistocene deposits has not been established in the Puget Lowland.

The generalized loess sequence presented by Fryxell (in Richmond et al., 1965) has been used to estimate the age of flood events on the Columbia Plateau. If the loess sheets and paleosols form a stratigraphic sequence that can be recognized throughout the Columbia Plateau, and if this sequence can be dated, then it could form the basis for a chronology which would be independent of suppositions about correlations with distant alpine glaciations.

PLEISTOCENE GEOLOGY OF THE WASHTUCNA AREA

The Washtucna Locality

Climate and Vegetation

The study area is situated between 3.2 and 6.8 kilometers west of the town of Washtucna in sections 19, 20 and 29 of Township 15N, Range 36E and sections 14 and 24 of Township 15N, Range 35E of Adams County (Fig. 2).

The climate is mainly influenced by the prevailing westerly winds and by the rainshadow effect caused by the Cascade Mountains. The area receives approximately 280 mm of precipitation annually, most of which falls from November to February. Temperatures range from maxima 100⁰F in midsummer to minima of about 15⁰F in midwinter. The wind direction varies from south to west with higher velocities from the west or southwest (Phillips, 1970). The study area falls within the Agropyron spicatum-Festuca idahoensis vegetation zone described by Daubenmire (1970), but it is almost completely cultivated in wheat at present.

Geomorphic Setting

The geomorphology of the area consists of southwest-northeast trending loess hills with a relief of approximately 50 meters (164 feet). The hilly topography is interrupted on the east by Washtucna Coulee whose floor is about 122 meters (400 feet) below the base of the loess hills at an elevation of 312 meters (1023 feet), and by Collier Coulee on the west, whose floor is at an elevation of 442 meters (1450 feet). Therefore the maximum relief in the area is 130 meters (427 feet).

Washtucna Coulee is a large channel eroded into the basalt bedrock originally by the ancestral Palouse River and then later by Scabland

flood waters (Fryxell and Cook, 1964). A bench at about 418 meters (1370 feet) elevation due west of Washtucna appears to be the maximum height eroded. The loess hills immediately west of this bench were not affected by flood erosion. A small roadcut along Highway 26 where it crosses this 418 meter (1370 foot) bench (roadcut #1, Fig. 2) exposes basaltic gravels unconformably overlain by Mazama ash.

Collier Coulee is a shallow channel originating at Rattlesnake Flat (Fig. 8). It contains an underfit intermittent stream and has been partially filled with loess. The coulee heads at a knick point between 503 (1650) and 488 meters (1600 feet) elevation carved into the basalt floor of Rattlesnake Flat (Fig. 8), part of the Cheney-Palouse Scabland tract. This coulee becomes very steep and narrow south of Highway 26 and contains deposits of flood gravel close to its confluence with Washtucna Coulee. Collier Coulee probably functioned as a flood channel during one or more of the flood episodes. Its shallow cross section, a result of filling with loess, its stratigraphic relationship to paleosols in roadcut #9 (discussed below), and its relatively high elevation argue for it being one of the older flood channels in the Scabland.

Soils

The modern soils near Washtucna, formed in the deep loess deposits, fall within the Aridisol and Mollisol soil orders (Soil Survey Staff, 1975). The dominant soil is the Ritzville series, a calcic Haploxeroll (Lenfesty, 1967). Gentry (1974), using the loess chronology of Fryxell (in Richmond *et al.*, 1965), suggested that the A horizons had formed in Holocene loess, whereas the B horizons had formed mainly in Pinedale (Wisconsin) loess. Bull Lake and pre-Bull Lake (pre-Wisconsin) loesses

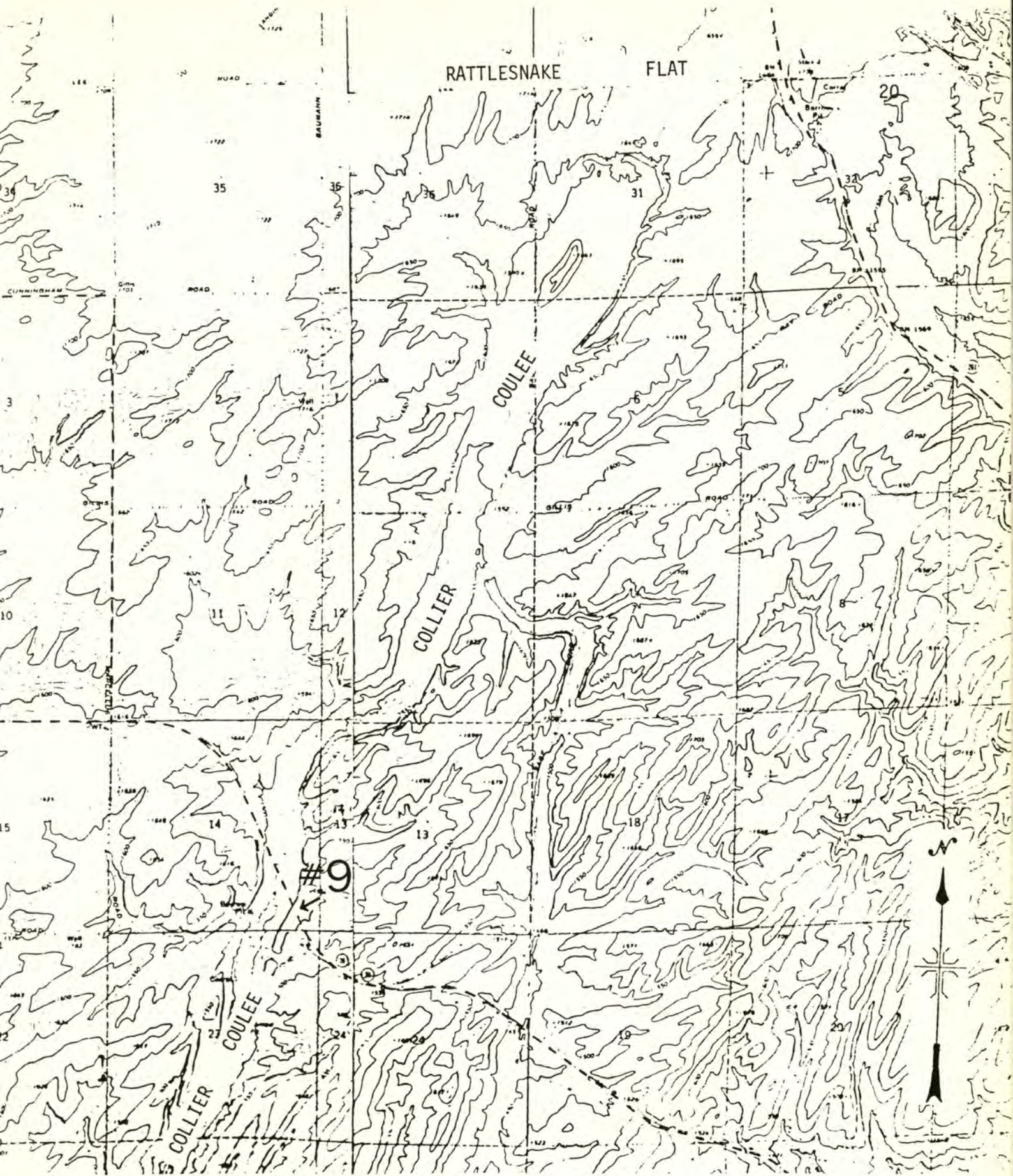


Figure 8: Location of Rattlesnake Flat and Collier Coulee relative to roadcut #9. Topography is from Washtucna Southwest and Washtucna Northwest 7½ minute quadrangles (U.S. Geological Survey). Contour interval is 10 feet.

are usually found near the base of the modern soil profile, where they exhibit strong degrees of soil structure and cementation. The stratigraphy in the Washtucna roadcuts shows that loess deposition was great enough to allow a sequence of buried soils to form rather than being incorporated in the modern soil profile.

Soil Stratigraphy

Five roadcuts were selected for detailed study of Pleistocene stratigraphy to establish a definitive sequence of buried soils and investigate field characteristics which might be used to distinguish the soils from each other. Soil descriptions are presented in the Appendix, and stratigraphic sections are shown in Figures 9 to 12.

The sediments in these roadcuts consist mainly of massive pale brown silt loam. Since no bedding is visible in the loess, stratigraphic units are distinguished by zones of carbonate accumulation which are considered to be soils that formed on a landscape in the past and which have been buried by younger sediments. Evidence supporting their designation as soils includes (1) soil morphology similar to that found in soils of arid regions elsewhere (Gile et al., 1966), (2) calcified root casts within some soils, indicating that soil development occurred near the ground surface, and (3) buried soils parallel the ancient land surface, the latter being shown by buried tephra layers.

The buried soils in the Washtucna roadcuts are extremely calcareous and exhibit morphological features which are mainly the result of cementation by calcium carbonate. Therefore, field descriptions of the soils (Appendix) include terminology proposed for calcareous soils by Gile et

DEPTH
(m.)

SOIL
HORIZON

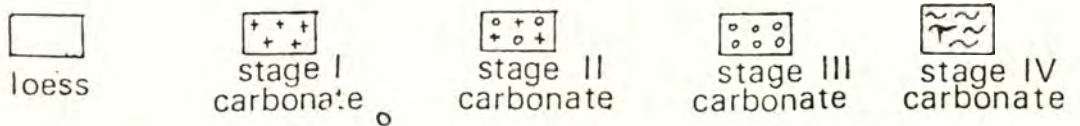
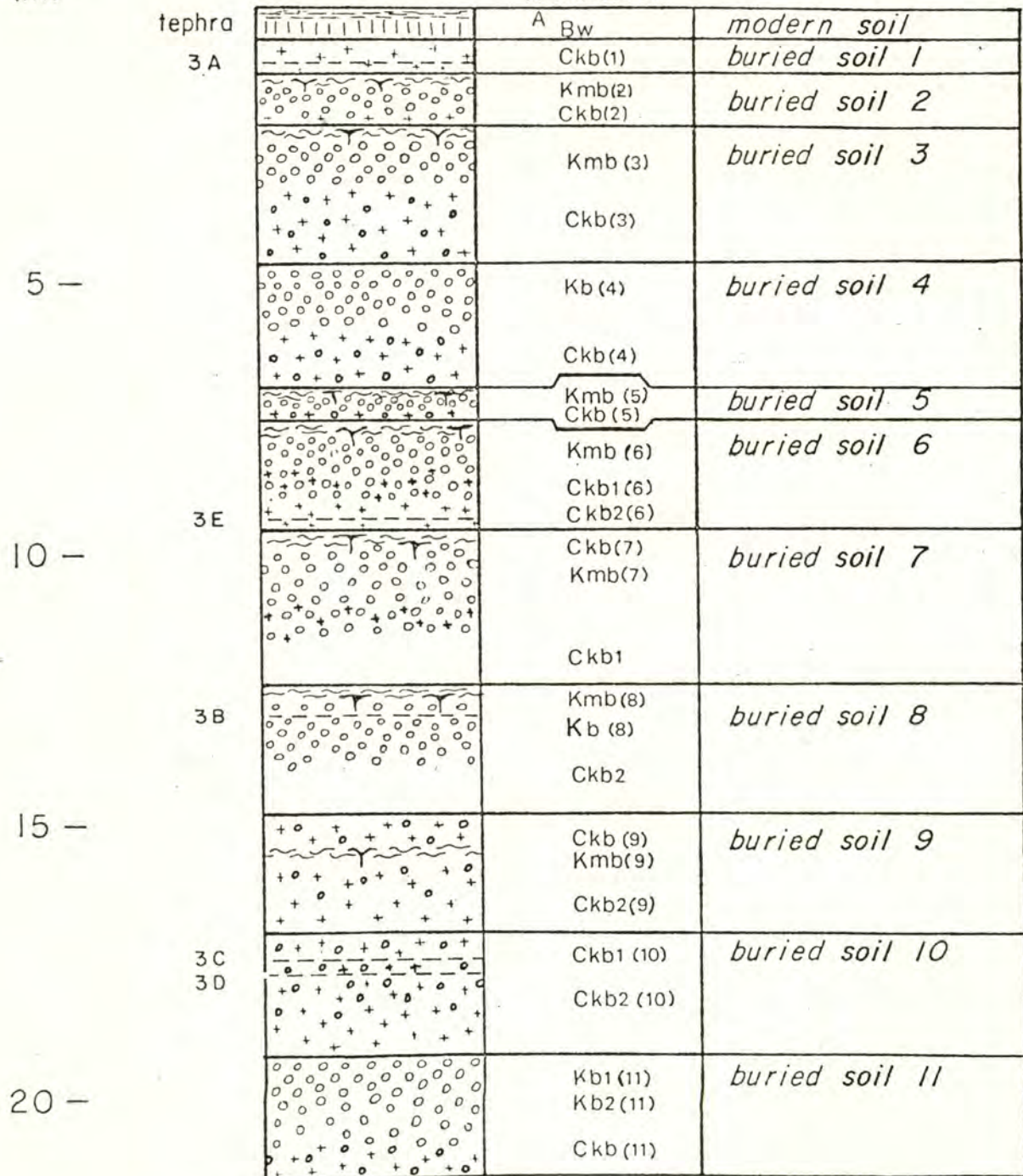


Figure 9: Stratigraphic column for roadcut #3. Soil horizon nomenclature is explained in the Appendix.

DEPTH
(m.)

SOIL
HORIZON

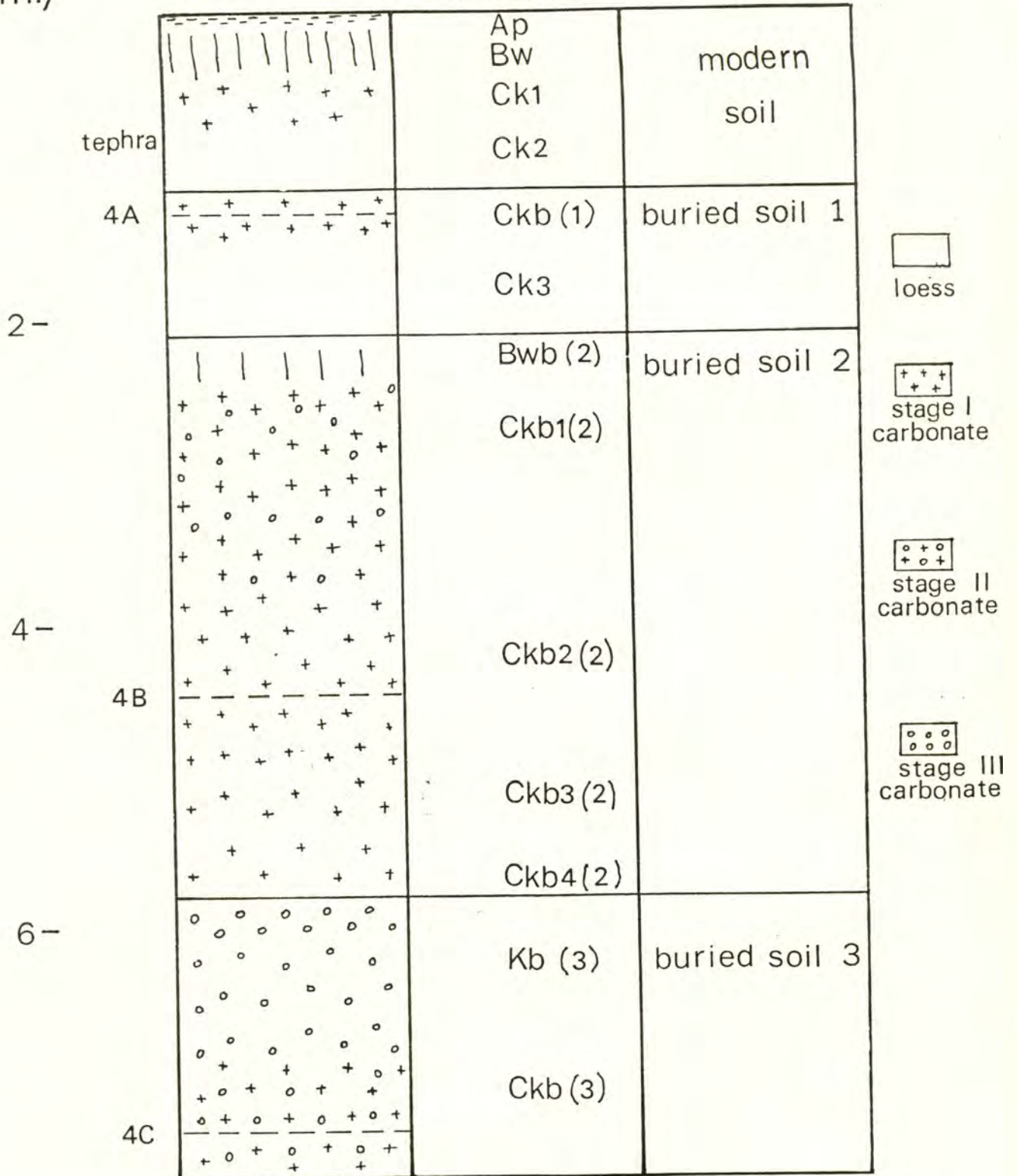


Figure 10: Stratigraphic column for roadcut #4. Soil horizon nomenclature is explained in the Appendix.

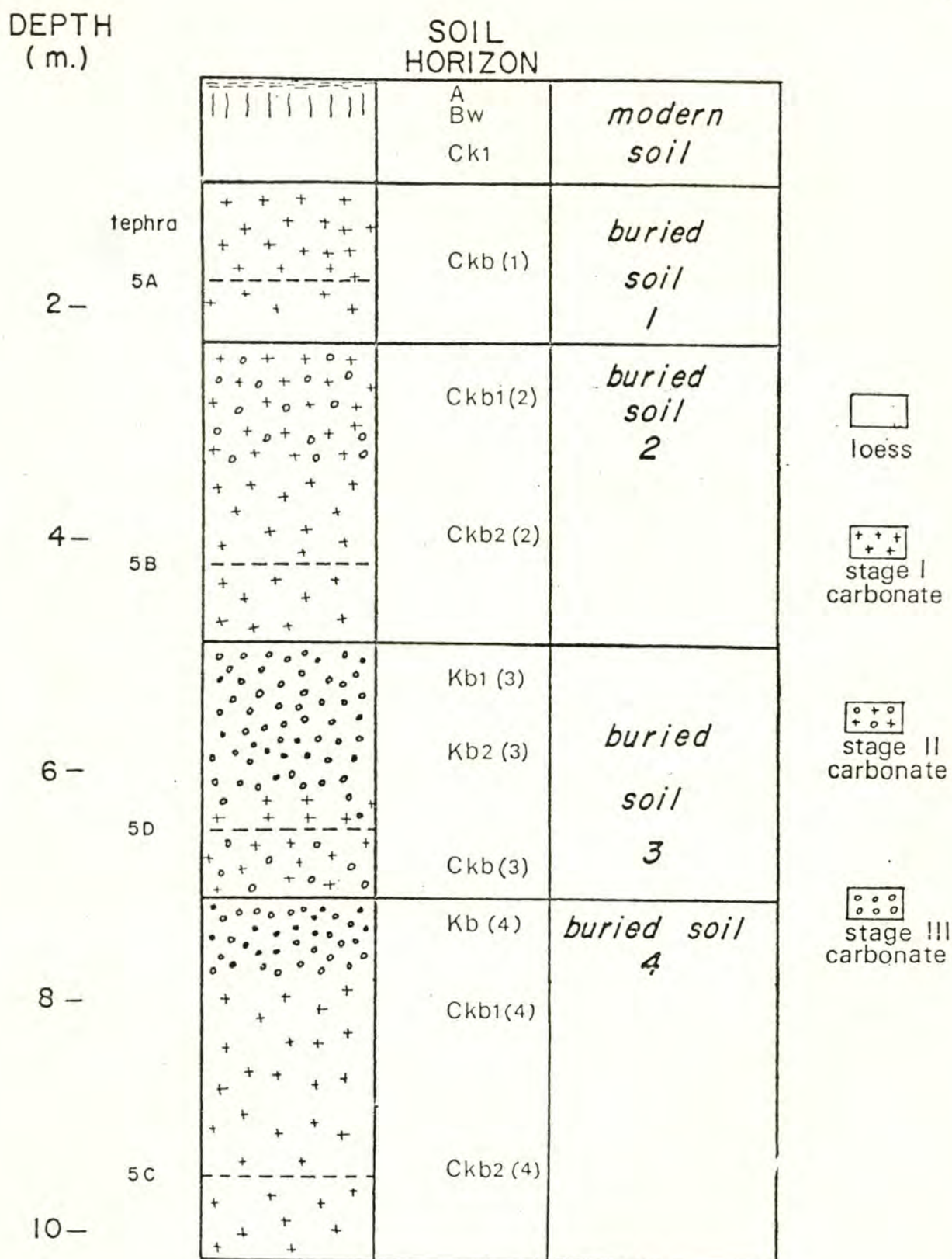


Figure 11: Stratigraphic column for roadcut #5. Soil horizon nomenclature is explained in the Appendix.

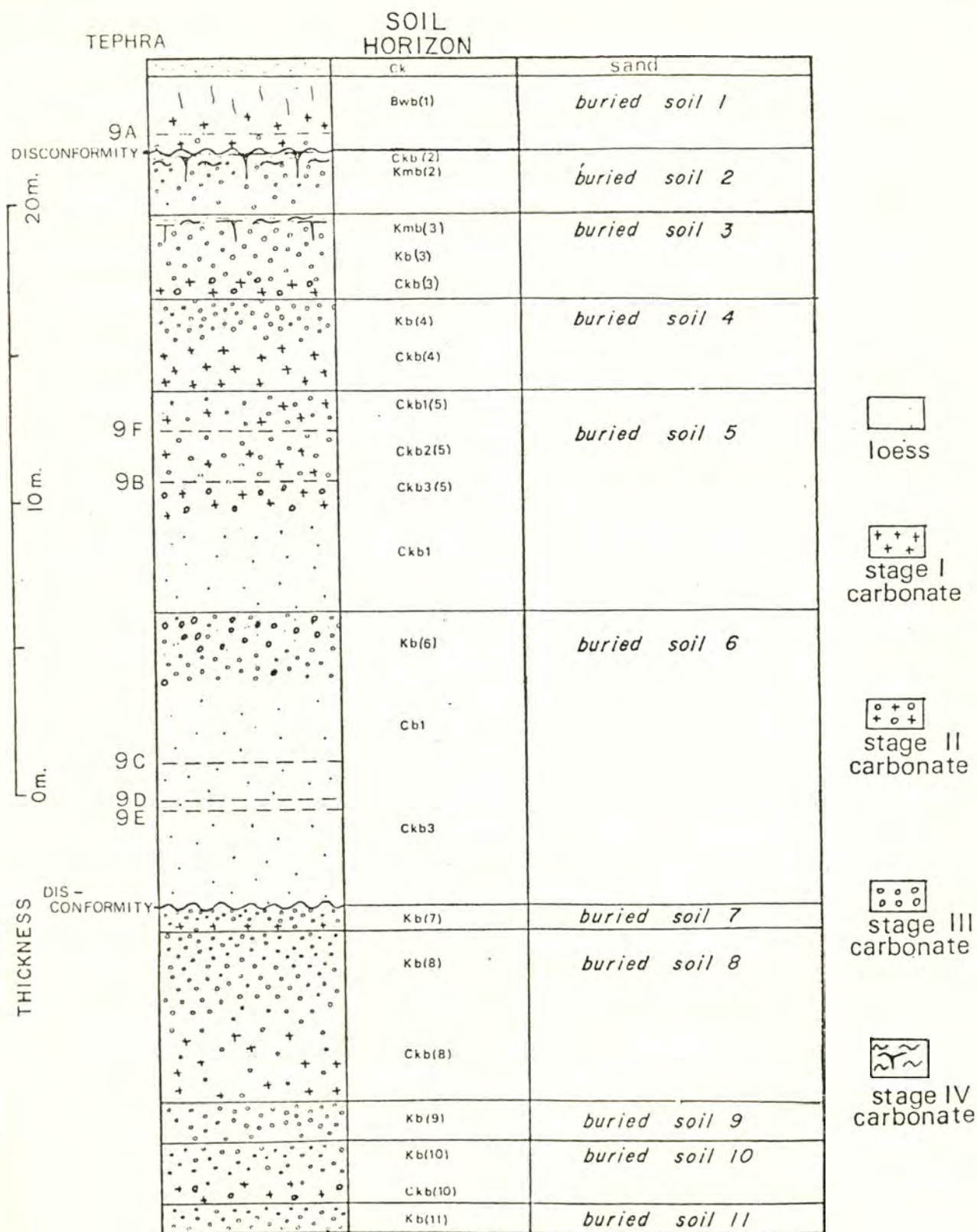


Figure 12: Stratigraphic column for roadcut #9, north. Soil horizon nomenclature is explained in the Appendix.

al. (1965) in addition to the standard terminology found in the Soil Survey Manual (Soil Survey Staff, 1951) and soil horizon nomenclature recently revised by the Soil Survey Staff (1981). The K horizon, proposed by Gile et al. (1965), is a soil horizon formed mainly by the accumulation of calcium carbonate, and has a diagnostic fabric which is called "K-fabric". K-fabric forms when fine-grained carbonate engulfs grains and forms a continuous coating. This seems to require a minimum of 15 to 40% carbonate in the soil.

Nongravelly calcareous soils can be classified by their degree of morphological development according to the scheme presented by Gile et

- al. (1966):
- Stage I: few filaments or faint calcareous coatings on sand grains
 - Stage II: few to common nodules of varying hardness with a calcareous matrix
 - Stage III: many nodules and internodule fillings coated with carbonate; voids can be filled with carbonate
 - Stage IV: laminar horizon of nearly pure carbonate usually overlying a plugged horizon of Stage 3 development

The Washtucna soils are classified according to the above sequence (Appendix).

Roadcut #3

Roadcut #3, 3.2 kilometers (1.9 miles) west-northwest of Washtucna (Fig. 2) is the largest roadcut examined and consists of 23 meters of loess with eleven buried soils and five tephra layers. The tephra descriptions are presented in the Tephra section. This roadcut was selected for magnetostratigraphic study in order to determine the age of loess (see Paleomagnetism section).

The stratigraphy exposed at roadcut #3 includes eleven buried soils which appear to be almost horizontal in cross section, but which overlap from west to east (Fig. 3), indicating that a westerly wind direction may have persisted throughout the deposition of the loess sheets.

The modern soil consists of an Ap-Bw-Ck horizon sequence formed in the top .56 meter of loess (Fig. 9). The cambic B horizon (Soil Surv. Staff, 1975) has weak subangular blocky structure and no field evidence of clay translocation. Below the modern soil is a buried soil which forms a vertical face at the east end of the roadcut (#1, Fig. 9). This buried soil contains carbonate accumulation of stages I and II. Tephra layer 3A is 30,000 to 37,000 years old; therefore, buried soil 1, as well as the modern soil profile, have formed within the past 30,000 years.

Buried soils 2, 3, 4, and 5 are characterized for the most part by strongly cemented stage IV carbonate which forms horizontal plates overlying zones of moderate to strong nodule development and lines vertical cracks. Since the cement does not completely dissolve in HCl, SiO_2 may act as a cementing agent as well as CaCO_3 . This possibility is supported by evidence discussed in the Clay Mineralogy section.

The sixth buried soil forms a very prominent vertical face about one meter high which protrudes from the surrounding loess, especially toward the eastern end of the exposure (Fig. 3). Horizontal plates of stage IV carbonate in a zone about 25 cm thick overlie a zone of moderately cemented stage III nodules with vertical cracks filled with carbonate. The soil also contains vertically oriented calcareous casts of ancient roots (Fig. 13), with some diameters as large as 4 cm. The Brunhes Normal-Matuyama Reversed polarity boundary is located within buried soil 6, so the soil is somewhat younger than 730,000 years B.P. (see Paleo-



Figure 13. Calcareous root cast in buried soil #6, roadcut #3.

magnetism section).

The seventh, eighth, ninth and tenth buried soils are similar to 6, except that 7 is not as strongly cemented as the others and is classified as stages I to III. Buried soils 7 and 8 also contain some calcareous root casts. Buried soil 10 is evident as a discontinuous zone between 85 and 95 meters west of the datum (Fig. 3).

Beneath tephra layer 3D, at a depth of 17.75 meters and to the base of the exposure at 21.45 meters, is buried soil 11 which contains strongly cemented nodules, but which is obscured by slopewash and slumped sediment from the overlying loess.

Roadcut #4

This exposure is 4.0 kilometers (2.4 miles) west-northwest of Wash-tucna and 0.8 kilometers (.5 miles) northwest of roadcut #3. The roadcut is 7.7 meters high (Fig. 4) at the southwestern end of a low loess hill which reaches a maximum height of 21.2 meters (70 feet). Three buried soils are distinguished in this roadcut (Fig. 10). The youngest occurs at a depth below the surface of 1.13-1.47 meters and contains tephra about 13,000 old (layer 4A), but is difficult to see because it has no structural or textural difference from the overlying Ck2 horizon. Buried soil #1 is recognized in the field by a marked increase in cementation by CaCO_3 (stage I) which causes it to be harder than the overlying loess. Tephra layer 4B, which is considered to be 30-37,000 years old (see Tephra section), occurs at a depth of 4.48 meters, .73 meter below the second buried soil, in relatively unweathered loess with stage I carbonate. Buried soil 2, therefore, represents a period of soil formation which occurred some time between about 30,000 and 13,000 years B.P.

The bottom 1.86 meters of the roadcut has stage II and III carbonate and is designated buried soil 3. The K horizon, between 5.80 and 6.60 meters deep (Fig. 10), is distinctly more developed than either of the overlying soils. Tephra layer 4C, which occurs at a depth of 7.36 meters, falls within the same group of tephra as 4B, and is also considered to be 30,000-37,000 years old (see Tephra section), but is probably one of the older members of this set. Buried soil 3 then must have formed between 30,000 and 37,000 years ago.

Roadcut #5

Roadcut #5, thirty meters west of roadcut #4 (Fig. 2), is in a north-east trending loess hill which has a maximum height of 16.8 meters. The roadcut is 10.25 meters high and exposes the same sequence of soils and tephra as roadcut #4, with the addition of 2.6 meters of loess at the base (Figs. 5 and 11).

Buried soils 1 and 2 (Fig. 11) are essentially the same in morphology and age as their counterparts in roadcut #4. Buried soil 3 is also correlated between these two roadcuts, but the base of the soil is not exposed in roadcut #4. Buried soil 4 consists of .72 meter of stage III carbonate with a distinctly more reddish hue than any of the other soils in these two roadcuts.

Roadcut #9

Roadcut #9 is 6.8 kilometers west-northwest of Washtucna (Fig. 2) and consists of two well-exposed sections on either side of Highway 26 (Figs. 6 and 7). The roadcut on the north side of the road has a more complete section, so the soil descriptions (Appendix) were made there.

The roadcut is formed where the highway cuts through a narrow, north-northeast trending ridge of loess on the east side of Collier Coulee (Fig. 8). The ridge is about 1.1 kilometers (.7 miles) long and a maximum of 100 meters high. The roadcut reaches a maximum height of 12.5 meters.

The stratigraphy in roadcut #9 north (Fig. 12) consists of three groups of buried soils, each group having been truncated by a disconformity. The oldest group contains five buried soils that have a horizontal attitude (Figs. 6 and 7). All five of these buried soils (7, 8, 9, 10, 11) have stage III carbonate. These soils are truncated by a channel which is filled with massive, well-sorted sandy loess. The lack of sedimentary structures and the good sorting suggest that the channel fill is of eolian rather than alluvial origin. The sand contains numerous krotovinas (rodent burrows) filled with CaCO_3 , as well as rodent bones and unidentified vertebrate bone fragments scattered throughout. Three tephra layers were found in this unit on the north side of the road, and four were found in the south roadcut (Fig. 7).

The next younger group of buried soils (numbers 2, 3, 4, 5, 6, Fig. 12) dips toward the west, possibly due to the redistribution of sediments in the channel by wind blowing up or down the coulee. Buried soils 2 and 3 have a zone of stage IV carbonate overlying a zone of stage III carbonate, whereas 4 and 5 exhibit only stage III carbonate, as shown by sparse weak nodule development.

Erosion in Collier Coulee has truncated buried soil 2 and all of the underlying loess. A small pocket of Mazama ash stratigraphically above this disconformity indicates that the erosion occurred prior to

6,700 years B.P. The ash occurs near the base of a loess deposit mantling the hill. This loess has a weak structural B (Bw) horizon developed in it and a layer of loose sandy loess has been deposited over the surface.

Discussion

The dominant characteristics of the Washtucna buried soils, nodular morphology and platy or laminar petrocalcic horizons, are caused by the precipitation of carbonate in the soil profile. The carbonate probably is derived from fine particles of calcium carbonate transported with the loess (Gile et al., 1966; Bachman and Machette, 1977). The Ringold Formation, thought to be the main source of the loess in this area (McCreery, 1954) is capped by a thick petrocalcic horizon (Newcomb et al., 1972) that may be a source of calcareous dust. Another possible source is the weathering of plagioclase feldspar which comprises 3 to 18% of the minerals in the loess. McCreery (1954) found that the amount of plagioclase diminishes downward through the soil profile, possibly due to weathering of the plagioclase near the surface and translocation of the calcium ions by water moving through the profile.

The genesis of the buried soils at Washtucna may be explained by a model developed for equivalent soil morphologies in southern New Mexico (Gile et al., 1966). In this model, calcium ions are transported from surface horizons downward through the profile and often precipitate within a pre-existing B horizon, forming a Bk horizon. Field evidence for previous translocation of clay into the B horizon is masked by the carbonate, which precipitates around grains, and as it engulfs the grains forms a nodule of cylindroidal structure (stage II morphology). Continued precipitation of carbonate within pores and root channels eventually

plugs the horizon so that water penetration is severely impeded. Lateral flow along the surface of the plugged K horizon leads to precipitation of carbonates with a laminar or platy morphology (stage IV morphology) and formation of a petrocalcic (K) horizon. Stage IV morphology in non-gravelly material in New Mexico is restricted to soils developed on surfaces of mid-Pleistocene age and older (Gile *et al.*, 1966).

The Washtucna soils show no field evidence of argillic B horizons, such as prismatic structure, fine texture, or clay films on ped surfaces. Buried soils in loess near the Washington-Idaho border, 88 kilometers east of Washtucna in an area with higher rainfall, have textural B horizons which show an increase in clay with age but do not have carbonate horizons (Krapf, 1977). These buried soils may have formed at the same time as some of the Washtucna soils, but under conditions of higher rainfall, or finer loess parent material may have supplied clays for translocation.

Fryxell and Cook (1964) describe a stratigraphic section near the town of Dusty, 53 kilometers east of Washtucna. The roadcut contains three paleosols, each with a textural B horizon, overlain by a K horizon. The two oldest paleosols, interpreted to be pre-Wisconsin, are strongly oxidized with partially indurated carbonate nodules, and each is capped by an indurated siliceous petrocalcic horizon. Early Wisconsin loess, capped by a calcareous horizon less indurated than the older ones, unconformably overlies these loess units (Fryxell and Cook, 1964).

Patton and Baker (1978) describe a sequence of three paleosols in loess parent material at a railroad cut near Marengo, 28 kilometers north of Washtucna. The proximity of this site to Washtucna suggests that paleoclimatic influences would be very similar in each, and, therefore, morphological characteristics of the soils should be comparable. The

oldest soil formed in younger pre-Palouse (pre-Bull Lake, pre-Wisconsin) loess consists of a Bt horizon with prismatic structure about 50 cm thick grading upward into a thick (50 cm) K horizon of platy carbonate and calcified root casts. It is called a superimposed petrocalcic paleosol implying that the carbonate formed after the soil. Two younger calcic paleosols, ascribed to the Palouse Formation (Bull Lake, early Wisconsin), do not have K horizons or characteristics of B horizons and are called Cca (Ck) horizons with platy structure. The oldest paleosol has characteristics which suggest that it formed by encroachment of carbonate from above onto a pre-existing textural B horizon. This soil differs from all of the Washtucna buried soils in thickness of the K horizon, presence of a Bt horizon, and lack of nodular morphology. The difference between the Marengo and Washtucna soils could be due to one of the following: (1) the Marengo soil may have formed over a much longer period of time than the Washtucna soils, or (2) it may be older than any of the paleosols exposed at Washtucna. In the first situation, the pre-Palouse Marengo soil could have formed in an area where loess deposition was minimal over a long period of time, allowing development of a strong Bt horizon, and later a thick petrocalcic horizon. At Washtucna, loess deposition may have been more sporadic, allowing shorter periods of time for soil development before a soil was buried beneath another deposit of loess. If this were the case, then the pre-Palouse soil at Marengo could correspond to more than one of the Washtucna soils. Another possibility is that the Marengo soil became exhumed by flood erosion and thereby exposed to weathering processes for a longer period of time.

The second explanation takes into account at least two episodes of flooding recorded at Marengo (Patton and Baker, 1978). It also accounts

for the thickness of the loess which is only five meters there, as compared to 23 meters at Washtucna #3 where none has been eroded by flood waters. Loess deposition and soil development possibly proceeded at the same rate in both localities, but the Marengo sequence may not be complete. The older Marengo loess and buried soil may correspond to the calcareous upper part of what has been called Ringold Formation elsewhere, and if so pre-date the Washtucna loess.

The two younger paleosols in the Palouse Formation at Marengo are similar in degree of development to a buried soil at Washtucna roadcuts #4 and #5, and their stratigraphic position beneath flood gravels, which are probably 13,000 years old, corresponds to the stratigraphic position of buried soil 2 below Mt. St. Helens S tephra (see Tephra section).

CLAY MINERALOGY

Methods

Soil samples from four of the Washtucna roadcuts (#3, 4, 5, 9 north) were analyzed to determine the type of clay minerals present and their relative abundance. Each sample was treated with a sodium acetate solution of pH 5 in order to dissolve the calcium carbonate cement, according to the procedure of Jackson (1974). A few of the samples were also treated with sodium carbonate which dissolves amorphous silica (Jackson, 1974) to see if orientation of the clays would improve, producing sharper peaks on the x-ray diffraction (XRD) pattern. After the sodium carbonate treatment, more clay was visible in suspension, which supports field evidence for cementation by amorphous silica and alumina in addition to CaCO_3 . The less than $2\mu\text{m}$ (micrometer) fraction was separated by centrifugation and then the clay was Mg^{++} saturated and suctioned onto a porous ceramic plate to produce an oriented aggregate for XRD analysis. Potassium-saturated plates were made for a few samples (3-1, 3-11, 5-2, 5-7, and 9-14) in addition to the Mg^{++} saturated ones. Oriented clay samples were analyzed on a G.E. XRD 5 x-ray diffractometer with a copper target tube at 35 kilovolts and 15 milliamps. X-ray patterns were run for samples that were air-dried and then submitted to the following sequence of treatments: glycolated, glycerolated, heated to 300°C for at least 2 hours and then 550°C for at least 2 hours. Four samples (3-24, 9-5, 9-9) were treated with dimethylsulfoxide (DMSO) according to the procedure of Abdel-Kader *et al.* (1978).

Samples were numbered with the designation of the roadcut from which they were taken (3, 4, 5, 9 north) followed by the sample number within

the roadcut, from top to bottom (lower numbers being higher in the section).

Identification of Clay Minerals

The XRD patterns show peaks which are diagnostic of mica, chlorite, smectite, vermiculite, and kaolinite. Since these minerals produce overlapping peaks, additional treatments were necessary in order to characterize the clay species.

(1) Mica: The mica group (muscovite, illite, biotite) is identified on x-ray patterns by the presence of peaks at 10, 5, and 3.3\AA in air-dry, Mg^{++} saturated samples that are unaffected by glycol, glycerol and heat treatments. Muscovite has a prominent 5\AA peak, whereas biotite has a very weak 5\AA peak which may not show up at all (Fanning and Keramidas, 1977). The dioctahedral mica (muscovite or illite) in the Washtucna loess is interpreted to be well-crystallized muscovite, since the peaks are relatively sharp. Figure 14 shows well-defined peaks at 10\AA and 5\AA in the Mg^{++} saturated air-dry pattern and is interpreted to indicate muscovite, whereas Figure 15 shows a smaller, more diffuse 5\AA peak, indicating that muscovite, and possibly biotite, are present. Because most of the XRD patterns for the Washtucna samples were run with low counting rates, the reproducibility of the peak intensities is not good enough to routinely distinguish between muscovite and biotite. Therefore these are combined under mica in Table 1.

(2) Chlorite: This mineral produces XRD peaks at 14\AA and 7\AA for air-dry, glycolated, glycerolated and heated (300°C) samples. The 7\AA peak disappears or is greatly diminished upon heating to 550°C , and the intensity of the 14\AA peak is enhanced. Figures 14, 15, and 16 show chlorite.

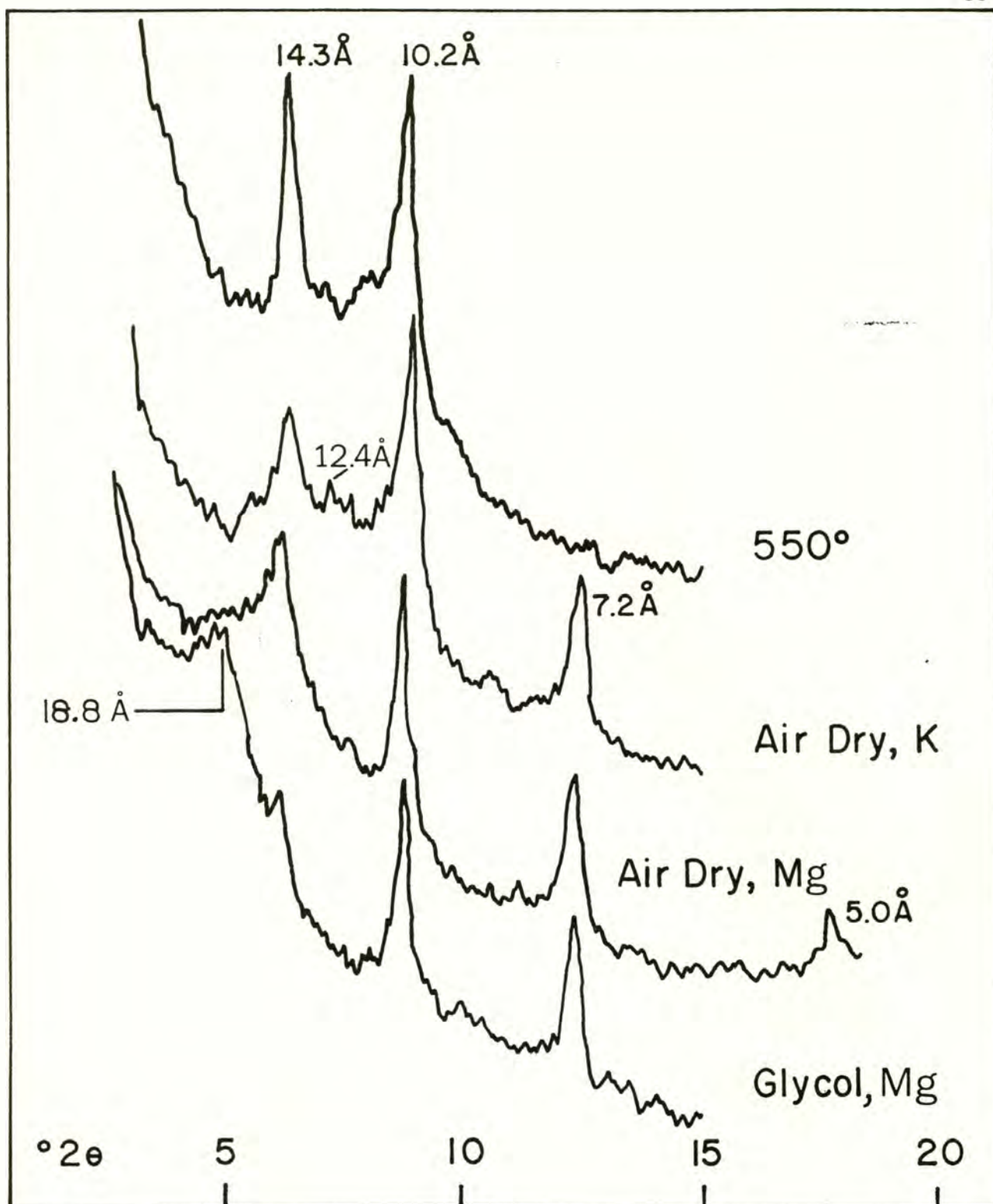


Figure 14: X-ray diffraction patterns for sample 5-2, from the modern soil profile. Clay minerals identified in this sample are: chlorite, mica (muscovite), smectite, vermiculite and mixed layer clays.

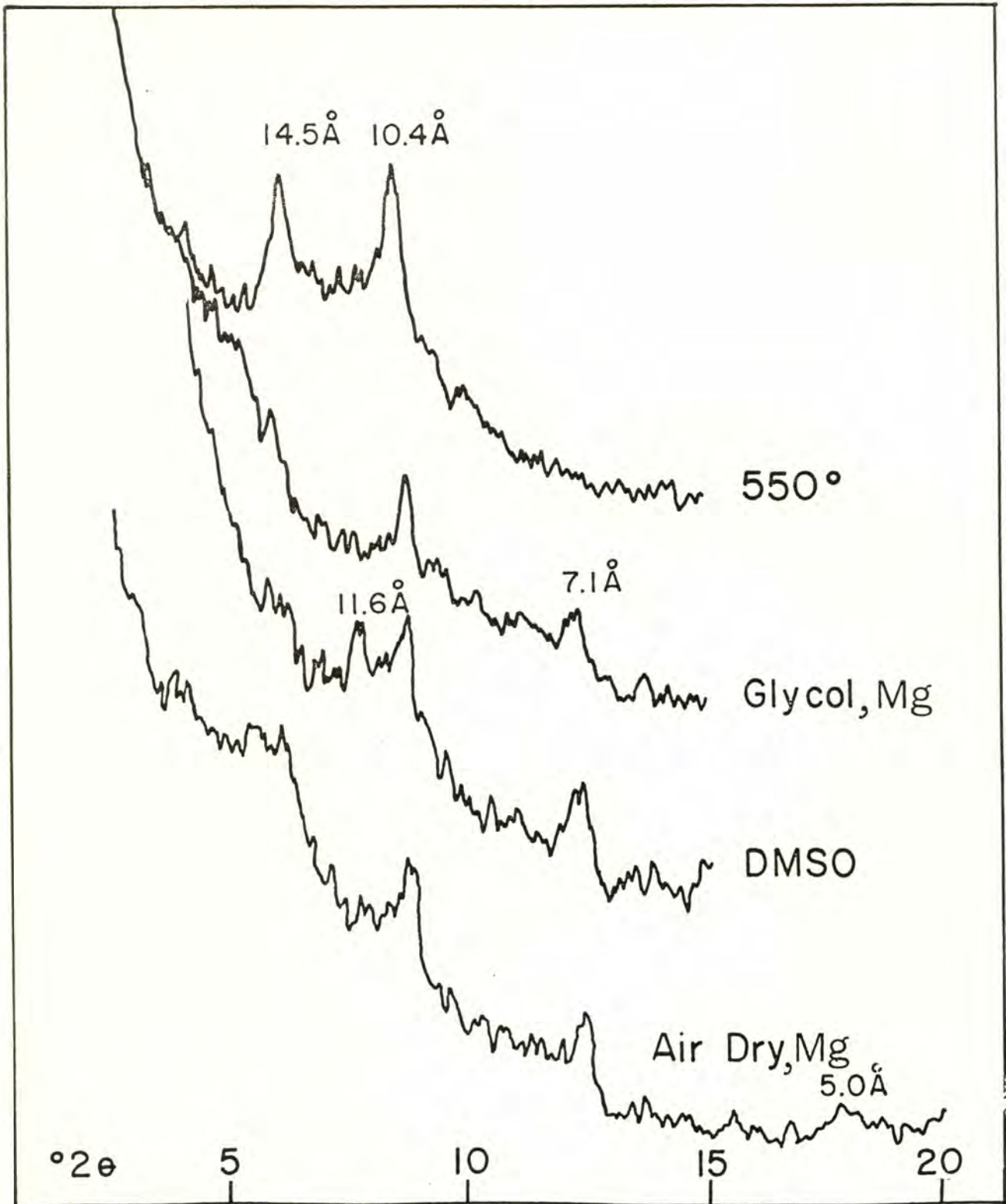


Figure 15: X-ray diffraction patterns for sample 9-9, from the K horizon in the 7th buried soil. Clay minerals identified in this sample are: chlorite, mica, smectite, vermiculite, mixed layer clays and kaolinite.

TABLE 1. Relative abundance of clay minerals in Washtucna soil samples. M = major component, m = minor component, t = trace. Samples are numbered with roadcut number first, followed by sample number. The lowest numbers represent samples from the top of the exposure (youngest soils) and the highest numbers are the deepest (oldest) soils.

Sample #	Buried Soil #	Soil Horizon	Chlo-rite	Mica	Smec-tite	Vermi-culite	Mixed Layer	Kaoli-nite
3-1	modern soil	BW	m	M	m	M	t	
3-2	1	Ckb1(1)	M	M	m			
3-3	2	Kmb(2)	M	M	m	t		
3-5	3	Kmb(3)	M	M	m			
3-7	4	Kb(4)	M	M	t	t	t	t
3-9	4	Ckb(4)	M	M	m			
3-10	5	Kmb(5)	M	M	t		t	
3-11	6	Kmb(6)	M	M	t		t	
3-12	6	Ckb2(6)	M	M	m		t	
3-13	7	Ckb(7)	M	M			t	
3-14	7	Kmb(7)	M	M	m		m	
3-15		Ckb1	m	M			t	
3-17	8	Kb(8)	M	M	m			
3-18		Ckb2	M	M	t			
3-19	9	Ckb1(9)	M	M				
3-21	9	Ckb2(9)	M	M				
3-22	10	Ckb2(10)	M	M	m	m	t	
3-23	10	Ckb2(10)	M	M	m		t	
3-24	11	Kb1(11)	M	M	M			t
3-25	11	Kb2(11)	M	M	t			
5-2	modern soil	Ck1	M	M	m	m	t	
5-3	1	Ckb(1)	M	M	m	m	t	
5-4	1	Ckb(1)	M	M	m	m	t	
5-5	2	Ckb1(2)	M	M	m	m	t	
5-6	2	Ckb2(2)	M	M	m	m	t	
5-7	3	Kb1(3)	M	M	m	M	m	

TABLE 1. Continued.

Sample #	Buried Soil	Soil Horizon	Chlo-rite	Mica	Smec-tite	Vermi-culite	Mixed Layer	Kaoli-nite
5-8	3	Kb2(3)	M	M	m	m	t	
5-9	3	Ckb(3)	M	M	m		t	
5-10	4	Kb(4)	t	M	M	m	m	
5-11	4	Ckb1(4)	m	M	M	t	t	
5-12	4	Ckb2(4)	M	M	m	m	t	
9-1	1	Bwb(1)	m	M	M	M	t	
9-2	2	Kmb(2)	M	m	M	t	m	
9-4	2	Kmb(2)	M	M	m		m	
9-5	3	Kb(3)	t	m	M	m	t	t
9-6	5	Ckb1(5)	m	m	M	t	t	
9-9	7	K1b(7)	M	M	m	t	t	m
9-10	7	K2b(7)	M	m	m		M	
9-11	8	Kb(8)	M	M	M	t	t	
9-12	9	Kb(9)	M	M	m	t	t	
9-13	10	Kb(10)	M	M	m	t	t	
9-14	11	Kb(11)	M	M	t	m	m	

Sample #	Buried Soil	Soil Horizon	Chlo-rite	Mica	Expandable*	Mixed Layer
4-3	modern soil	Ck1	M	M		m
4-4	modern soil	Ck2	M	M	m	
4-5	1	Ckb(1)	M	M	m	t
4-6		Ck3	m	M	m	t
4-7	2	Bwb(2)	M	M	m	t
4-8	2	Ckb(2)	M	M	m	t
4-9		Ckb3(2)	m	M	m	
4-12	3	Kb(3)	m	M	m	t
4-13	3	Ckb(3)	M	M	m	t

*Samples from roadcut #4 were treated with glycol, but not with glycerol. Therefore a distinction between smectite and vermiculite could not be made.

(3) Smectite: Smectite (montmorillonite) also produces a 14\AA peak in Mg^{++} saturated, air-dry samples, but is distinguished from chlorite by expansion of the d-spacing to 17\AA when the sample is treated with ethylene glycol (Figs. 16 and 17) and collapse to 10\AA upon heating to 550°C (Fig. 16). Glycerol treatment expands smectite to 18\AA , and saturation with K^{+} makes it collapse to $\sim 12\text{\AA}$. The samples illustrated in Figures 14, 16, and 17 show a 14\AA peak in air dry, Mg^{++} saturated samples which collapse to between 10\AA and 14\AA with K^{+} saturation.

(4) Vermiculite: This mineral also has a d-spacing of 14\AA in air-dry Mg^{++} saturated samples, but it can be distinguished from smectite and chlorite by saturation with K^{+} which causes collapse to 10\AA in vermiculite. Like smectite, vermiculite collapses to 10\AA upon heating to 550°C . Glycerol and glycol treatments may also distinguish vermiculite from smectite, since Mg^{++} saturated vermiculite may expand slightly with glycol, but not with glycerol (MacEwan and Wilson, 1980). The Washtucna samples were treated with both glycol and glycerol in order to recognize vermiculite, and, in addition, a few samples were saturated with K^{+} in order to confirm the presence of vermiculite. Figure 16 shows an example of a sample which expands with glycol to 17\AA but does not expand with glycerol treatment. The presence of vermiculite is further substantiated by comparing the Mg^{++} saturated pattern with the K^{+} saturated pattern: the 14\AA peak in the Mg^{++} saturated pattern is diminished in the K^{+} saturated pattern, whereas the 10\AA peak becomes slightly larger. Comparison of the Mg^{++} and K^{+} saturated patterns in Figure 17 shows that vermiculite is a major component of the sample and that smectite and chlorite are also present.

(5) Kaolinite: This mineral is difficult to recognize when chlorite is also present. Kaolinite produces a 7\AA peak in air-dry samples, and

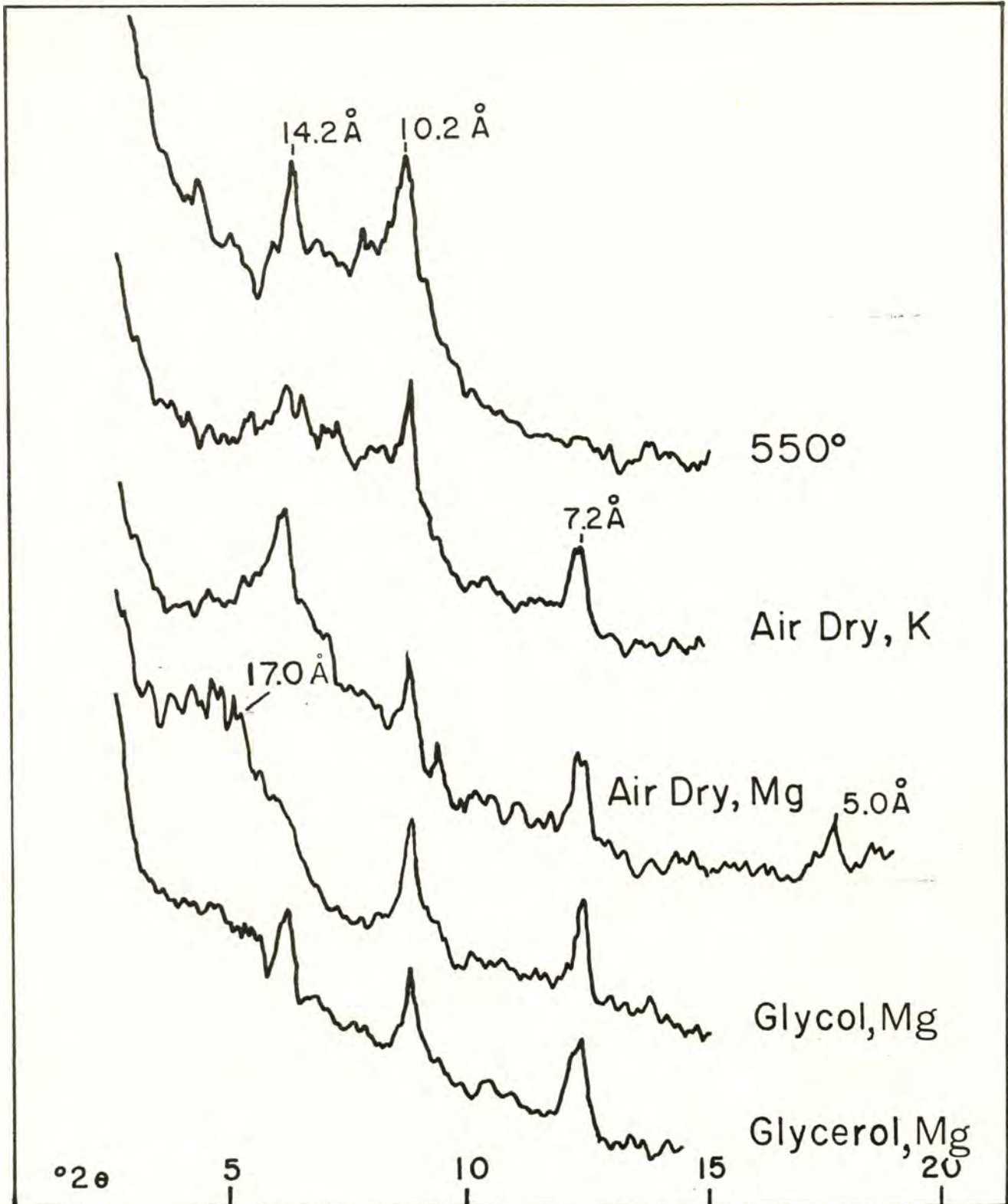


Figure 16: X-ray diffraction patterns for sample 5-7, from the K horizon in the 3rd buried soil. Clay minerals identified in this sample are: chlorite, mica (muscovite), smectite, vermiculite and mixed layer clays.

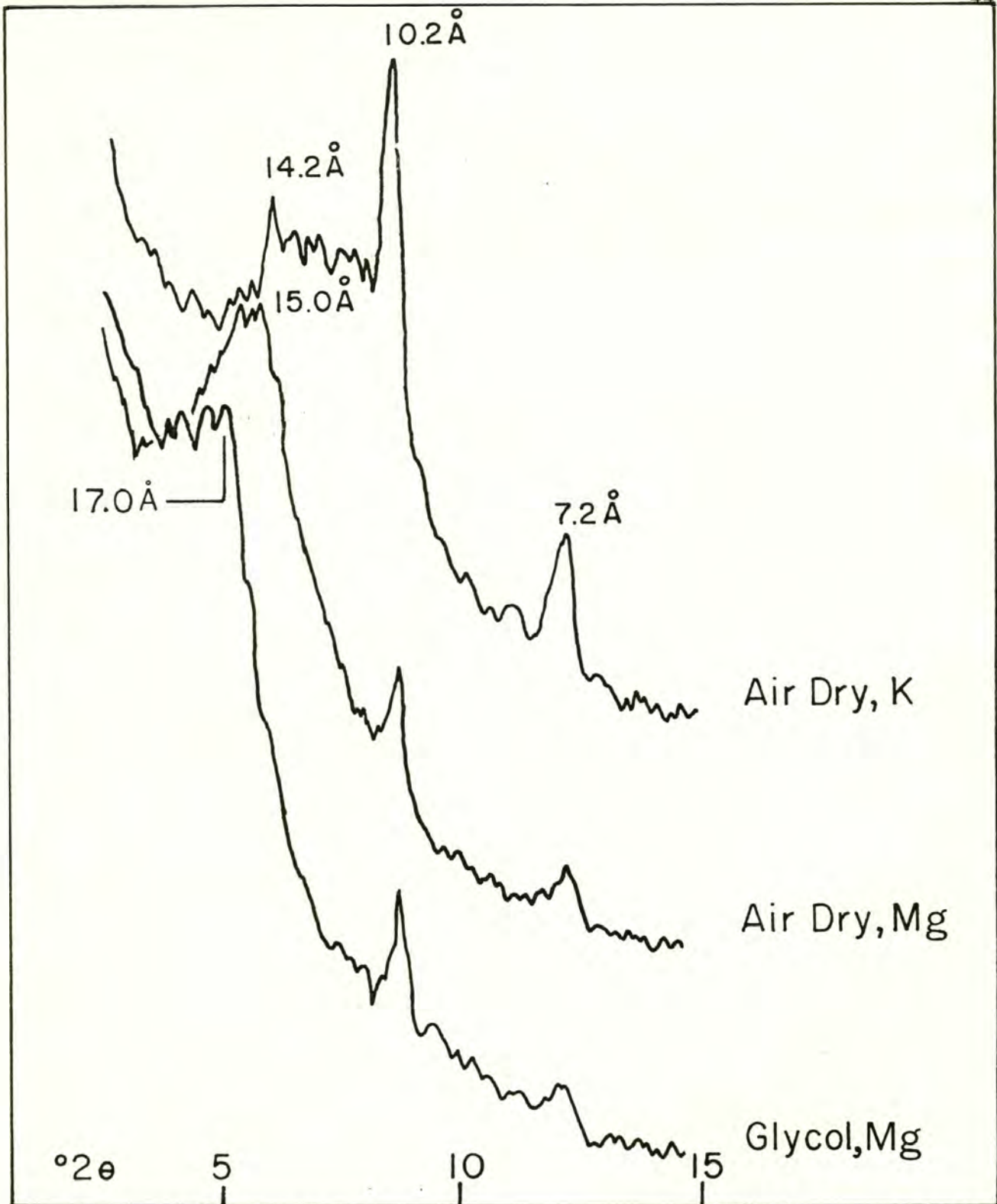


Figure 17: X-ray diffraction patterns for sample 3-1, from the modern soil profile. Clay minerals identified in this sample are: chlorite, mica, smectite, vermiculite and mixed layer clays.

this peak disappears upon heating to 550°C. Therefore, if a sample produces 14Å and 7Å peaks it may contain either chlorite alone or chlorite plus kaolinite. If the 7Å peak is unusually large for the amount of chlorite in the sample (judging from the size of the 14Å peak in a heated sample) then kaolinite may be present. The only way to identify kaolinite positively in this instance is to treat the sample with dimethylsulfoxide (DMSO), which produces a peak at ~11Å. Four of the Washtucna samples were treated with DMSO (3-24, 3-22, 9-5, and 9-9). Three of these were found to contain kaolinite (3-24, 9-5, and 9-9; Table 1) in small amounts. A fourth sample (3-7; Table 1) is thought to contain kaolinite because of the presence of a peak at 3.58Å in the air-dry pattern. This peak represents the second order reflection of the kaolinite 7Å d-spacing. Figure 15 is an example of a sample treated with DMSO and showing an 11Å peak. This sample also contains chlorite, mica, and smectite.

(6) Mixed-layer clays: The presence of mixed-layer chlorite-smectite and/or chlorite-vermiculite in many of the Washtucna samples is deduced from the appearance of a bulge (diffuse peak) between 10Å and 14Å on the pattern of heated samples (Fig. 18). This bulge is a result of the presence of OH⁻ interlayers (chloritic intergrade) which do not collapse as easily as H₂O interlayers (vermiculite, smectite). Superlattice reflections were not seen on any of the x-ray patterns, which suggests lack of order in the mixed layering.

Results

The clay mineral assemblage identified in each Washtucna soil sample is presented in Table 1. The relative abundance of each mineral is a qualitative estimate based on the peak intensities on the x-ray pattern.

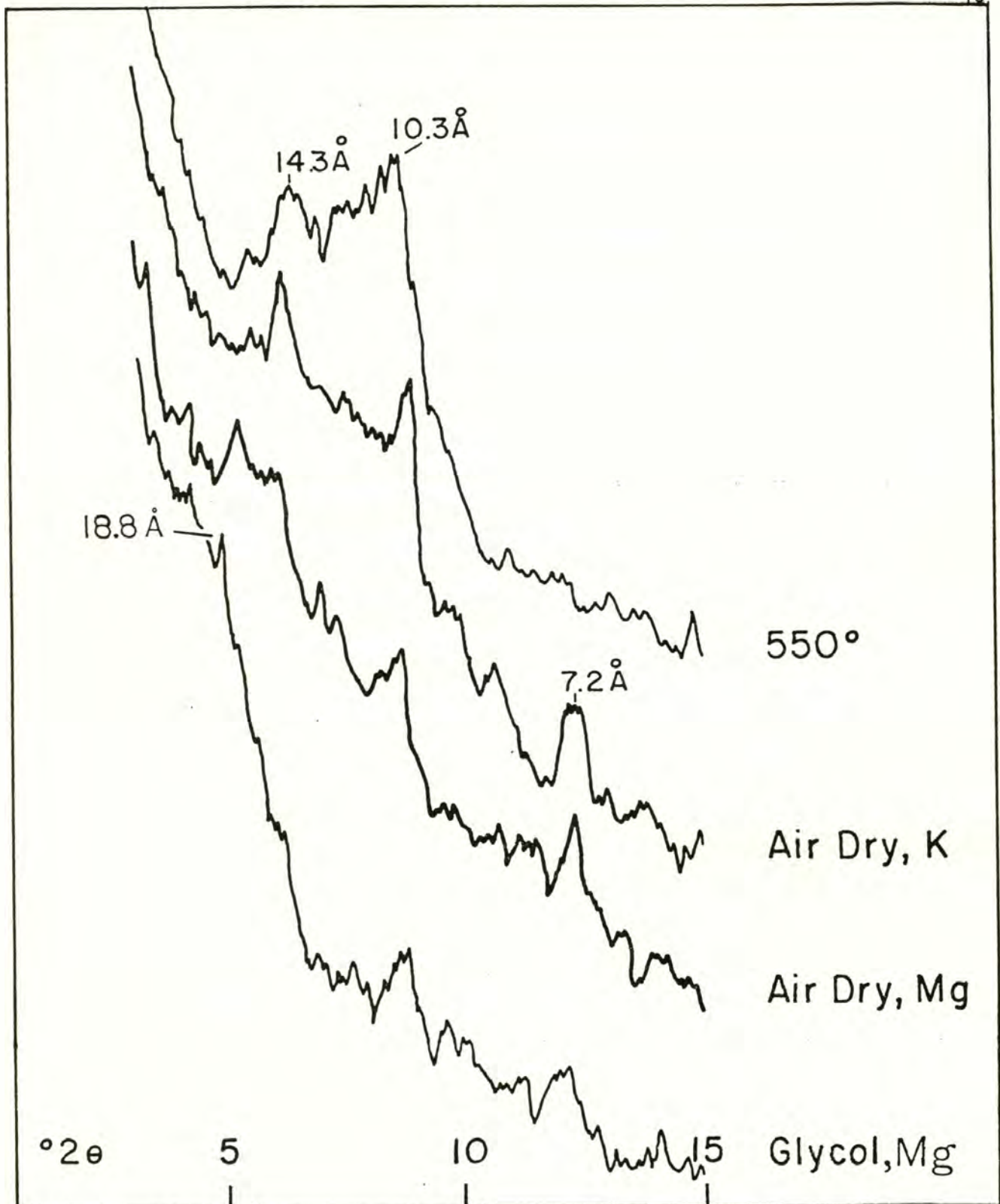


Figure 18: X-ray diffraction patterns for sample 9-14, from the K horizon in the oldest buried soil (#11) in roadcut #9. Clay minerals identified in this sample are: chlorite, mica, smectite, vermiculite, and mixed layer clays.

Minerals which produce the most intense peaks are considered to be major (M) components. Those which produce strong to moderate peaks, but which are about half as strong as the major (M) peaks, are considered to be minor (m) components. Minerals which produce barely discernible peaks on the x-ray pattern are considered to be present in trace (t) amounts.

Samples of relatively unweathered loess (3-15, 3-21, 4-3, 4-4, 4-6, 4-9, 5-2, 5-11, 5-12) all contain chlorite and mica. Expandable clays (smectite and vermiculite) are minor or trace constituents in 6 out of 9 (67%) of these samples and smectite is a major component in one sample. Mixed-layer clays (chlorite/smectite and/or chlorite/vermiculite) occur in 60% of the samples as trace components.

One sample (3-1) from the B horizon of the modern soil contains mica (biotite) as the major constituent, with minor chlorite and smectite and a trace amount of mixed-layer chlorite/expandable clay. The Ck horizon of the modern soil (sample 5-2) contains major mica (muscovite) and chlorite, with minor smectite and vermiculite, and trace mixed-layer chlorite/expandable clay.

Buried soils that consist of Ck horizons (stage I or II carbonate) contain predominantly chlorite and mica. Expandable clays, either smectite or vermiculite or both, are present in minor amounts in all of these soils. Mixed-layer clays are present as trace constituents in 75% of these samples.

Chlorite and mica are the major constituents of most K horizons. Smectite is a major component in 22% of these soils and is found as a minor or trace component in the rest. Vermiculite is less common; it is a major component of only one sample (5-7) but is found in 56% of the samples. Out of the four samples of K horizons which were treated with

DMSO, kaolinite was identified in three of them (14% of all K horizon samples). It was also identified from the air-dry XRD pattern of sample 3-7. These data suggest that kaolinite may be present in all of the samples but could not be identified with the treatments that were conducted.

In summary, chlorite and mica are the major constituents of the clay mineral assemblage of the loess at Washtucna. Expandable and mixed-layer clays are present as minor components, and kaolinite is present in small amounts in a few of the loess soils.

Origin of the Clay Minerals

Chlorite is abundant in almost all of the Washtucna samples, including both unweathered and highly weathered loess; this indicates that chlorite has been inherited from the parent material rather than being pedogenic. Chlorite was found in the clay and very-fine sand fractions of the modern Ritzville soil (McCreery, 1954), although it was not the dominant clay mineral.

Micas, both muscovite and biotite, are also probably inherited from the parent material. They have been found to be a dominant component of the Palouse loess (McCreery, 1954; Krapf, 1978) and of some of the Ringold sediments (Moodie *et al.*, 1966).

Smectite is present in small amounts in the unweathered loess, is abundant in the B horizon of the modern soil and in some of the more strongly developed (K horizons) buried soils, and is a minor element in the less developed (Ck horizons) buried soils. The presence of smectite in the unweathered loess indicates that it is not entirely the result of weathering and/or soil development. The presence of smectite in

unweathered loess could be explained by either of the following: (1) it was formed from weathering of volcanic glass and other materials which were then redeposited and mixed with the loess, or (2) it was part of the original airfall ash (Pevear et al., 1982) which became mixed with the fresh loess in transport. The abundance of smectite in the modern soil is probably related to the fact that, in general, the upper meter of Palouse loess contains more volcanic glass than the underlying older loess (Lotspeich and Smith, 1953; Cunningham, 1964; McCreery, 1954). Smectite may also be inherited from the Ringold sediments, a main source of the loess, in which smectite (montmorillonite) has been found to be the dominant clay mineral in selected samples (Moodie et al., 1966).

Vermiculite can form from the weathering of chlorite (Smith, 1962; Johnson, 1964) or mica (Barshad, 1948) and is a common clay mineral in soils (Douglass, 1977). Mica is weathered to vermiculite in an environment which allows for oxidation of ferrous iron and leaching of the interlayer potassium ion. Oxidation of ferrous iron lowers the negative charge on the 2:1 mica layers so that potassium is lost as the interlayer cation. Magnesium replaces potassium as the interlayer cation, and H₂O molecules are attracted to fill the interlayer position (Bray, 1937; Jackson et al., 1952), thus forming vermiculite. Vermiculite forms from chlorite by hydration of the interlayer hydroxyl sheet (Droste and Tharin, 1958). Vermiculite is a minor component in most of the unweathered loess samples and moderately developed (Ck horizons) buried soils, but it is found in only trace amounts in many of the strongly developed (K horizons) buried soils.

Mixed-layer chlorite/smectite and chlorite/vermiculite are present in minor and trace amounts in most of the soil samples from Washtucna (Table 1). These mixed-layer clays are the result of weathering of chlorite and micas (Johnson, 1964; Senkayi *et al.*, 1981; Jackson, 1965).

The clay mineral assemblage which occurs in a particular soil is a function of the parent material, the climatic conditions under which the soil has formed, the chemical environment within the soil profile, and the amount of time during which soil development has taken place. If the mineralogy of the loess parent material can be assumed to be relatively uniform in the Washtucna soils, then differences in the clay mineral assemblage may be attributed to either differences in the length of time during which the soil formed or to differences in the type of weathering environment involved. Barshad (1966) studied the clay mineral assemblages in surface horizons of soils developed under different amounts of precipitation and found that montmorillonite is confined to areas with less than 40 inches of precipitation and is most abundant in areas with less than 10 inches. Vermiculite is found in areas with up to 60 inches of precipitation but is abundant in areas with between 40 and 60 inches of precipitation. The relative amounts of illite to vermiculite, and illite to smectite (montmorillonite) suggest that illite weathers to montmorillonite in areas with less than 10 inches of precipitation, whereas vermiculite forms from illite in zones with higher precipitation. Kaolinite was found to be the dominant clay mineral in areas with more than 20 inches of precipitation. Ismail (1969) found that smectite will form from biotite under neutral and alkaline conditions because the oxidation of ferrous iron causes a reduction in layer charge. Under acidic conditions the reduction of ferrous iron is balanced by a decrease in the octahedral

charge through the loss of iron and magnesium from octahedral sites; the result is that vermiculite forms.

Whether these data are applicable to the Palouse soils is debatable, but general inferences about paleoclimates can be attempted. The presence of kaolinite in four of the buried soils may be an indication of a more highly leaching environment due to higher precipitation in the past. However, only one sample contains kaolinite in a significant amount, and further sampling and DMSO treatments are needed to verify these findings. The presence of smectite in most of the buried soils indicates that the soil-forming environment may have been similar to that of the present, and precipitation may not have been substantially higher. Vermiculite, which is abundant in the modern soil (sample 3-1), is present in most of the buried soils in minor and trace amounts and may indicate that slightly less leaching occurred in the past than is occurring at present.

TEPHRA

Introduction

Tephra carried eastward by prevailing winds from volcanoes in the Cascades has blanketed the landscape of eastern Washington many times during the Quaternary. Layers of tephra are commonly visible in exposures of sediments on the Columbia Plateau and have been useful in working out the Quaternary stratigraphy of the region (Fryxell, 1965; Hammatt, 1976; Moody, 1977; Mullineaux et al., 1978). Three volcanoes have been identified as the sources of many of the tephra layers: Mount Mazama (Crater Lake) which erupted about 6,700 years ago, Glacier Peak, which erupted about 12,000 years ago, and Mount St. Helens, which has erupted at least 20 times in the last 40,000 years.

Source of Tephra

Ash from the eruption of Mt. Mazama forms a widespread, prominent deposit in alluvial terraces in eastern and southeastern Washington (Hammatt, 1976) and in altithermal loess (Fryxell, 1965). Mazama ash is also an important constituent of the modern soil in the Palouse loess, although it is rarely found as a distinct layer. Because of its widespread distribution, Mazama ash is important as a time stratigraphic horizon in archaeological and geological sites, as well as in dating palynological profiles. It is identified petrographically by phenocrysts of hornblende, augite and hypersthene in the heavy mineral fraction and by the modal refractive index and chemical composition of the glass (Wilcox, 1965; Kittleman, 1973; Smith et al., 1977b).

Glacier Peak tephra has been found in floodplain deposits overlying sediments of the last major Scabland flood (Moody, 1977) and in loess overlying recessional glacial deposits near the mouth of the Okanogan Valley (Porter, 1978). It has also been found in Creston Bog, in the northeastern Scablands (Smith et al., 1977a). Two major layers of Glacier Peak tephra have been distinguished on the basis of glass chemistry (Porter, 1978; Smith et al., 1977a). The older tephra, which was deposited in a northeast lobe across Washington into Idaho and Alberta, is dated at about 12,750 years before present (B.P.) (Lemke et al., 1975). The younger layer, which was deposited in an easterly direction across Washington, Idaho, and into Montana and Wyoming, is dated at about 11,250 years B.P. (Mehring et al., 1977).

Mount St. Helens is the source of at least eight layers of tephra as old as 37,000 years found on the Columbia Plateau. Tephra Set C, between 30,000 and 37,600 years old (Mullineaux et al., 1978), has been identified in Pleistocene alluvium underlying Scabland flood deposits in the Snake River Canyon (Hammatt et al., 1976). Tephra Set S is found in slack water sediments associated with the last major Scabland flood and has been dated at about 13,000 years B.P. (Mullineaux et al., 1978). Set J, 8,000 to 11,000 years old (Hyde, 1975), has been identified in alluvium overlying Scabland flood sediments at Lind Coulee (Moody, 1978). The younger sets, Y, W, and T have also been identified in Holocene deposits on the Columbia Plateau (Smith et al., 1975, 1977b).

In addition to deposits correlated with dated tephra near the source volcanoes, many unidentified tephra layers in loess roadcuts throughout the Palouse region are found beneath well-developed paleosols suggesting that these tephra may be older than any of the identified tephra. The

Washtucna roadcuts contain several unidentified tephra layers.

This investigation of the stratigraphy at Washtucna began in 1976 when I sampled the prominent tephra layers to see if any of them could be correlated with known sources. Twenty-six layers were sampled from seven roadcuts at that time. Additional field work by Henry W. Smith of the Agronomy and Soils Department, Washington State University, in 1977 and by me in 1979 revealed tephra which had not been sampled previously.

Tephra Analysis

Sample preparation and petrographic examinations were conducted by Rose Okazaki of the Agronomy and Soils Department, Washington State University, except for samples 9L, 9M, and 5D, which were cleaned and examined petrographically by me. Electron microprobe analyses were conducted by Okazaki and Knowles, following the method described in Smith et al. (1977b). The data were compiled by Smith and Okazaki, and correlations with source tephra were made where possible. They have generously allowed me to use these unpublished data for interpreting the loess stratigraphy in the Washtucna area.

The Washtucna Tephra

Twenty-four tephra layers were collected from the four roadcuts described in this report. Tephra layers are given letter designations which have no stratigraphic significance. The tephra layers are noted in the soil descriptions (Appendix) only if they crop out at the location where the description was made. Since they are discontinuous (Figs. 3 to 7), the tephra layers were not always visible in the section des-

cribed. Their relative stratigraphic positions are illustrated in Figure 19.

Descriptions of the tephras in the Washtucna roadcuts proceed from youngest to oldest since the age and source of younger tephras can be identified and thus form a reference point for comparison with the older tephras.

The youngest tephra in the Washtucna exposures is correlated petrographically and chemically with tephra from the eruption of Mount Mazama on the basis of its phenocryst suite (Tables 2, 3), refractive index of the glass (Fig. 20) and glass composition (Table 4). It was found mixed with loess at the west end of roadcut #9 (layer 9A) (Fig. 6). A thick (20 cm) deposit of Mazama tephra was observed in roadcut #1 (Fig. 2), where it fills a small channel in Scabland flood gravel.

Roadcuts #4 and #5 (Figs. 4 and 5) are adjacent to each other and contain a sequence of four buried soils and four tephra layers. The youngest tephras in these roadcuts (4A and 5A) contain green hornblende, cummingtonite, and magnetite as the dominant ferromagnesian phenocrysts. One weathered flake of biotite found in a sample of tephra 4A (Table 3) may be a contaminant from an older tephra layer. Layer 5A also contains sparse amounts of orthopyroxene. The phenocryst suite is similar to tephra from Sets S and M of Mt. St. Helens. When plotted on a Ca:K:Fe ternary diagram for the glass (Fig. 21), samples 4A and 5A fall within the range for these tephra sets. Sets S and M are not distinguishable by glass chemistry (Table 5), so samples 4A and 5A may be correlated with either. Since Set S has been identified elsewhere on the Columbia Plateau, especially to the west (upwind) from Washtucna, it is a more likely candidate than Set M for correlation, so a correlation with Set S will

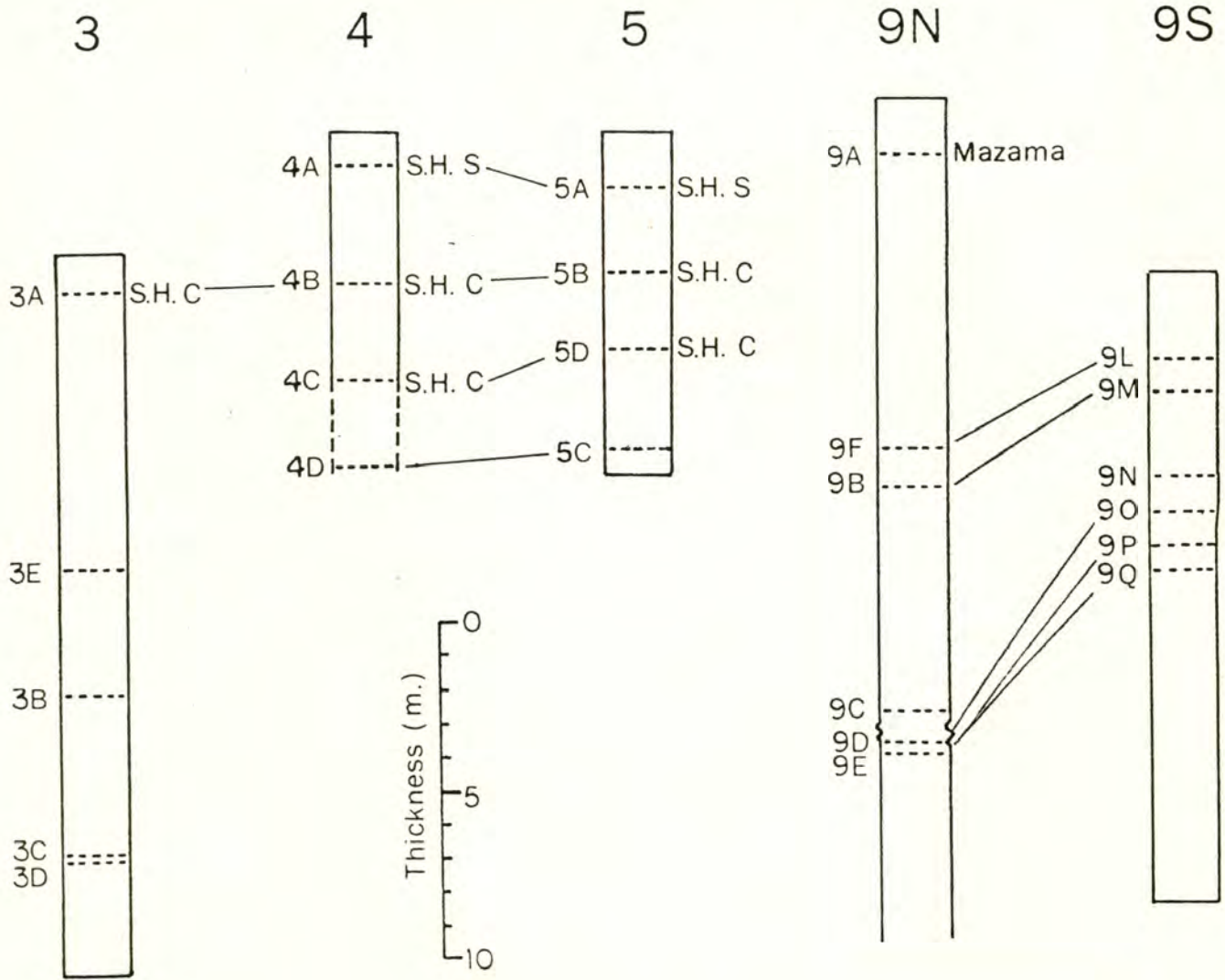


Figure 19: Correlation of tephra layers in the Washtucna roadcuts

TABLE 3. Petrographic data for Washtucna tephra samples.

Sample #	FeMg Phenocrysts						mag/ ilmen
	hornblende green	brown	cummingtonite	opx	cpx	biotite	
3A	x		x			x	x
3E	x			x	x		x
3B	x	x		x	x		x
3C	x	x		x			x
3D	x	x		x		P	x
4A	x		x			P	x
4B	x		x	x		P	x
4C	x		x			x	x
4D	x		x				x
5A	x		x	x			x
5B	x		x			P	x
5C	x		x				
5D	x		x				x
9A		x		x	x		x
9F	x		x	x			x
9B	x		x			P	x
9C	x	x			x		x
9D	x	x		x		P	x
9E	x			x	x		x
9L*	x		x	x			x
9M	x		x				x
9N*	x					P	x
90*	mostly glass						
9P	x	x		x			
9Q	x	x		x			x

x = present

P = biotite present, but with no adhering glass (see discussion, p.)

* = poor sample, mostly detrital grains or glass

opx = orthopyroxene; cpx = clinopyroxene; mag = magnetite; ilmen = ilmenite

TABLE 2. Correlation of Washtucna tephra layers with tephra of known source and age.

<u>Field Designation of Tephra Layer</u>	<u>Source</u>	<u>Tephra Set</u>	<u>Correlative Layers</u>	<u>Age (yrs. B.P.)</u>
Roadcut #3:				
3A	Mt. St. Helens	C	4B, 5B	30-37,600*
3E	Unknown			>730,000
3B	Unknown			>730,000
3C	Unknown			>730,000
3D	Unknown			>730,000
Roadcut #4:				
4A	Mt. St. Helens	S(M?)	5A	13,000*
4B	Mt. St. Helens	C	3A,5B	30-37,600*
4C	Mt. St. Helens	C	5D	30-37,600*
4D	Unknown		5C	~50-100,000?
Roadcut #5:				
5A	Mt. St. Helens	S(M?)	4A	13,000*
5B	Mt. St. Helens	C	3A,4B	30-37,600*
5D	Mt. St. Helens	C	4C	30-37,600*
5C	Unknown		4D, (Okanogan Centre?) ²	~50-100,000?
Roadcut #9 North:				
9A	Mt. Mazama			6,700 ¹
9F	Unknown		9L	>6,700
9B	Unknown		9M	>6,700
9C	Unknown			
9D	Unknown		9O	>6,700
9E	Unknown		9P or 9Q	>6,700
Roadcut #9 South:				
9L	Unknown		9F	>6,700
9M	Unknown		9B	>6,700
9N	Unknown			>6,700
9O	Unknown		9D	>6,700
9P	Unknown		9E?	>6,700
9Q	Unknown		9E?	>6,700

* from Mullineaux *et al.* (1978)

¹ from Mehringer *et al.* (1977)

² from Westgate and Fulton (1975)

FIGURE 20. Refractive indices of glass from the Washtucna tephra 59 samples.

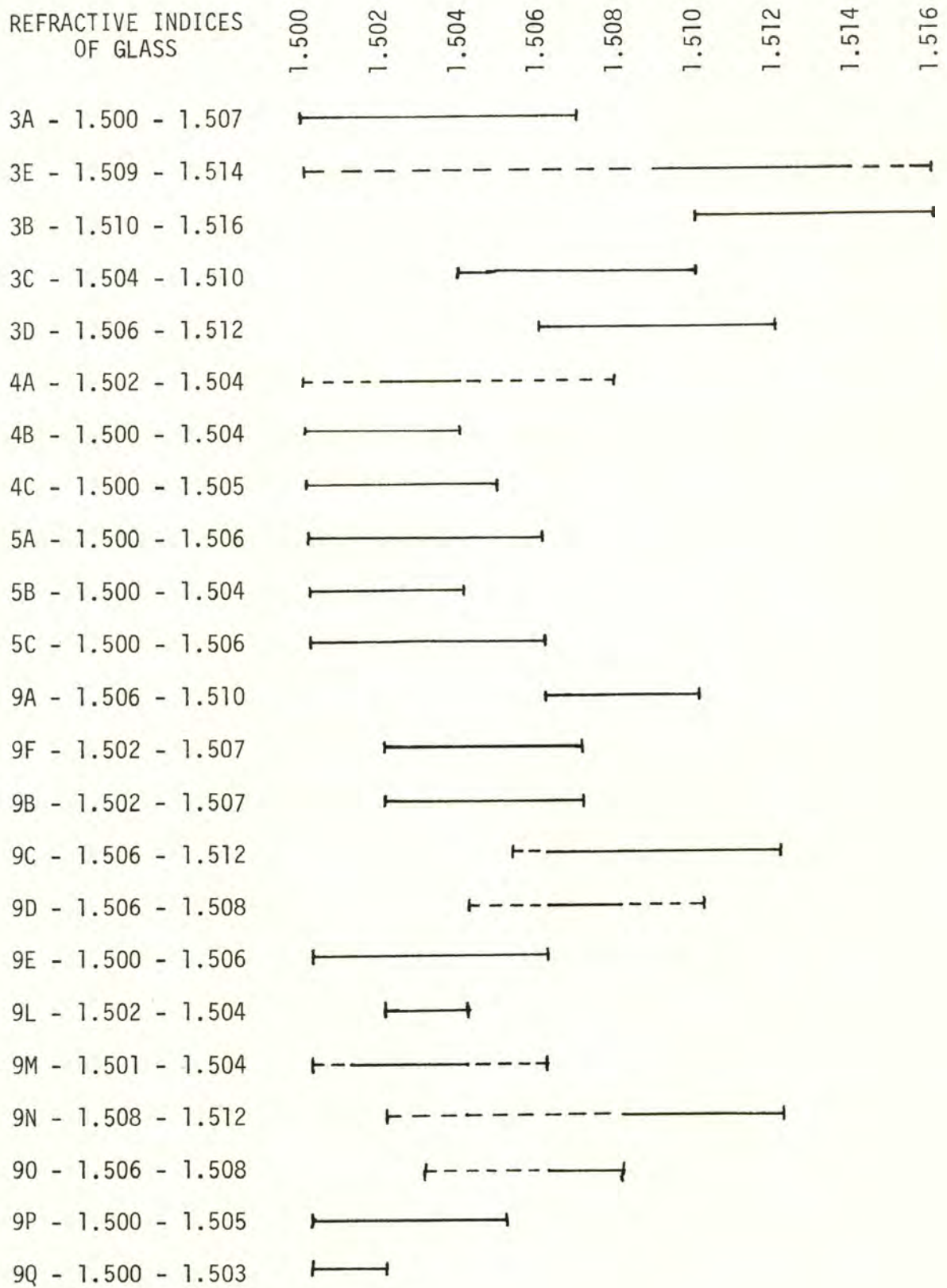


TABLE 4. Electron microprobe data for glass from Washtucna tephra samples.¹

Sample #	% Ca	%K	% Fe	% Ca +	%K +	% Fe = 100
3A	1.20	1.74	0.66	33.3	48.3	18.3
3E ²	1.53	1.57	1.88	44.1	25.4	30.5
			2.79	38.4	22.2	39.4
3B	1.53	1.82	1.78	29.7	35.5	34.8
3C	1.24	1.85	1.39	27.7	41.3	31.0
3D	1.86	1.41	1.81	36.6	27.8	35.6
4A	1.18	1.71	0.96	30.6	44.4	24.9
4B	1.16	1.77	0.72	31.8	48.5	19.7
4C	1.21	1.82	0.67	32.7	49.2	18.1
4D	1.22	1.80	0.78	32.1	47.4	20.5
5A	1.16	1.75	0.93	30.2	45.6	24.2
5B	1.18	1.85	0.73	31.4	49.2	19.4
5D	n.d.					
5C	1.34	1.80	0.81	33.9	45.6	20.5
9A	1.10	2.16	1.50	23.1	45.4	31.5
9F	1.08	1.99	0.70	28.6	52.8	18.6
9B	1.39	1.64	0.92	35.2	44.2	29.6
9C	1.39	2.34	1.57	26.2	44.2	29.6
9D	0.69	2.40	1.60	14.7	51.2	34.1
9E	0.69	2.82	1.08	15.0	61.5	23.5
9L	n.d.					
9M	n.d.					
9N	1.32	2.54	1.46	24.8	47.7	27.4
9O	0.65	2.39	1.68	13.8	50.6	35.6
9P	0.63	2.88	0.98	14.0	64.1	21.8
9Q	0.54	2.78	0.95	12.6	65.1	22.2

¹The data were collected on an ARL-EMX microprobe at the Idaho Bureau of Mines and Geology, and are relative to obsidian standard U of A 5831 (Smith and Westgate, 1969).

²Sample 3E contains two glass components.

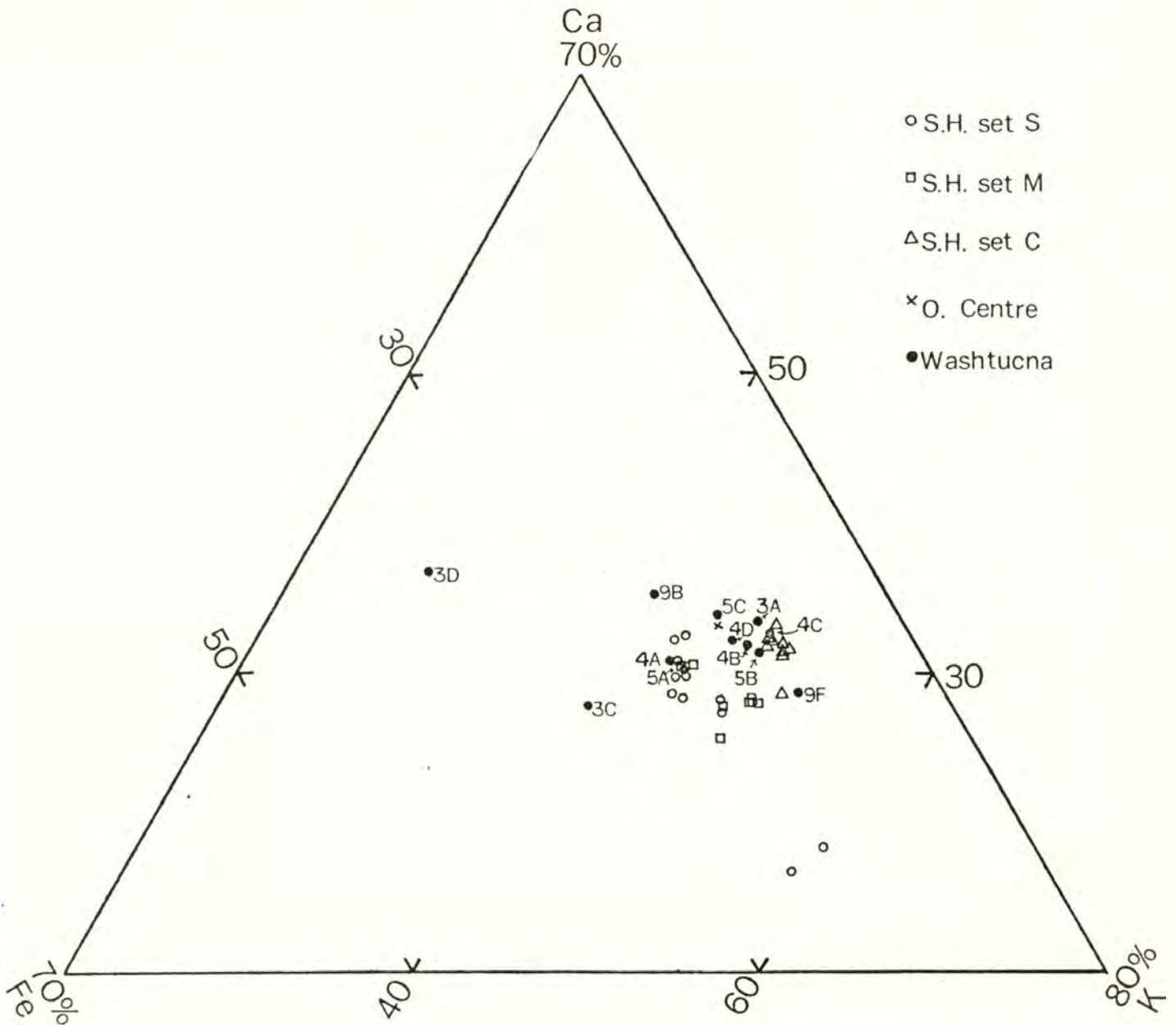


Figure 21: Graph of Ca:K:Fe ratios (total=100%) in glass shards from cummingtonite bearing tephra from Washtucna, and from reference samples of Mount St. Helens tephra Sets S, M, and C, and from the Okanogan Centre tephra (Westgate and Fulton, 1975). Data are presented in Tables 4 and 5.

TABLE 5. Electron microprobe data for reference samples of Mount St. Helens tephra sets S, M, and C.*

Tephra	Sample Source	Sample #	% Ca	%K	% Fe	% Ca + %K + % Fe = 100		
So	1	3-12-71-3	0.95	1.72	0.82	27.2	49.3	23.5
So	2		0.98	1.69	0.81	28.2	48.6	23.3
Sg	1	8-12-71-4	1.04	1.66	0.93	28.6	45.7	25.6
Sg	2		1.05	1.73	0.93	28.3	46.6	25.1
S	1	8-12-71-5	1.06	1.62	0.86	29.9	45.8	24.3
S	2		1.05	1.60	0.88	29.7	45.3	24.9
S	1	8-12-71-6	0.59	1.92	0.72	18.3	59.4	22.3
S	2		0.55	1.95	0.83	16.5	58.6	24.9
S	1	8-12-71-7	1.14	1.56	0.85	32.1	43.9	23.9
			1.08			30.9	44.7	24.4
S	2		1.14	1.56	0.81	32.5	44.4	23.1
M	1	8-12-71-9	1.02	1.80	0.87	27.6	48.8	23.6
M	1	8-12-71-10	1.01	1.82	0.78	28.0	50.4	21.6
M	1	8-12-71-11	0.93	1.82	0.09	25.5	49.9	24.6
M	1	8-12-71-12	1.01	1.84	0.77	27.9	50.8	21.3
M	1	8-12-71-13	1.16	1.76	0.93	30.1	45.7	24.2
M	1	8-12-71-14	1.14	1.71	0.88	30.6	45.8	23.6
Cy	1	8-12-71-15	1.00	1.82	0.68	28.6	52.0	19.4
C	1	8-12-71-16	1.13	1.85	0.67	31.0	50.7	18.4
C	1	8-12-71-17	1.15	1.85	0.65	31.5	50.7	17.8
C	1	8-12-71-18	1.15	1.80	0.68	31.7	49.6	18.7
Cw	1	8-12-71-19	1.09	1.72	0.61	31.9	50.3	17.8
C1	3		1.14	1.76	0.65	32.1	49.6	18.3
C2	3		1.13	1.83	0.64	31.4	50.8	17.8
C3	3		1.15	1.77	0.66	32.1	49.4	18.4
C4	3		1.13	1.68	0.60	33.1	49.3	17.6

*The data were collected on an ARL-EMX microprobe at the Idaho Bureau of Mines and Geology and are relative to obsidian standard U of A 5831 (Smith and Westgate, 1969).

- 1 - Samples collected by D. R. Mullineaux and analyzed by Okazaki and Knowles.
- 2 - Samples collected by D. R. Mullineaux and analyzed by Moody (1978).
- 3 - Samples collected by Smith, Fryxell, and Moody and analyzed by Okazaki and Knowles.

be used for stratigraphic interpretation. Set S is about 13,000 years old and Set M is 18,000-20,000 years old (Mullineaux et al., 1978).

Set C, which is greater than 30,000 years old (Mullineaux et al., 1978), is distinguished from Sets M and S near their source by the presence of biotite. However, biotite crystals tend to break along the 001 cleavage plane in transport and to separate from the enclosing glass. For this reason, glass-encased biotite is sparse in downwind samples of Set C. Distinguishing detrital biotite from pyroclastic biotite is not possible in the Washtucna samples without glass attached to the crystal.

Tephra layer 3A, the youngest tephra in roadcut #3 (Fig. 3) is correlated with Mt. St. Helens Set C (Table 2) by glass composition (Tables 4 and 5), phenocryst suite, and glass-encased biotite (Table 3). It is recognizable in the field by its relatively coarse texture.

Layers 4B and 5B have similar composition to layer 3A (Table 4), are in a comparable stratigraphic position (Figs. 10 and 11), and also appear relatively coarse. They contain green hornblende, cummingtonite, and biotite, although the origin of the biotite is questionable. They are separated from layers 4A and 5A by one buried soil (Figs. 10 and 11) which is 1.0 to 1.5 meters thick. Layers 4B and 5B are also correlated with Set C.

Tephra layers 4C and 5D occur in small pockets within buried soil 3 in roadcuts #4 and #5 (Figs. 10 and 11). They also contain green hornblende and cummingtonite. Glass-encased biotite was found in a sample of layer 4C. Microprobe data are available only for layer 4C, and the data compare favorably with reference samples for Set C (Table 4, Fig. 21). These two tephras (4C and 5D) are therefore correlated with Mt. St. Helens Set C (Table 2).

Layer 5C is clearly visible in pockets near the base of roadcut #5 (Fig. 5) where it is 2.5 cm thick. It contains green hornblende and cummingtonite phenocrysts (Table 3). The glass chemistry (Table 4) is unlike that of any identified tephra from the Cascades, although the proportion of Ca:K:Fe plots in the general vicinity of Mt. St. Helens tephra Set C (Fig. 21, Table 5). The amount of these elements in the glass is similar to that in the Okanogan Centre tephra (Fig. 21) found in southwestern British Columbia by Westgate and Fulton (1975). Unfortunately, the age of the Okanogan Centre tephra is unknown, although the sediments which contain the tephra are thought to date from the Olympia interval between the last two glaciations (Westgate and Fulton, 1975). The stratigraphic equivalent of layer 5C is not visible in roadcut #4, but was discovered by Smith in an auger hole 2.2 meters below the base of the roadcut (Fig. 19); it was designated layer 4D. The petrographic (Table 3) and chemical (Table 4) data support correlation of layers 4D and 5C, although no source can be identified.

The age of tephras 4D and 5C can be approximated from their stratigraphic position relative to the older Mt. St. Helens Set C tephra; they are separated from it by about 3 meters of loess containing one buried soil. This soil (buried soil 4) could have formed in approximately 10,000 years if conditions were similar to the interval when buried soil 3 developed and if the rate of loess deposition was constant. A rough estimate for the age of the tephra layer at the base of the roadcut then is 50,000-100,000 years.

Roadcut #3 contains five tephra layers (from youngest to oldest, 3A, 3E, 3B, 3C, 3D). The youngest layer, 3A, is correlated with Set C from Mt. St. Helens (Table 2), which is older than 30,000 years (Mullineaux

et al., 1978). The four older tephra layers must be at least 730,000 years old, since they are older than the Brunhes Normal-Matuyama Reversed polarity boundary which has been located in this section (see Paleomagnetism section). No correlative tephra layers have been found in other exposures, and no source has been identified. Fission track dating of layers 3B and 3D was attempted, but no zircons were present in the samples and the glass shards are too fine to allow analysis (N. Briggs, 1982, oral communication).

These four old tephra layers contain phenocrysts of hornblende and orthopyroxene (Table 3). Tephra 3E and 3B also contain clinopyroxene, while layers 3C and 3D contain sparse cummingtonite. The refractive indices of glass in these tephra tend to be higher than in Mt. St. Helens tephra (Fig. 20). The Ca:K:Fe percentages are distinct for each (Figs. 21 and 22).

Roadcut #9 consists of exposures on both sides of the road. On the north side, six layers of tephra were identified (9A, 9F, 9B, 9C, 9D, and 9E). The south roadcut also contains six tephra layers (9L, 9M, 9N, 9O, 9P, 9Q). Correlations between the north and south sides of the road are presented in Figure 19. The correlations of 9F with 9L and 9B with 9M are based on stratigraphic position and petrographic characteristics. In the north roadcut, a group of three thin tephra layers occurs in one stratigraphic unit, while in the south roadcut, four thin layers are found within this same unit. Microprobe data suggest the correlation of 9D with 9O and the correlation of 9E with either 9P or 9Q.

Izett (1981) mentions four dacitic tephra interpreted to be roughly 1.5 million years old found in the Pleistocene Bruneau Formation and the Tuana Gravel in Idaho, and suggests that they may be from a source in the

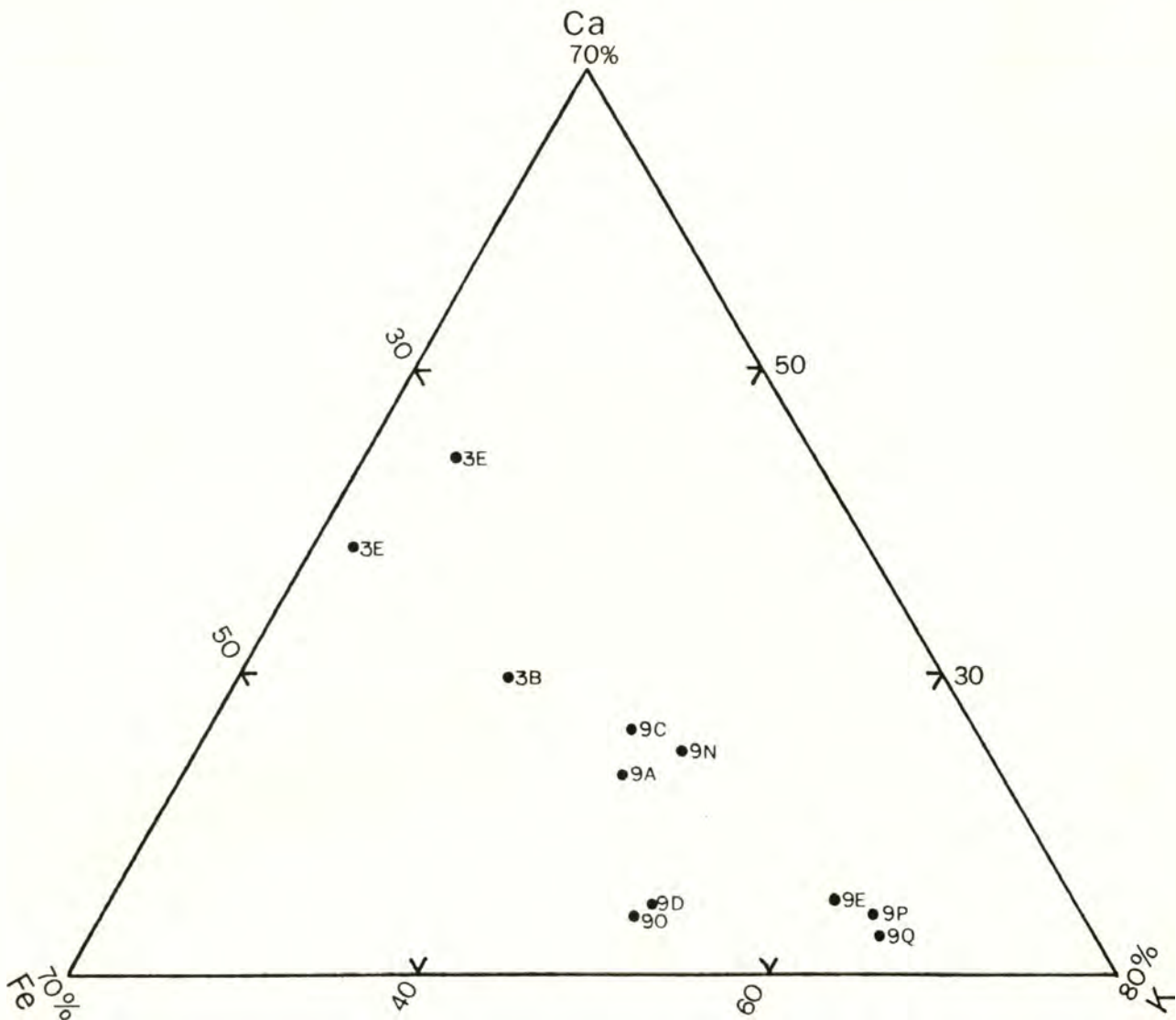


Figure 22: Graph of Ca:K:Fe ratios (total=100%) in glass shards from non-cummingtonite bearing layers from Washtucna. Sample 3E is plotted twice since it contains two glass components. Data are presented in Table 4.

Cascades. Comparison of chemical and petrographic data for older Pleistocene tephras such as these may allow correlations with the older Washtucna tephras in the future. Tephra layers approximately .8 million years old in the Puget Lowland (Easterbrook et al., 1981) may also be correlative with the older unidentified Washtucna tephras.

PALEOMAGNETISM

Paleomagnetism has been used extensively as a chronological tool for Pleistocene terrestrial sediments. The principle underlying the use of paleomagnetism for dating Quaternary rocks and sediments is that the earth's polarity that existed when these materials were magnetized is usually preserved in them. Normal and reversed polarities, and the transitions which separate them, are recorded in lavas and sediments which have been dated radiometrically and can be used for stratigraphic correlation over the entire earth. The geomagnetic polarity time scale (Cox, 1969; Cox et al., 1968; Mankinen and Dalrymple, 1979), which is a compilation of these dated sequences, can be used to correlate stratigraphic sequences for which radiometric dates are not available. The most recent major polarity change, known as the Brunhes Normal-Matuyama Reversed boundary, occurred approximately 730,000 years (Mankinen and Dalrymple, 1979), but may be as old as 790,000 years (Johnson, 1982).

Most of the paleomagnetic studies of Quaternary loess deposits have been conducted in Europe for the purpose of correlating glacial sequences. Some of these data are presented in the reports of the International Geological Correlation Program (Koci, 1974; Bucha et al., 1975, 1978; Hus et al., 1976; Koci and Sibrava, 1976; Fink et al., 1978) as well as in other journals (Fink and Kukla, 1977; Kukla and Koci, 1972; Kukla, 1975; Koci and Sibrava, 1976). ^{MISSING} Tcholka (1976) investigated the remanent magnetization of loess and found that magnetite and hematite were the predominant minerals to retain a remanence.

Magnetostratigraphic work on loess has been less extensive in North America. In the Pacific Northwest, paleomagnetism has been used to work

out the glacial history of the Puget Lowland (Easterbrook, 1973, 1974, 1976a, 1977a; Easterbrook and Briggs, 1979; Easterbrook and Othberg, 1973; Easterbrook et al., 1981). Packer (1979) and Kukla and Opdyke (1980) have identified the Brunhes-Matuyama boundary in loess sections in central and eastern Washington. The mechanics of acquisition of remanent magnetization are reasonably well understood for fine-grained waterlain sediments (Benedict, 1943; Nagata, 1962, 1962; King and Rees, 1966; Verosub, 1977; Henshaw and Merrill, 1979). Silt and clay sized grains of magnetite and hematite that have been magnetized previously are subjected to torque exerted by the earth's magnetic field while they are settling in a fluid. These grains tend to become aligned with the ambient magnetic field direction, yielding a depositional remanent magnetization (DRM). Disturbance of the sediment after deposition may re-align the grains, resulting in post-depositional remanent magnetization (PDRM) (Irving and Major, 1964; Verosub, 1977).

Eolian sediments also acquire a remanent magnetization, as demonstrated by the magnetostratigraphic work on Pleistocene loess mentioned above, but the mechanism of acquisition is poorly understood. Steele (1981), in a study of tephra from the 1980 eruption of Mt. St. Helens, found that subaerially deposited ash records the true magnetic field direction.

Since the age of the Palouse loess is poorly known, a magnetostratigraphic study was undertaken in the hope that magnetic polarity changes could be delineated to reveal dateable horizons such as the Brunhes-Matuyama boundary. Washtucna roadcut #3 (Fig. 2) was chosen for paleomagnetic study because its sequence of eleven buried soils indicated that the section might possibly be older than 730,000 years, and because of the possibility of obtaining fission track dates from tephra layers 3B and 3D

(Fig. 9). Tephra layer 3A, near the top of the section (Fig. 9), provides some chronologic control, since it is correlated with Mt. St. Helens tephra Set C (Table 2) which is about 30,000-40,000 years old.

Sampling Procedure

Four stratigraphic sections were sampled at roadcut #3 (Fig. 3). Twenty-five pairs of samples were taken at 90 meters west in vertical spacings of .2 to 1.5 meters, dictated by the degree of cementation (more indurated sediments being more difficult to sample). Paired samples were collected to determine variability in the stability and magnetic direction within a stratigraphic horizon. The youngest (highest) sample pair was collected just below the third buried soil (Fig. 9), 1.5 meters below the surface, and the lowest pair just above the tenth buried soil, 14.35 meters below the surface. Fifteen pairs were collected in a column at 130 meters west (Fig. 3), 40 meters away from and parallel to the first section, to see if the data were replicable. The sample pairs at 130 meters west are more widely spaced and extend to a depth of 19.1 meters. In order to extend the sampling to the oldest part of the section, three pairs were sampled at 180 meters west (Fig. 3). After the approximate location of a polarity transition zone was established, nine closely-spaced pairs were collected from its vicinity in the column at 90 meters west (samples 26 to 34) as well as three pairs from 98 meters west.

The paleomagnetic samples were obtained by cutting into the face of the exposure to remove any disturbed material on the surface. Plastic vials, 4.5 cm long and 2.5 cm in diameter, were driven into the loess, oriented with a Brunton compass, and removed. The vials and contents were cut to a length of 2.5 cm and any loose sediment was removed. The

open ends of the cylinders were sealed with paraffin, yielding a sample with a volume of approximately 7 cubic cm. Visual inspection showed little or no disturbance of the sediment within the vials.

Magnetic Cleaning and Measurements

The magnetization of each sample was measured with a Schonstedt Spinner Magnetometer, model SSMI-A. Secondary components of magnetization with low coercivity were cleaned by alternating field (AF) demagnetization in a Schonstedt model GSD-5, AC, tumbling demagnetizer. The demagnetization program was tailored to each sample, depending on its directional stability and intensity. Most demagnetizations were carried out in steps of 100 oersteds (oe), up to a maximum of 800 oe, at which point the magnetization of most of the samples was randomized.

The stable end point obtained at the demagnetization level that fully removed the low coercivity component with minimum effect on the high coercivity component was determined subjectively from computerized orthogonal projections of the magnetization vectors (Zijderveld, 1967). Assessment of the integrity of the magnetization was also made individually by calculating the angular standard deviation of individual measurements on the spinner using the method of Harrison (1980), and by comparing the directions of paired specimens.

Results

The high coercivity (primary) direction of magnetization of each sample is presented in Table 6 with the demagnetization level that was required to remove the secondary components of magnetization. These directions are plotted against depth in Figures 23 and 24. The reliability

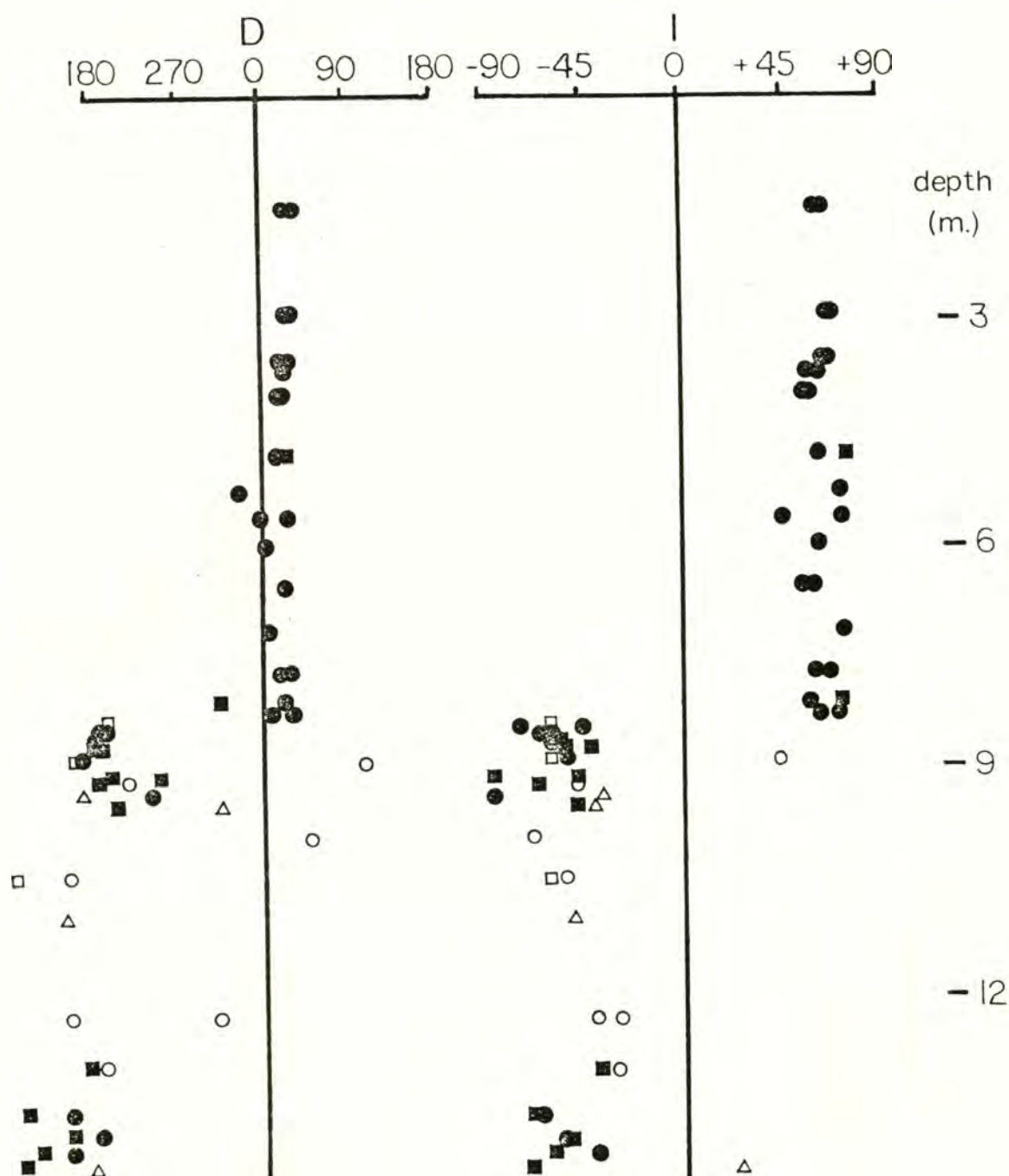


Figure 23: Graph of paleomagnetic direction versus depth for samples from roadcut #3, at 90 meters west of the datum, at selected demagnetization levels. Each pair of samples is represented by two points plotted at the same depth below surface. In some cases the points are plotted on top of each other, and in some only one sample was available. The reliability of each sample is denoted by angular standard deviation after Harrison (1980): ● = 0-5, ■ = 6-10, ○ = 11-15, □ = 16-20, △ = >20. These data are listed in Table 6.

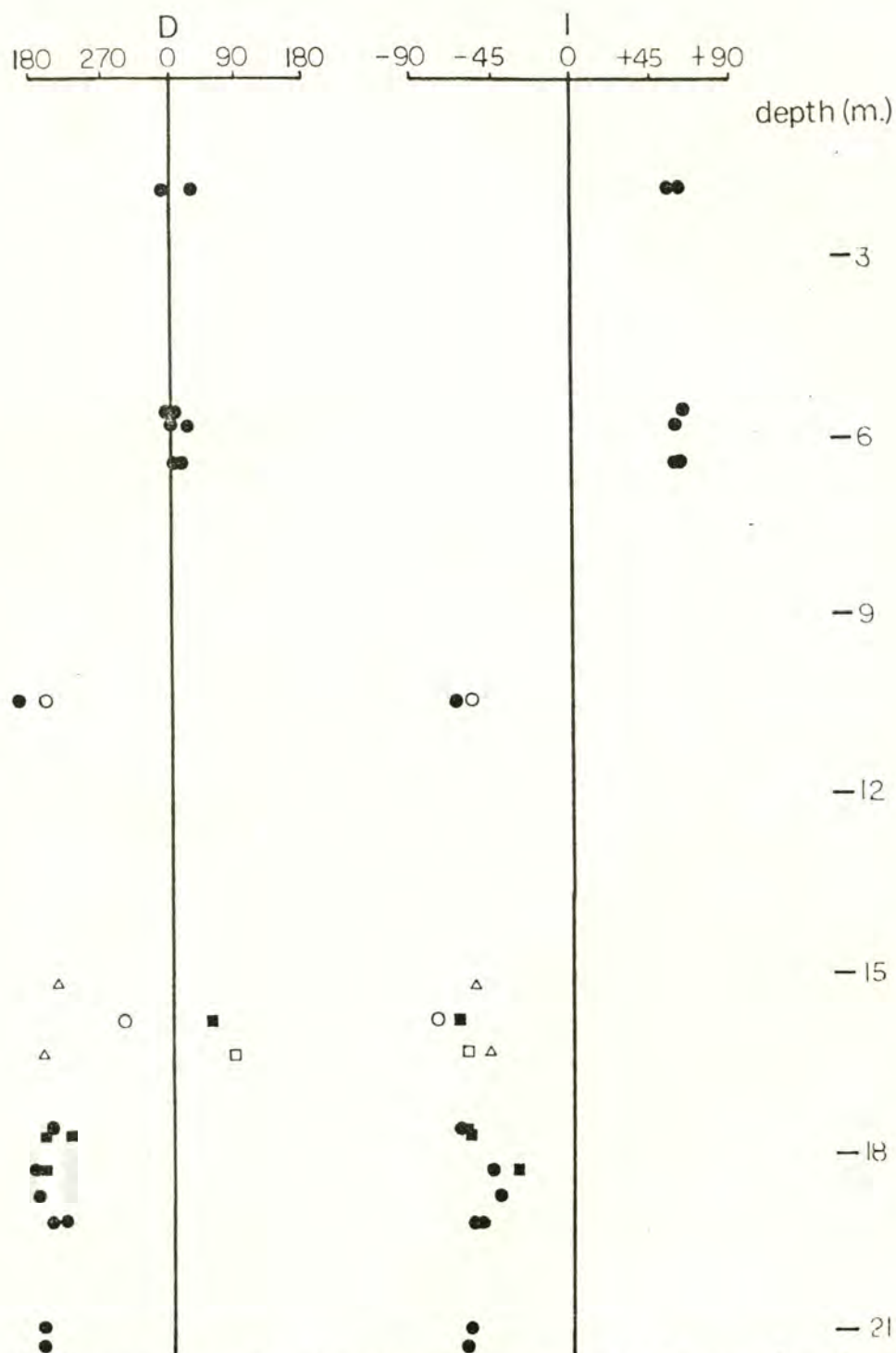


Figure 24: Graph of paleomagnetic direction versus depth for samples from roadcut #3, at 130 and 180 meters west of the datum, at selected demagnetization levels. Each pair of samples is represented by two points plotted at the same depth below surface. In some cases the points are plotted on top of each other, and in some only one sample was available. The reliability of each sample is denoted by angular standard deviation after Harrison (1980): ● = 0-5, ■ = 6-10, ○ = 11-15, □ = 16-20, △ = >20. These data are listed in Table 6.

of each sample's direction was evaluated by the angular standard deviations for the measurements, and this information is presented in Table 6 and Figures 23 and 24. The mean direction for each pair of samples from all four sections is plotted against depth in Figure 25 and the data are listed in Table 7.

Samples from the upper 8.3 meters of roadcut #3 are normally magnetized, while those below 8.3 meters have a reversed magnetization. The transition from normal to reversed magnetization takes place within a 10 cm vertical interval in section #3. The closely spaced samples (90-26 to 33, Fig. 25), thought to traverse the transition zone, turned out to be wholly in the reversed part of the section.

The samples with normal magnetization appear to have one stable component of magnetization which approximates the present magnetic field direction ($D = 20^{\circ}$, $I = +69^{\circ}$). Most of the samples were demagnetized to 500 oe, but the few that were demagnetized to 800 oe retained their stability with angular standard deviations (ASD) of 8° or less. The excellent stability of the normal samples is illustrated in Figure 26 which is a Zijderveld plot showing the change in direction and intensity of sample 90-01-02 with each step of demagnetization. The direction of magnetization changes very little, while the intensity decreases with each demagnetization step, indicating most likely a stable magnetization. The low discrepancy in direction within each pair of samples is visible graphically in Figures 23 and 24.

The samples showing reversed magnetization have an overprint of secondary magnetization in a normal direction as shown in Figure 27. The reversed samples were much less stable than the normal ones, have lower intensities (Table 6), and show more variation within the pairs.

TABLE 6. Magnetic directions for samples from roadcut #3 at selected demagnetization levels.

Sample #	Demagnetization (oe) ¹	D	I	A.S.D. ²	Intensity ³ ($\times 10^{-5}$)
90-01-01	150	34.1	+57.3	1	4.31
01-02	300	25.3	+60.9	3	3.78
04-01	150	31.0	+58.2	4	2.47
04-02	200	28.2	+67.4	4	2.21
02-01	200	24.4	+61.4	2	3.89
02-02	200	22.3	+63.6	3	3.17
03-01	200	25.9	+60.2	4	3.95
03-02	600	24.6	+55.5	1	2.69
05-01	200	19.5	+53.5	3	3.15
05-02	400	14.0	+59.1	3	3.59
06-01	150	25.5	+73.5	9	0.94
06-02	200,300	15.7	+60.1	3	4.84
07-01	sample discarded				
07-02	200	338.5	+67.5	4	2.23
08-01	150	27.8	+70.5	3	0.92
08-02	300,400	2.1	+43.8	3	1.48
09-02	200,300	6.6	+59.6	2	1.83
10-01	400	17.5	+56.9	3	3.71
10-02	100	17.8	+53.1	2	8.18
11-01	300	7.3	+70.2	2	1.86
11-02	300	8.0	+70.0	3	2.63
12-01	150	20.3	+59.3	4	0.56
12-02	100	30.8	+64.1	5	0.84
13-01	200	317.4	+69.8	8	0.35
13-02	200	26.2	+56.7	2	3.72
14-01	200	13.2	+68.5	3	3.11
14-02	100,200,300,400	36.6	+60.6	3-5	2.07
26-01	200	191.3	-75.3	3	1.13
26-02	100,200	198.5	-59.8	13-17	0.99
27-01	300	193.7	-45.6	3	1.01
27-02	100,200,300	199.0	-73.7	3	1.30
28-01	200,300,400	189.4	-57.4	3-6	2.54
28-02	100,200,300	181.8	-63.3	3-4	2.01
29-01	100,200,300,400	181.9	-59.4	4-6	1.04
29-02	100,200,400	175.9	-54.2	6-7	1.63
30-01	300,400	177.4	-53.5	5-7	0.12
30-02	200,300,400	190.8	-41.3	3-6	1.99

¹Level (oe) at which low coercivity component removed. The mean direction from several demagnetization levels is used for some samples, so the levels used are listed.

²Angular standard deviation after Harrison (1980). The range of values is given for samples with averaged directions.

³The intensity of magnetization (J) is a mean for those samples with averaged directions.

TABLE 6. Continued

Sample #	Demagnetization (oe) ¹	D	I	A.S.D. ²	Intensity ³ ($\times 10^{-5}$)
90-31-01	200,300	160.2	-59.5	18	0.47
31-02	300	168.6	-52.3	4	0.86
32-01	200	102.7	+44.3	11	0.36
33-01	300,400	201.8	-86.2	7-9	0.76
33-02	200,300	250.9	-47.9	4-7	0.67
34-01	100,200,300,400	185.9	-65.6	6-8	1.89
34-02	200,300,400	219.5	-47.7	5-14	1.35
15-01	200	241.2	-86.1	5	1.20
15-02	300,400	170.6	-36.7	21-24	0.57
16-01	150,200,250,300,400	204.9	-43.5	6-11	0.60
16-02	unstable				
17-01	150,200,300	50.4	-68.7	12-13	0.41
18-01	300	166.0	-52.3	12	0.29
18-02	300	102.4	-58.2	20	1.33
19-01	unstable				
19-02	300	151.2	-50.6	26	0.26
20-01	300,400	156.8	-30.0	6-15	0.37
20-02	200	316.7	-39.7	13	0.45
21-01	100,200,300,400	191.0	-30.6	8-13	0.34
21-02	200	177.0	-39.3	6	0.96
22-01	200	156.4	-66.0	4	2.08
22-02	400	110.1	-68.5	7	1.05
23-01	400	185.1	-51.2	3	0.26
23-02	300,400,500,600	153.5	-47.6	4-7	1.66
24-01	300	156.9	-40.7	3	0.96
24-02	400	117.8	-62.0	6	0.62
25-01	300,400	103.9	-69.7	3-6	0.42
25-02	300,400	180.5	+24.2	27-30	0.34
98-01-01	400	184.8	-68.5	4	3.18
01-02	100,200,300,500	193.7	-84.3	4-7	0.24
02-01	300,400	157.4	-57.9	7-8	0.66
02-02	300	209.3	-40.7	4	2.19
03-01	400	204.2	-27.9	13	0.76
03-02	unstable				
130-01-01	300	27.1	+57.0	1	3.17
01-02	300	36.3	+58.7	2	2.24
02-01	200	2.8	+63.1	2	1.30
02-02	300	353.6	+60.7	4	0.92
03-01	150	359.0	+60.8	1	2.16
03-02	200	353.6	+60.7	4	2.03
04-01	200	14.7	+60.9	3	2.52
04-02	200	7.3	+60.3	1	3.12
05-01	300	195.3	-58.2	15	0.27
05-02	200	158.7	-66.6	2	1.44
06-01	discarded due to orientation uncertainty				
06-02	discarded due to orientation uncertainty				

TABLE 6. Continued.

<u>Sample #</u>	<u>Demagnetization (oe)¹</u>	<u>D</u>	<u>I</u>	<u>A.S.D.²</u>	<u>Intensity³ (x10⁻⁵)</u>
130-07-01	unstable				
07-02	unstable				
16-01	unstable				
16-02	unstable				
17-01	unstable				
17-02	600,650,700	208.0	-56.8	26-44	0.31
08-01	150	298.5	-78.4	14	0.46
08-02	400	53.1	-65.2	10	0.32
10-01	300	82.4	-59.6	17	0.22
10-02	200	189.1	-49.3	24	0.17
11-01	200	197.4	-66.1	5	0.91
11-02	200,400	203.5	-60.8	6-7	0.94
12-01	200	190.3	-58.5	5	0.69
12-02	200	227.8	-65.3	6	0.86
13-01	300	175.0	-46.8	4	2.67
13-02	300,400,500	187.3	-32.1	4-12	0.41
14-01	200	177.1	-42.3	5	0.76
14-02	200,300	183.5	-52.3	7-8	0.61
15-01	unstable				
180-17-01	300	197.5	-51.9	3	1.93
17-02	300	215.2	-56.0	6	2.33
18-01	200	180.8	-68.0	5	0.67
18-02	200	190.1	-59.2	5	0.72
19-01	200	196.0	-62.2	6	0.69
19-02	200	189.1	-61.0	5	1.07

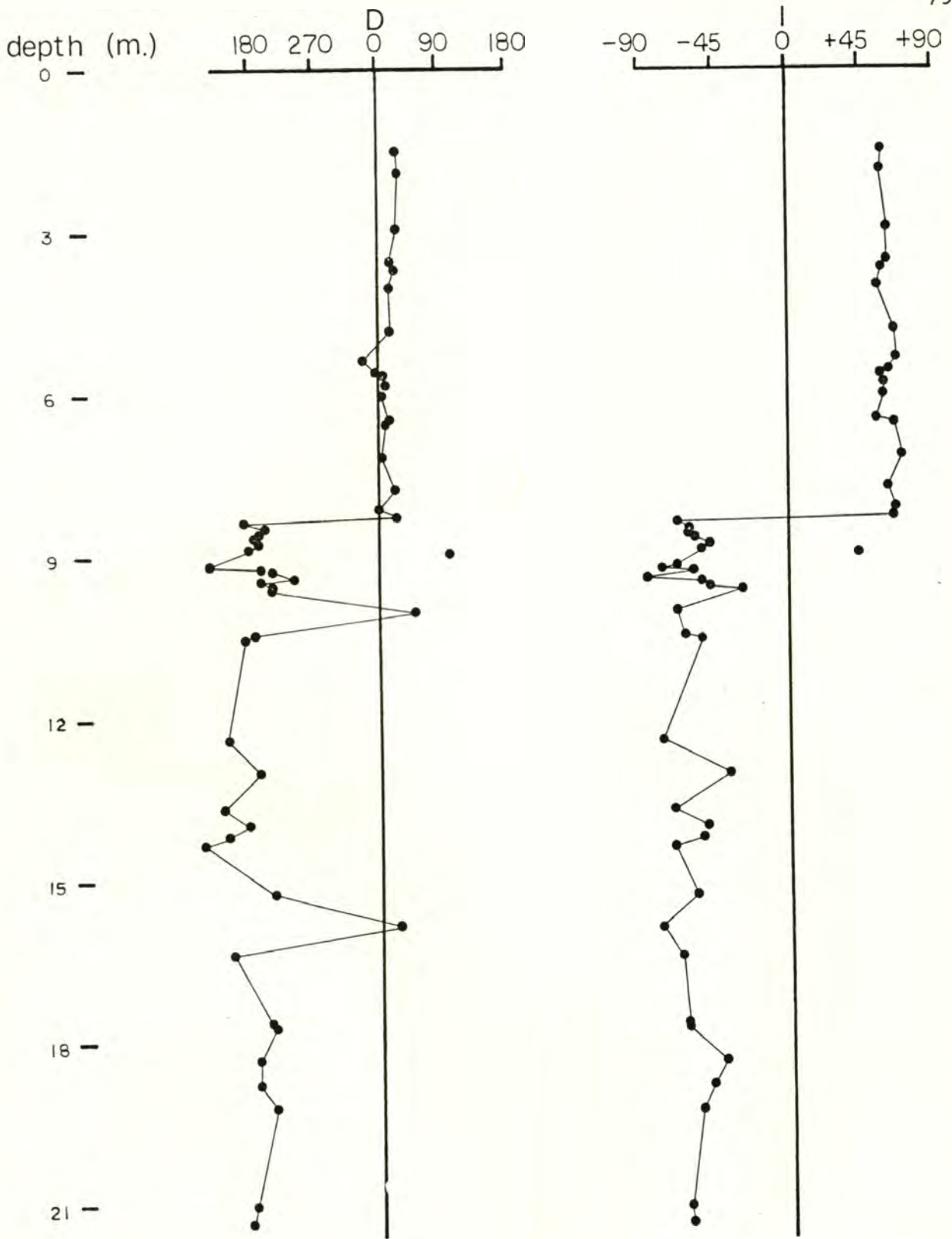


Figure 25: Graph of the mean paleomagnetic direction versus depth from each pair of samples in roadcut #3. The data are presented in Table 7.

TABLE 7. Mean magnetic directions for sample pairs listed in Table 6. These data are plotted as a graph in Figure 25.

Sample #	\bar{D}	\bar{I}	R^1	Depth(m)
90-01	29.9	+59.2	2.00	1.5
04	29.8	+62.8	2.00	2.9
02	23.4	+62.5	2.00	3.5
03	25.2	+57.8	2.00	3.7
05	17.0	+56.3	2.00	4.0
06	19.2	+66.9	1.99	4.8
07	338.5	+67.5	----	
08	10.1	+57.7	1.93	5.6
09	6.6	+59.6	----	6.0
10	17.6	+55.0	2.00	6.4
11	7.6	+70.1	2.00	7.2
12	25.1	+61.8	2.00	7.8
13	359.8	+66.8	1.92	8.1
14	26.6	+65.0	1.99	8.25
26	196.1	-67.6	1.98	8.35
27	195.2	-59.7	1.94	8.45
28	185.9	-60.4	2.00	8.60
29	178.7	-56.8	2.00	8.70
30	184.9	-47.6	1.98	8.75
31	168.6	-52.3	----	8.85
32	102.7	+44.3	----	8.95
33	246.9	-67.6	1.88	9.15
34	206.8	-57.7	1.95	9.25
15	241.2	-86.1	----	9.40
16	204.9	-43.5	----	9.6
17	50.4	-68.7	----	10.0
18	166.0	-52.3	----	10.5
20	218.3	-75.2	1.18	12.4
21	184.4	-35.2	----	13.0
22	134.5	-68.9	1.98	13.6
23	168.7	-50.5	1.97	14.0
24	142.1	-52.9	1.92	14.2
25	103.9	-69.7	----	14.8
98-01	186.7	-76.4	1.98	9.2
02	188.2	-52.2	1.90	9.4
03	204.2	-27.9	----	9.6
130-01	31.5	+57.9	2.00	1.9
02	358.0	+62.0	2.00	5.5
03	11.5	+59.5	2.00	5.8
04	11.0	+60.7	2.00	6.5
05	179.7	-63.6	1.97	10.4
17	208.0	-56.8	----	15.2
08	24.5	-78.5	1.93	15.8
10	145.4	-66.6	1.77	16.4

TABLE 7. Continued.

Sample #	\bar{D}	\bar{I}	R^1	Depth(m)
130-11	200.7	-63.5	2.00	17.6
12	206.9	-63.2	1.97	17.7
13	181.8	-39.6	1.99	18.3
14	180.00	-47.3	1.99	19.1
180-17	205.9	-54.3	1.99	19.2
18	186.2	-63.7	1.99	21.0
19	192.5	-61.6	2.00	21.3

¹R is the length of the resultant vector (McElhinny, 1973) and is a measure of the similarity of the two samples being averaged. The closer R is to 2.00, the more similar are the directions of the two samples. Samples for which a pair was either not available, unstable, or if the other member of the pair was judged to be less reliable (by A.S.D.), do not have an R value.

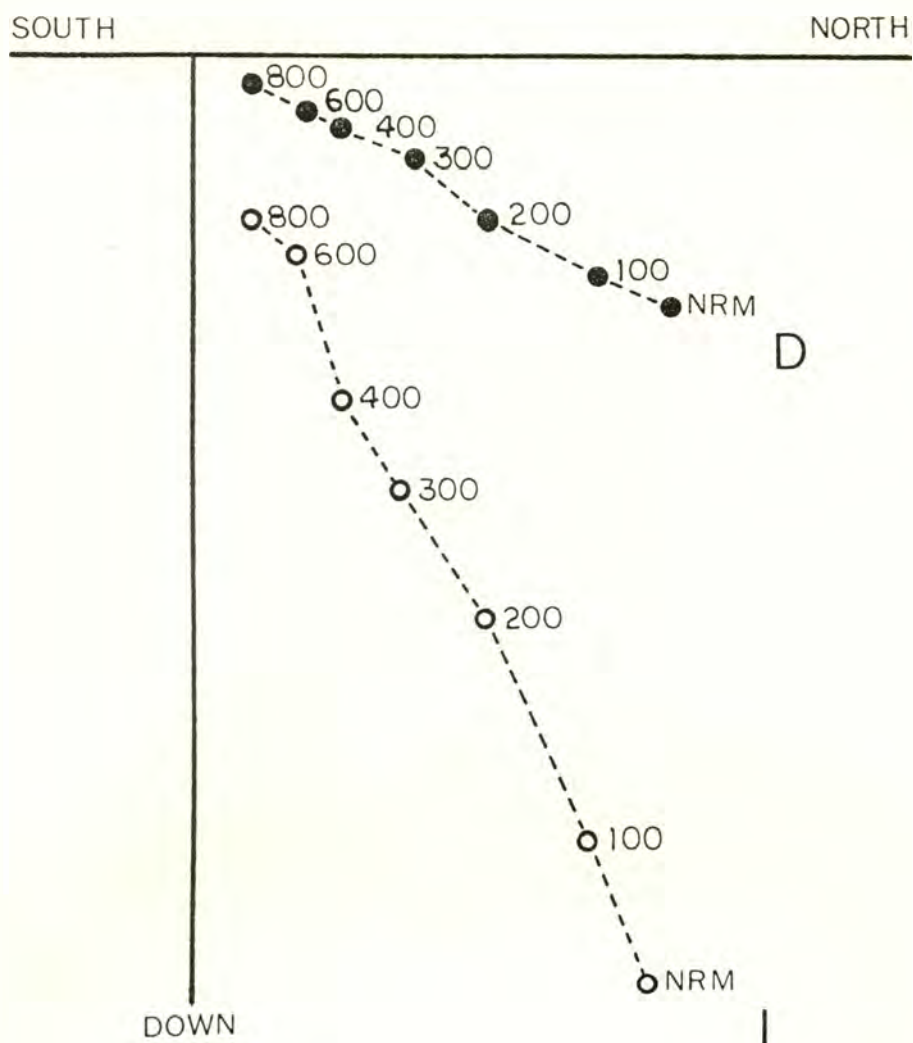


Figure 26: Orthogonal projection of the magnetization vectors (Zijderveld, 1967) in sample 90-01-02. This sample shows a single component of magnetization with normal polarity. Numbers represent AF demagnetization levels (oe).

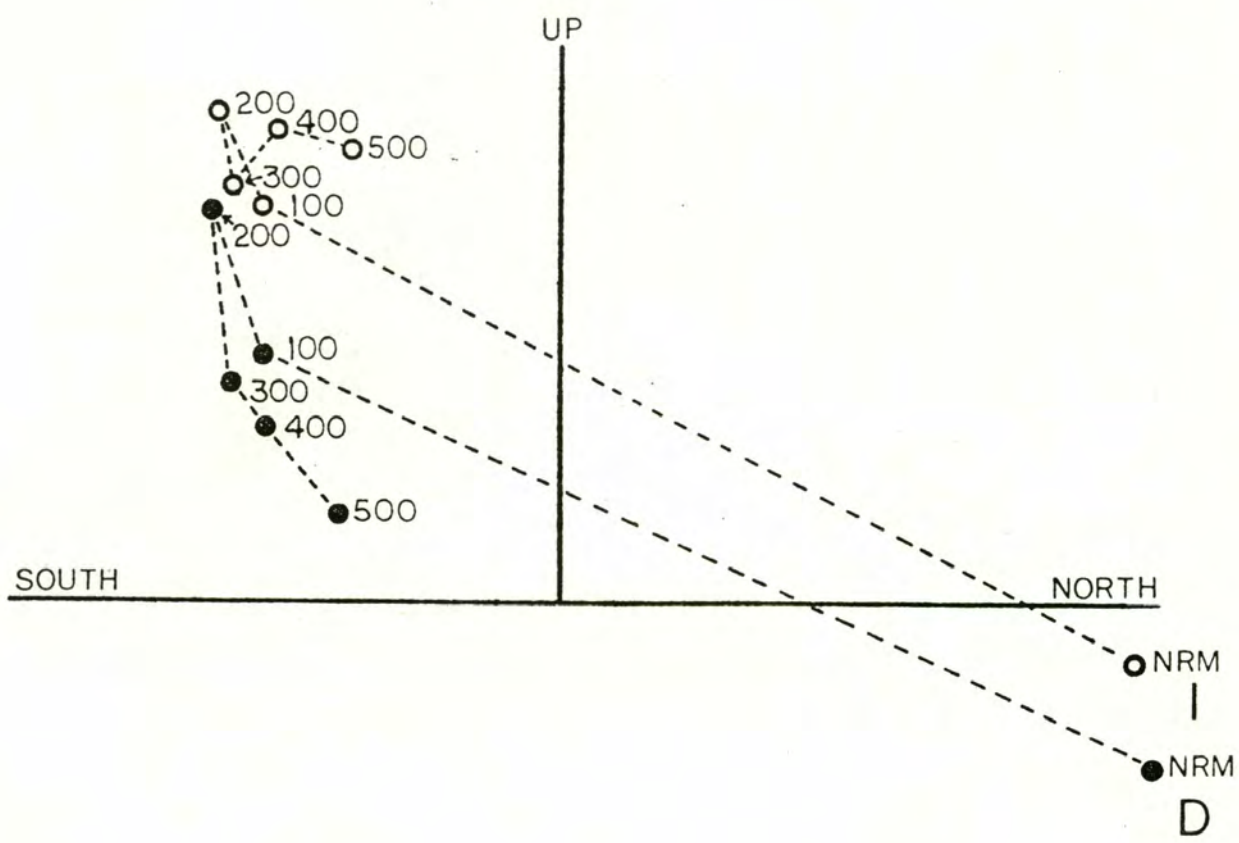


Figure 27: Orthogonal projection of the magnetization vectors (Zijderveld, 1967) in sample 90-34-02. This sample contains two components of magnetization: a component with reversed polarity with an overprint by a component with normal polarity which is removed by AF demagnetization of 100 oe. Numbers represent AF demagnetization levels (oe).

The scatter of the directions is illustrated in a stereographic projection (Figure 28).

Three sample means show primary directions (Fig. 25) that might be interpreted as the result of normal polarity events during the Matuyama Reversed Epoch since their declinations are closer to a normal axial dipole field direction than to a reversed one. Two of these samples, however, show inclinations that are well reversed (-68.3° and -78.5°). The third sample (90-32, Table 7), at 8.9 meters depth below the surface, shows a normal inclination as well as declination. A Zijdeveld plot for progressive demagnetizations (Fig. 29) shows an erratic pattern that acquires a reversed inclination at 400 oe. Because this is only a single sample, not a pair, with weak intensities of magnetization and an unstable demagnetization pattern, its use as an indicator of a polarity event cannot be justified.

Discussion

The samples from more than 8.3 meters below the surface consistently show a reversed magnetization after AF cleaning. Their mean primary direction ($D = 184.5^{\circ}$, $I = -62.8^{\circ}$) approximates that of an axial dipole field ($D = 180^{\circ}$, $I = -65^{\circ}$), although the directions show a large scatter (Fig. 28) and the age span covered by these samples is not known. Most of the reversed samples have a secondary low coercivity overprint in a normal direction that is mostly removed by demagnetizing at 200 oe (Fig. 27). The mean direction of the component that was removed from these reversed samples by 100 oe cleaning is $D = 37^{\circ}$, $I = +47^{\circ}$. If the scatter (Fig. 28) and low intensities (Table 6) are due to this normal overprint not being completely removed, then the mean primary reversed component

- lower hemisphere (N) × axial dipole field
- upper hemisphere (R) * present magnetic field
- mean direction of Normal samples
- mean direction of Reverse samples

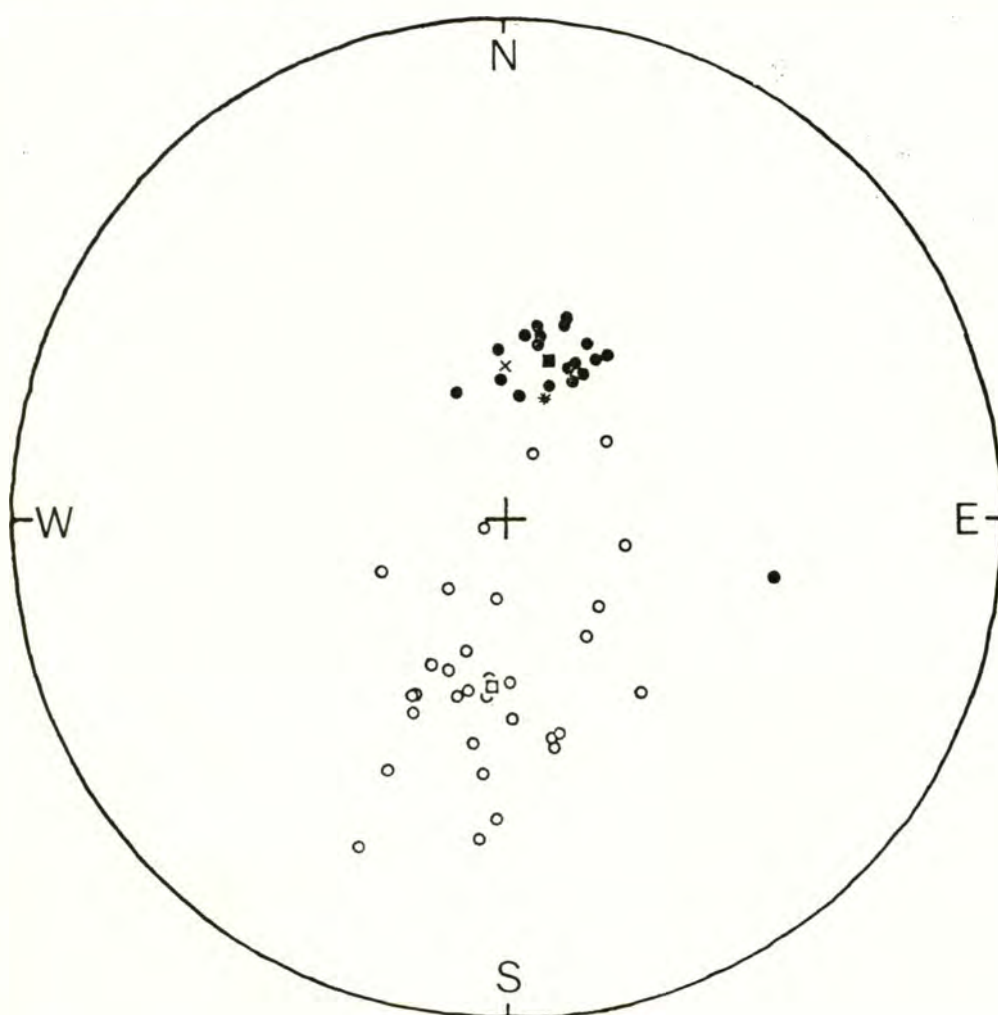


Figure 28: Stereographic projection of the mean paleomagnetic direction from each pair of samples in roadcut #3. The data are presented in Table 7.

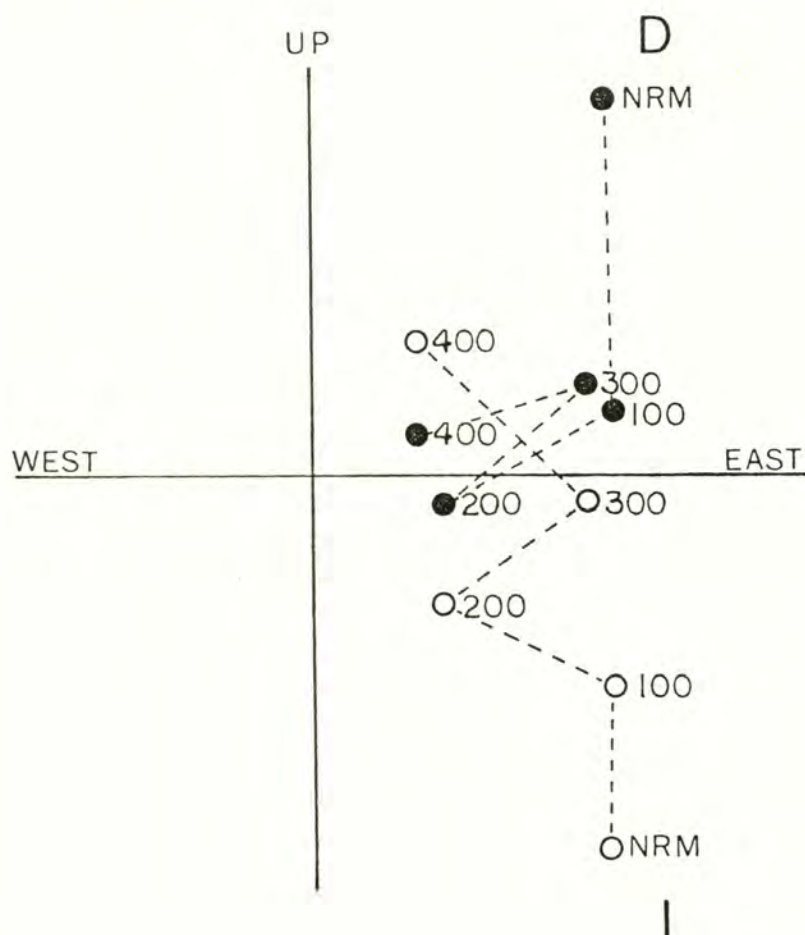


Figure 29: Orthogonal projection of the magnetization vectors (Zijderveld, 1967) in sample 90-32-01. Numbers represent AF demagnetization levels (oe).

would not be that of an axial dipole. Alternatively, the reversed direction may be the result of a weak and variable field. Regardless, the direction and the intensities of these samples indicate that these sediments are capable of recording and preserving the original polarity and approximate field direction.

The eighteen pairs of samples with normal magnetization, from the upper 8.3 meters of the section, probably record a long period of normal polarity, at least a large part of the Brunhes Normal Epoch, that spanned the last 730,000 years. Shorter polarity changes, such as the Blake (reversed) Event which occurred about 110,000 years ago, were not found in the section. Possible explanations are that (1) loess deposition is too erratic to record short term events, (2) the samples were spread too far apart, or (3) the record has been completely overprinted by secondary magnetization in a normal field.

The mean direction of the normal samples ($D = 16.2^{\circ}$, $I = +62.9^{\circ}$) is anomalous because it does not approximate the axial dipole field direction ($D = 0^{\circ}$, $I = +65^{\circ}$) (Fig. 28). One would expect the samples to average an axial dipole if they extend uniformly over the past 730,000 years and as a result average out the secular variation (slow change of the magnetic field about the axial dipole field direction). Because loess deposition is erratic, and the existence of buried soils indicates that there are gaps in the stratigraphic record, the paleomagnetic record cannot be assumed to be continuous through this section. However, that only loess that was deposited during the presence of an easterly bias to the magnetic field was sampled seems unlikely. Figure 25, a magnetostratigraphic section and Tables 6 and 7 illustrate that most of the normally magnetized samples record this easterly declination and that the mean is reflective of this bias.

The anomalous mean direction of the normal samples cannot be attributed to an overprint of the axial dipole field direction by the present field direction ($D = 20^{\circ}$, $I = +69^{\circ}$), because this overprint would produce a mean direction that on a stereonet would fall along a great circle between the two. The mean direction clearly does not fall on this great circle (Fig. 28).

Another possibility is that the samples have been wholly remagnetized in the present magnetic field. If the anomalous declination is due to a viscous remanent magnetization (VRM), a low intensity of magnetization affecting a rock over a long time, then the older samples would have been more affected than the younger ones, which is not the case since the reversed samples do not exhibit an anomalous declination. If the older, reversed samples are more cemented, they may be less susceptible to VRM, but they do not appear to be more cemented on the whole (Appendix).

Another way that the samples could have been remagnetized is by jostling of the sediment either during or after sampling, thereby remobilizing the high coercivity grains. However, that the 18 pairs of samples from the upper part of the section would be consistently disturbed, while the lower samples were not, is highly unlikely. In order to test the vulnerability of the samples to remobilization, a few samples were given an anhysteritic remanent magnetization (ARM) in a designated direction, and then the remanence was measured on a spinner magnetometer. Between each measurement, the sample was knocked against a hard surface in order to remobilize the grains. The remobilization of the grains did not affect the direction or magnetization of the sample, but the intensity of the magnetization decreased with each jostling step.

Another set of possible explanations for the easterly declination of the normally magnetized samples is based on the supposition that they were only partially, if at all, affected by a secondary magnetization. The easterly bias may be attributed to prevailing wind currents which flowed generally from west to east during the Pleistocene (Fryxell and Cook, 1964), and which may have affected the grains in a manner similar to the way water currents bias declinations in fluvial environments (Rees, 1961).

Another possibility is that the normal samples recorded a far-sided and right-handed magnetic field direction which may have been typical of the Brunhes Normal Epoch (Wilson and McElhinny, 1974).

The sediments in roadcut #3 may have been affected by a secondary overprint which has augmented the stability of the normal samples and degraded the stability of the reversed samples. However, the remanence appears to be dominated by the original remanence (DRM), permitting the Brunhes-Matuyama boundary to be established in this roadcut. The sediments below a depth of 8.3 meters in this roadcut are greater than 730,000 years old. This date is a minimum age for the sediments because erosion may have occurred removing the top of the reversed section prior to the beginning of the Brunhes Normal Epoch.

QUATERNARY CHRONOLOGY

Age of the Washtucna Loess

The age of the younger (<40,000 years) loess near Washtucna has been determined by the correlation of tephra layers which bracket these deposits with tephra of known age from Mount St. Helens and from Mount Mazama. The age of the older (>40,000 years) loess deposits can only be estimated from their stratigraphic position and from paleomagnetic evidence that establishes the Brunhes Normal-Matuyama Reversed polarity epoch boundary (730,000 years B.P.) in roadcut #3 (Fig. 30). The loess is divided into units which are bounded by time marker horizons.

Loess Younger Than 40,000 Years B.P.

The youngest eolian deposit in the Washtucna roadcuts is the layer of sand at the top of roadcut #9 (Fig. 12) which buries a loess sheet containing a buried soil with a cambic B horizon and Mazama ash. This uppermost loess unit is also recognized in roadcuts #4 and #5 where an Ap-Bw-Ck horizon sequence, the modern soil (Figs. 10 and 11), has formed. The Mazama ash at the base of this loess unit in roadcut #9 provides a maximum age of 6,700 years for the loess and for the modern soil.

The next older loess deposit immediately underlies the modern soil in roadcuts #4 and #5 and contains Set S tephra from Mount St. Helens which is about 13,000 years old (Mullineaux *et al.*, 1978). This loess contains a zone of carbonate accumulation (buried soil #1) which is distinct from the modern soil (Appendix) and that may have resulted from a period of landscape stability between 13,000 and 6,700 years B.P. Since this soil is buried by only about one meter of loess, it is within the maximal wetting depth associated with the present land surface (H. W.

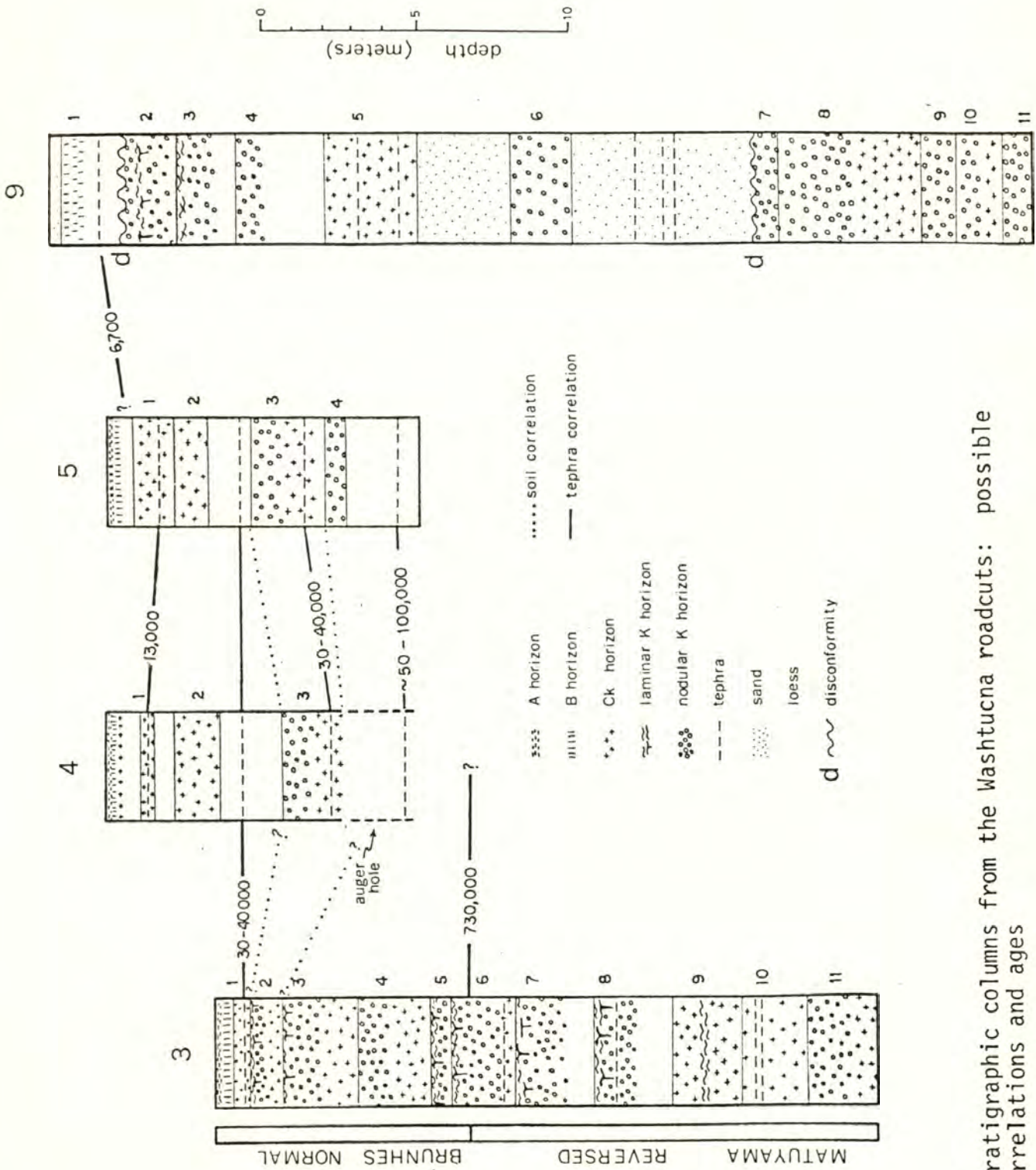


Figure 30: Stratigraphic columns from the Washtucna roadcuts: possible correlations and ages

Smith, oral communication) and may be influenced by continuing carbonate accumulation.

A loess unit which is bracketed by tephra Sets S and C from Mount St. Helens is identified in roadcuts #4 and #5 (Figs. 10 and 11). This loess unit, which is about 2.5 meters thick, accumulated between at least 30,000 B.P. (the minimum age of Set C) and 13,000 B.P. (the age of Set S) (Fig. 30). A zone of stage II carbonate (buried soil #2 in roadcuts #4 and #5), one to two meters thick, is found within this loess unit. Since this zone of carbonate occurs in the middle portion of the loess unit (Figs. 10 and 11) the carbonate probably resulted from soil formation on a stable land surface between 30,000 and 13,000 years B.P. rather than from development of the younger overlying soils.

The next older loess unit is well defined in roadcuts #4 and #5 where it is bracketed by two tephra layers attributed to eruptions of Mount St. Helens which occurred between about 30,000 and 40,000 years ago (Set C) (Fig. 30). This loess unit is about 2.5 meters thick and contains a zone of stage III carbonate (buried soil #3) about two meters thick. This carbonate appears to have formed sometime during the deposition of the 30 to 40,000 year old loess unit because the carbonate is everywhere contained within the loess unit (Figs. 4 and 5). If the carbonate had formed later its configuration would not necessarily follow the stratigraphy of underlying units but would parallel a younger land surface.

In summary, about seven meters of loess have accumulated in roadcuts #4 and #5 during the last 40,000 years. The loess is subdivided into four units bracketed by four dated tephra layers. Each of the loess units contains a soil which is characterized by a zone of carbonate

accumulation. The significance of this soil sequence will be discussed after the entire loess chronology is established.

Loess 40,000 to ~50-100,000 Years Old

Loess deposited during this time interval is found at the base of roadcut #5 where it underlies Mount St. Helens Set C tephra and overlies tephra estimated to be about 50 to 100,000 years old (layer 5C) (Fig. 30). The sediment is 3 meters thick and contains a buried soil (#4) with stage III carbonate that is .7 meter thick.

This time period may be represented in roadcut #3 by a soil (buried soil #2) that is buried beneath a 30 to 40,000 year old tephra (Fig. 30). This soil is more strongly developed (stage IV carbonate) and may be correlative with the two buried soils at the base of roadcut #5, or it may be older than these two soils (ie., older than ~50 to 100,000 years). If the second alternative is accepted, then erosion in roadcut #3 would have removed the two soils that formed between 40,000 and ~50-100,000 years ago.

Loess 40,000 to 730,000 Years Old

Loess which was deposited during this time interval is found in roadcut #3 where tephra from Mount St. Helens Set C occurs near the top of the section, and where the Brunhes-Matuyama paleomagnetic boundary is defined at a depth of 8.3 meters below the surface (Fig. 30). At least 7 meters of loess accumulated between 40,000 and 730,000 years ago, and five soils formed. These soils are distinctly more calcareous than the soils younger than 40,000 years old (in roadcuts #4 and #5) and, for the most part, have well-developed K horizons with stage IV carbonate. The thickness of this loess (7 meters) is the same as the thickness of

the post-40,000 year B.P. loess in roadcuts #4 and #5 suggesting either a slow rate of deposition or an incomplete stratigraphic record in roadcut #3. The post-40,000 year B.P. stratigraphy is incomplete in this roadcut, which suggests that erosion may have removed some of the older loess as well. The strong development of the soils during this time also suggests that the apparent slow deposition rate may be due to long periods of non-deposition.

Loess Older Than 730,000 Years B.P.

Twelve meters of loess in roadcut #3 have reversed magnetic polarity and are interpreted to have accumulated during the Matuyama Reversed polarity epoch prior to 730,000 years ago. Five buried K horizons are observed in these deposits, but no characteristics have been found to distinguish these soils from those between 40,000 and 730,000 years old.

Soil Development

The dated sequence of loess deposits and soils in roadcuts #4 and #5 can be used to define soil-forming intervals (Morrison, 1967; Birkeland, 1974; Birkeland and Shroba, 1974) during the late Quaternary. The soil forming factors which determine the degree of soil development at this site are: parent material, topography, time, rate of loess accumulation, and rate of carbonate translocation and accumulation. Parent material and topography are constant at this locale, and the amount of time during which soil development took place can be estimated from the tephrostratigraphy. The rate of loess accumulation can only be guessed at based on the thickness and bracketing ages of each loess unit. If the carbonate in the Palouse loess originates in the Ringold Formation,

which is considered to be one of the sources of the loess (Rieger, 1952; McCreery, 1954), then carbonate is present in the soil parent material and "the rate of buildup in the soil is a function of the rate at which it can be translocated by leaching waters in the soil profile" (Birkeland, 1974:168). If this is the case in the Washtucna soils, then the degree of carbonate cementation may be related to the degree of leaching in the profile, which may have been determined by changes in effective precipitation in the past. The carbonate stages of the buried soils in the Washtucna roadcuts give a rough measure of the amount of carbonate present. These stages are plotted against depth in Figures 31, 32 and 33.

Comparison of the Holocene (modern) soil which has formed in about 7,000 years with the buried soil formed in 30 to 40,000 year old loess (buried soil #3 in roadcuts #4 and #5), which may have formed in about the same amount of time, shows that the rate of soil genesis was accelerated between 30,000 and 40,000 years ago. The Holocene soil has a cambic B horizon and slightly calcareous C horizon, whereas the 30 to 40,000 year soil consists of approximately two meters of stage III carbonate (Fig. 31). The difference in the amount of carbonate could be related to the rate of loess accumulation and/or to the rate of leaching of carbonate from the parent material and its accumulation near the base of the soil profile. Possibly, the older soil formed under conditions of slower loess deposition and higher effective precipitation than have prevailed during the Holocene. The presence of vermiculite as a major constituent in the clay assemblages of the 30 to 40,000 year soil (sample 5-7 in Table 1) supports this interpretation.

The fact that stage III carbonate can form in less than 10,000 years could indicate that soils in the older part of the section (>40,000

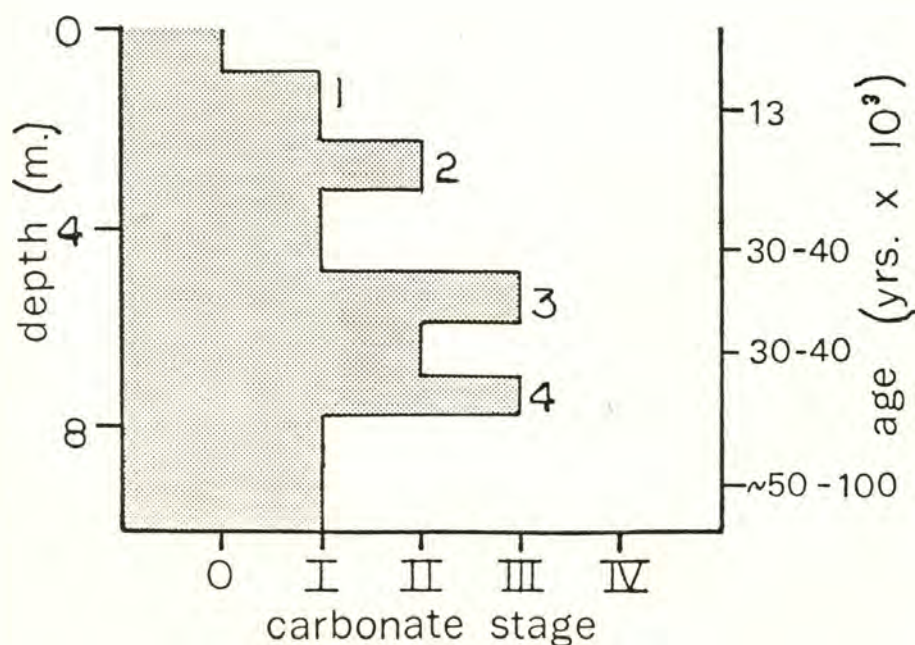
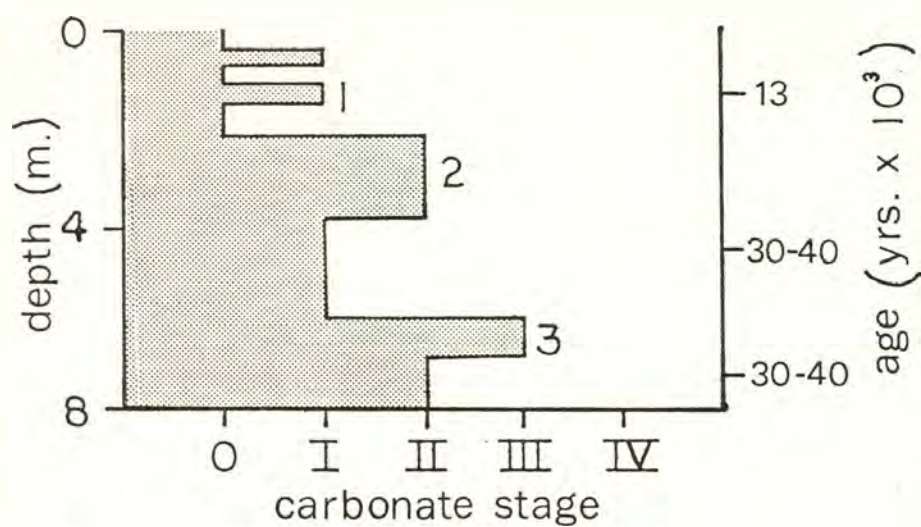


Figure 31: Graph of depth below surface versus carbonate stage (Gile *et al.*, 1966) of buried soils in roadcuts #4 (above) and #5 (below)

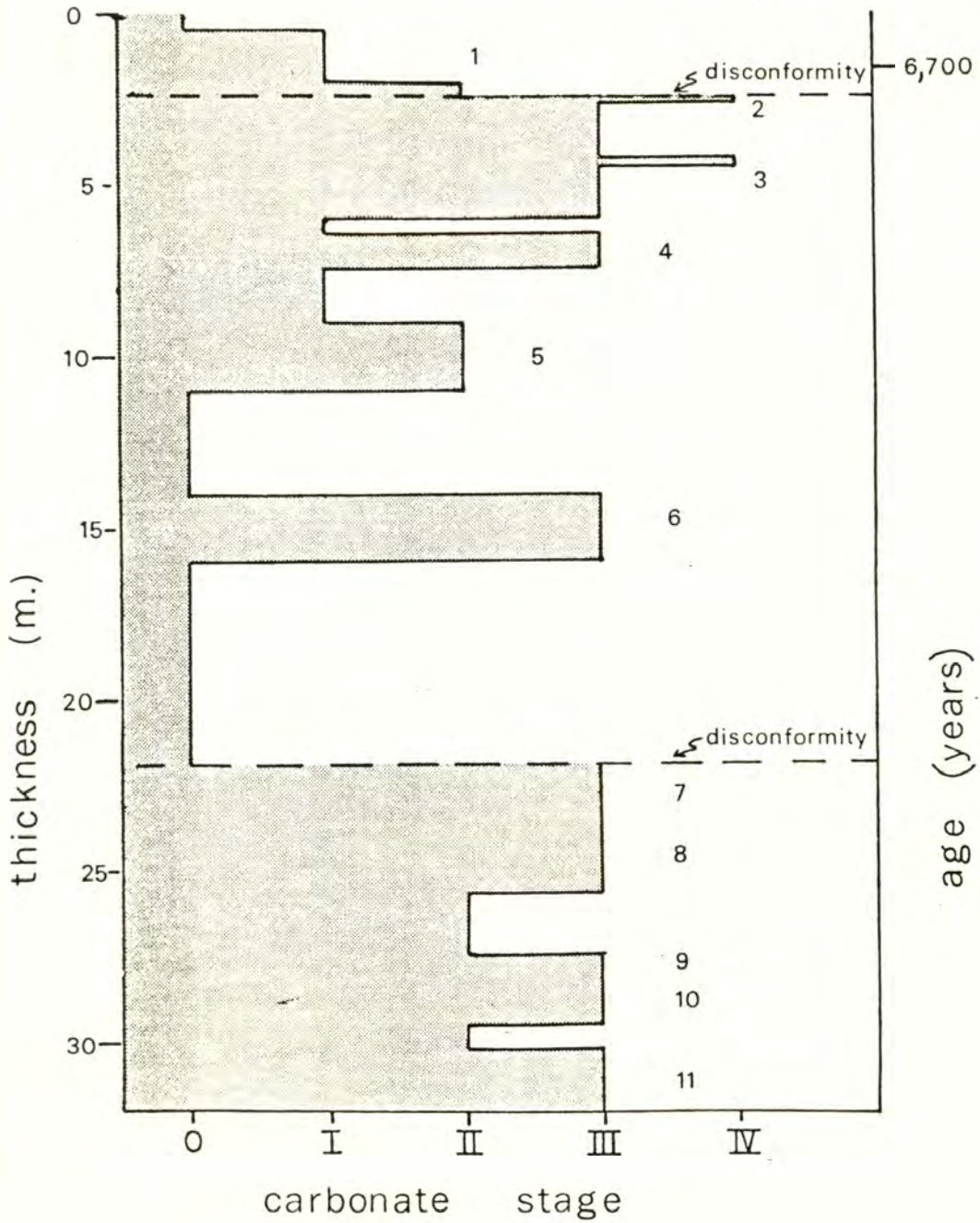


Figure 32: Graph of depth below surface versus carbonate stage (Gile et al., 1966) of buried soils in roadcut #9

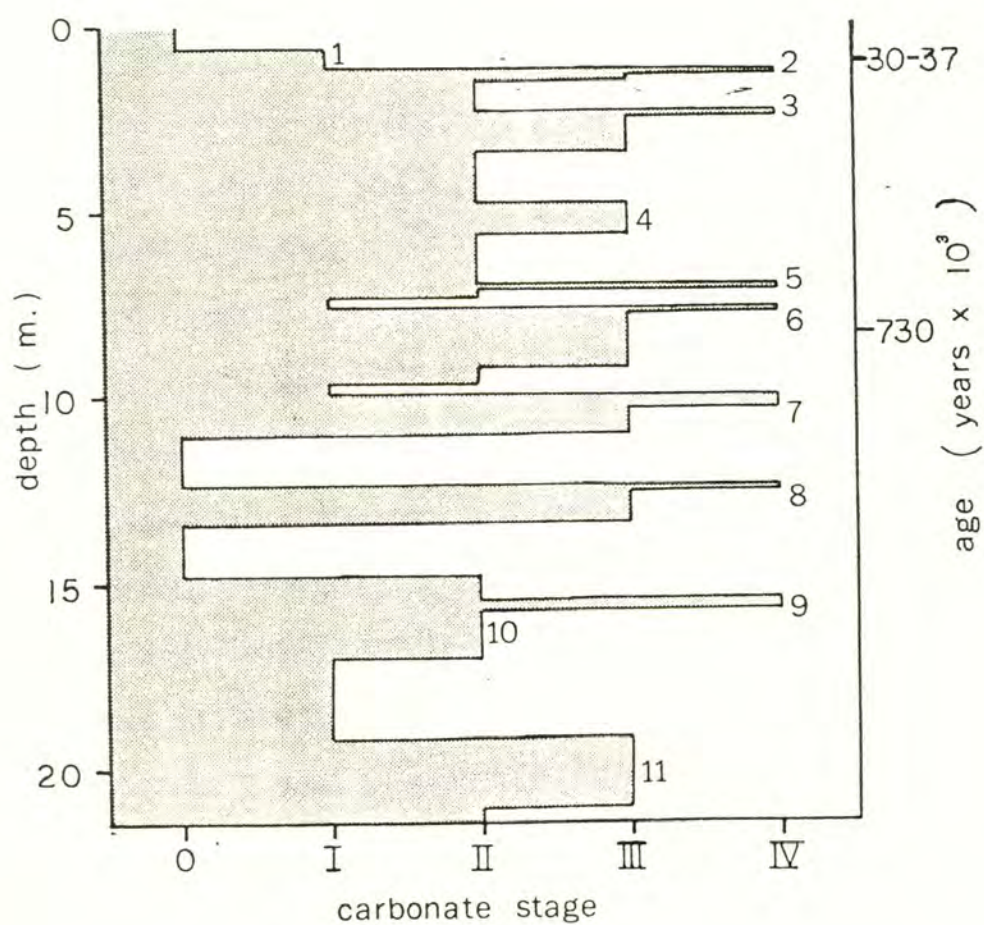


Figure 33: Graph of depth below surface versus carbonate stage (Gile et al., 1966) of buried soils in roadcut #3

years) with stage III and IV carbonate (Figs. 32 and 33) do not necessarily represent long periods of time of soil development, but instead represent periods of relatively rapid development separated by episodes of slower or negligible soil formation (Morrison, 1978).

The soil which formed between 13,000 and 30,000 years B.P. (buried soil #2 in roadcuts #4 and #5) consists of one to two meters of stage II carbonate (Fig. 31) and is intermediate in degree of development between the 30 to 40,000 year soil and the Holocene soil. The time period of 13 to 30,000 years B.P. generally corresponds with the Olympia non-glacial interval and the early and middle Fraser Glaciation in the Puget Lowland (Easterbrook, 1981). If similar climatic influences could be inferred for eastern Washington, then it would be possible to reconstruct the environment under which this soil formed. In roadcuts #4 and #5, 2.5 meters of loess were deposited some time after about 30,000 years B.P., possibly during a non-glacial interval corresponding to the Olympia, and then a two meter thick soil formed, perhaps during a time of slowed loess accumulation and higher precipitation associated with the Fraser Glaciation to the west. Renewed deposition prior to 13,000 years B.P. buried this soil with about a half meter of loess.

Although the factors influencing soil genesis at Washtucna are not well defined, the relative degree of soil development, especially carbonate accumulation, can be used to distinguish soils of different ages. The buried soils fall into three groups on the basis of age and degree of development:

- (1) Two buried soils younger than about 30,000 years B.P. are weakly to moderately cemented and have stage I and II carbonate;

(2) two buried soils, one between 30,000 and 40,000 years old and one older than 40,000 years B.P. but possibly younger than about 50-100,000 years B.P., are moderately cemented and have stage III carbonate; and

(3) ten buried soils are strongly cemented with stage III and IV carbonate (K horizons) and are older than 40,000 years B.P. (five are older than 730,000 years B.P.).

Comparison With Columbia Plateau Loess Chronology

The traditional loess chronology for the Columbia Plateau established by Fryxell (in Richmond et al., 1965) and used in subsequent stratigraphic studies (Baker, 1971, 1978; Patton and Baker, 1978) consists of a sequence of loess units and paleosols that were not dated directly but whose ages were estimated by correlation with the Rocky Mountain glacial sequence of Richmond (1965) (Fig. 34). Fryxell distinguished three Pleistocene loess units by their color and relative degree of soil development: (1) "Pinedale" (late Wisconsin) loess is pale brown with moderately developed structural and textural B horizons, and is less calcareous than older soils, (2) Bull Lake (early Wisconsin) loess contains three soils with well developed structural and textural B horizons and with non-indurated carbonates in the more arid portions of the Plateau, and (3) Pre-Bull Lake (pre-Wisconsin) loesses which have strongly developed structural and textural B horizons and indurated petrocalcic (K) horizons (Richmond et al., 1965).

The three groups of buried soils recognized at Washtucna seem to correspond in the degree of carbonate cementation with the three groups of soils in Fryxell's generalized Columbia Plateau loess stratigraphy

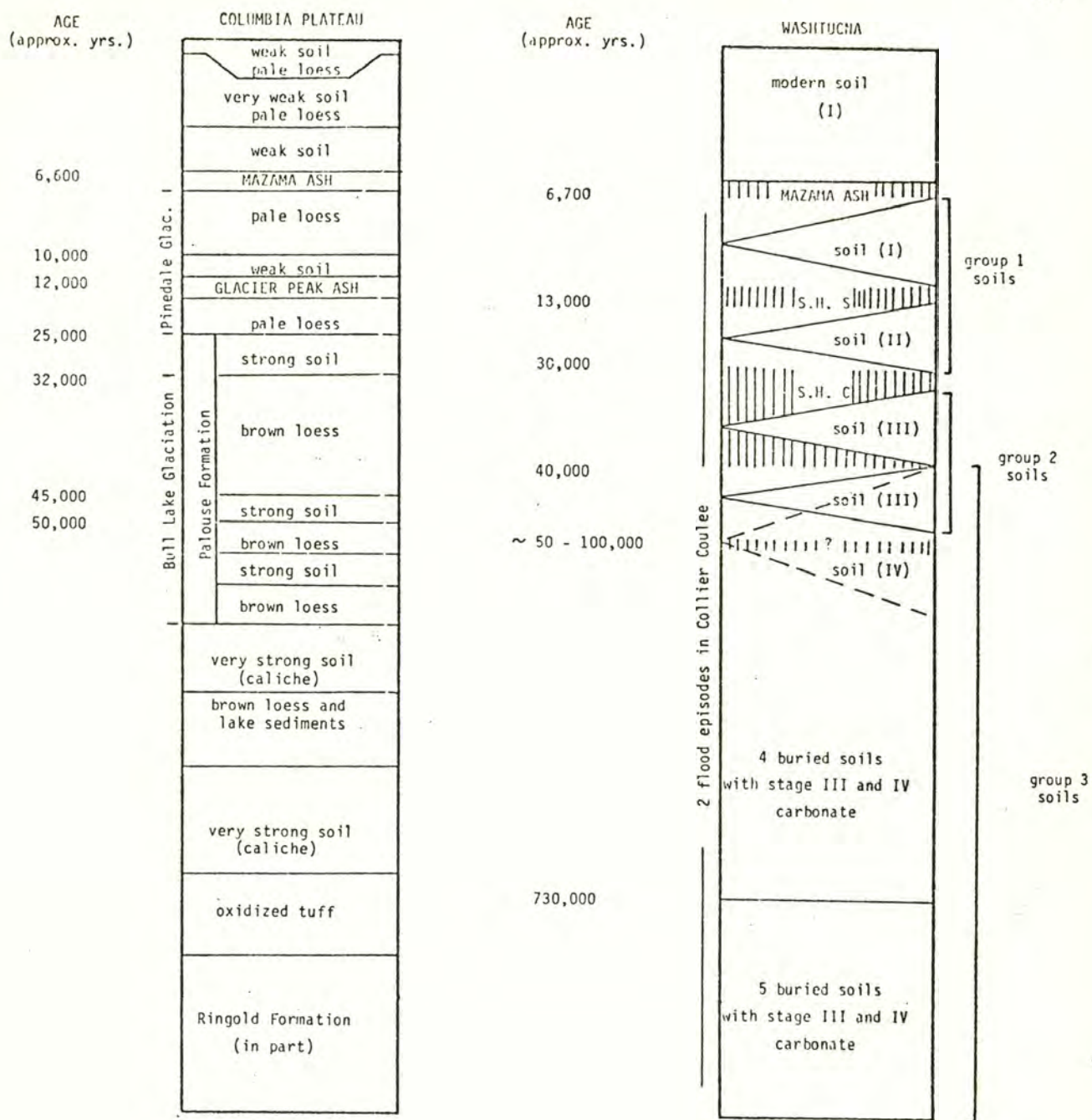


Figure 34: Comparison of the Washtucna stratigraphy with the Columbia Plateau loess chronology of Fryxell (in Richmond et al., 1965). Roman numeral in parentheses is carbonate stage; vertical lines are tephra layers or sets; S.H. S= Mount St. Helens tephra set S; S.H. C= Mount St. Helens tephra set C; ?= tephra of unknown source and estimated age.

(Richmond et al., 1965), and the estimated ages are not dissimilar (Fig. 34). The number of loess units and buried soils does not correspond well. At Washtucna, two buried soils, 7,000 to 13,000 years old, and 13,000 to 30,000 years old (group 1) have weak soil development characteristic of Fryxell's Pinedale soils, two soils (group 2), 30,000 to ~50,000-100,000 years old, are similar to his Bull Lake soils, and ten soils (group 3) have characteristics similar to his Pre-Bull Lake soils.

Recent investigations of glacial deposits in Yellowstone National Park by Pierce (1979) and Colman and Pierce (1981) have led to a revision of the chronology of Rocky Mountain glaciation. Some Pinedale deposits are considered to be between about 35,000 and 50,000 (mid-Wisconsin) (Colman and Pierce, 1981). If these ages are applied to the Columbia Plateau loess stratigraphy of Fryxell (in Richmond et al., 1965), then there is no correlation with the Washtucna stratigraphy. Fryxell's original age estimates for the loess stratigraphy generally correspond with the data collected at Washtucna, but the terms Pinedale and Bull Lake should not be applied to these deposits since these terms now imply ages different from the original estimates used in the Columbia Plateau loess chronology of Richmond et al. (1965).

Evidence for Scabland Floods

Two disconformities in roadcut #9 (Fig. 30) are attributed to flood waters from Rattlesnake Flat (Fig. 8), part of the Cheney-Palouse Scabland tract, that flowed down Collier Coulee and entered Washtucna Coulee south of the study area (see discussion on page 19). The age of the two floods can be approximated from interpretation of the loess and tephra stratigraphy.

The younger disconformity underlies Mazama tephra and is therefore older than 6,700 years. The flood disconformity could be related to the last major flood in the Scablands of about 13,000 years ago (Mullineaux *et al.*, 1978), evidence for which has been recognized in the Cheney-Palouse tract (Baker, 1978). However, three lines of evidence argue for an earlier age: (1) in contrast to the bare, rugged channels which characterize the Cheney-Palouse tract, Collier Coulee is partially filled with loess and has a smooth rounded cross-section; (2) the mouth of Collier Coulee contains gravels and sands with attitudes indicating that water flowed from Washtucna Coulee up into lower Collier Coulee during the last episode of flooding; and (3) the elevation of Rattlesnake Flat (~1,700 feet) is much higher than Washtucna Coulee (~1,000 feet) suggesting that Rattlesnake Flat was formed by earlier floods. If the upper disconformity was formed by a pre-late Wisconsin Scabland flood, then one would expect to find a soil or multiple soils formed between (or upon) the disconformity and the Mazama-bearing loess which overlies it, but none are evident (Fig. 6). Since these soils could be missing from the stratigraphic record because of erosion, their absence is not compelling evidence for a younger age for this disconformity.

In summary, the stratigraphic evidence suggests that this flood is late Wisconsin (~13,000 years B.P.) in age, but geomorphic evidence suggests it is older. Certainly, the flood occurred prior to 6,700 years ago.

The older disconformity is separated from the younger disconformity by about 10 meters of loess and eolian sand as well as by five buried soils (Fig. 31), which are similar in degree of development to soils older than 40,000 years B.P. in roadcut #3. The flood that caused this disconformity may be related to the older flood gravels at the base of the

Marengo section which are considered to be pre-Wisconsin (Baker, 1978). Paleomagnetic stratigraphy in roadcut #9 would add important chronologic information to the history of Scabland flooding.

Regional Correlations

Correlation of the loess and soil stratigraphy at Washtucna with glacial chronologies either in the Pacific Northwest or in the Rocky Mountains is difficult because: (1) the relationship between loess deposition on the Columbia Plateau and glaciation at the northern margin of the Plateau has not been established; and (2) the type of climate (interglacial versus glacial) under which the Washtucna paleosols formed is not clear. The chronology interpreted from roadcuts #4 and #5 tends to support an argument for accelerated loess deposition during times of retreat of the Cordilleran Ice Sheet, and for stability and soil formation during maximum stands of the Ice Sheet. This scenario is supported by the supposition that more sediment would be available for eolian transport following each Scabland flood, which may have occurred at the initiation of retreat of the Pend Oreille lobe of the Cordilleran Ice Sheet. If this generalized situation applies to Washtucna, then the soils would not be correlative with interglacial soils described in glaciated areas.

The chronologic data from the tephra layers and magnetostratigraphy do allow for broad comparisons with soils and deposits described in other regions, however.

The loess deposits which are older than 730,000 years at Washtucna can be generally correlated with glacial deposits in the Cascade Range and in the Puget Lowlands which also have demonstrated reversed polarity

(Porter, 1976; Easterbrook et al., 1981). Tephra layers found in some of these reversely magnetized sediments in the Puget Lowland (Easterbrook et al., 1981), may be correlative with one or more of the older unidentified tephras at Washtucna, in which case a more specific correlation of the deposits would be possible; but comparative data are not available at this time.

The relative degree of development of buried soil #2 in roadcut #3, which antedates 30 to 40,000 year old eruptions of Mount St. Helens, compared to soils younger than 30,000 years old, is similar to the difference between the post-Lakedale and post-Kittitas soils in the Cascade Range (Porter, 1975) and the post-Pinedale and post-Bull Lake soils in southeastern Idaho (Pierce et al., 1982). Whether buried soil #2 in roadcut #3 formed over the same time span as buried soils #3 and #4 in roadcut #5 (between 30,000 and ~50-100,000 years ago) or whether it formed earlier cannot be determined from the stratigraphy at Washtucna (Fig. 30). Due to this stratigraphic uncertainty, and the fact that all of the soils which underlie Mount St. Helens Set C tephra in roadcut #3 are more strongly developed than those which overlie this tephra in roadcuts #4 and #5, a specific soil corresponding in age with the last interglaciation (<120,000 years ago) cannot be identified at Washtucna. The two most likely candidates are buried soils #2 and #3 in roadcut #3.

Two weakly developed soils which have been demonstrated to be younger than 13,000 years old at Washtucna (the modern soil and buried soil #1 in roadcuts #4 and #5) can be correlated with the post-Lakedale soil in the Cascade Range (Porter, 1976) and the post-Pinedale soil in southeastern Idaho (Pierce et al., 1982).

The great number of buried soils at Washtucna is anomalous when compared with the loess stratigraphy described elsewhere on the Columbia Plateau (Richmond *et al.*, 1965; Baker, 1978) and in southeastern Idaho (Pierce *et al.*, 1982). This stronger stratigraphic resolution at Washtucna seems to indicate that this site may be more sensitive to changes in climate (temperature, precipitation, wind direction or velocity) or that the soil stratigraphy is better preserved.

Summary

The roadcuts at Washtucna contain a thick sequence of loess deposits and paleosols which, along with dated tephra layers, provide a basis for a loess chronology on the Columbia Plateau. The upper part of the combined section (Fig. 34) which is reasonably well dated, spans the last 40,000 years and appears to contain a continuous sequence of loess deposits. The buried soils which are older than at least 40,000 years are more strongly developed than the younger soils and represent either longer soil forming intervals or climatic conditions more favorable to soil formation.

Two episodes of Scabland flooding are recognized in roadcut #9. Chronologic control in this exposure is poor, but magnetostratigraphy and further tephra correlation could provide better age resolution in the future.

CONCLUSIONS

This study of the loess in four of the Washtucna roadcuts uses four lines of evidence to work out the Quaternary chronology at this locality: (1) tephrostratigraphy; (2) magnetostratigraphy; (3) field descriptions of the soils; and (4) clay mineralogy of the loess. The following conclusions are drawn from this evidence:

(1) Tephra from eruptions of Mount Mazama and Mount St. Helens are present in the late Quaternary part of the stratigraphic sections. Mazama ash is identified in one roadcut; Mount St. Helens Set S (or possibly Set M) is found as an intermittent layer in two roadcuts; and Mount St. Helens Set C occurs in three roadcuts. Two stratigraphically distinct layers of Set C are identified in two roadcuts; indicating that this tephra set was erupted over a relatively long time span, possibly as long as 10,000 years.

(2) Several tephra layers of unknown source, but probably of Cascade provenance, are present in the Washtucna roadcuts. The youngest of these occurs in two roadcuts and is estimated to be 50,000 to 100,000 years old based on its stratigraphic position. Four tephra layers in one roadcut were deposited during the Matuyama Reversed polarity epoch and are therefore older than 730,000 years B.P. Five tephra layers underlie Mazama ash in one roadcut. Stratigraphic evidence suggests that these five tephras are pre-late Quaternary in age, but chronologic data are lacking. These tephras are not correlated with tephras in the other three roadcuts.

(3) Magnetostratigraphy conducted in one roadcut resulted in demonstrating that (a) the Palouse loess carries a measurable remanent

magnetization which is dominated by the original remanence, and (b) the Brunhes-Matuyama boundary can be delineated in these sediments. The loess with a component of reversed magnetization is considered to be greater than 730,000 years old.

(4) Field characteristics, especially carbonate stage of development, can be used to distinguish three broad age groupings of paleosols: soils which formed after about 30,000 years ago are weakly developed with stage I and II carbonate; soils which formed between 30,000 and at least 40,000 years ago have stage III carbonate; and soils which formed prior to at least 40,000 years ago have stage III and IV carbonate.

(4) The clay mineral assemblage of the Palouse loess consists of chlorite and mica with minor amounts of expandable clays (smectite and vermiculite). Kaolinite was identified in three samples, indicating that it may be present in others, but analysis for this mineral was conducted on only four samples. Clay mineralogy did not prove useful as a method for distinguishing paleosols, but could be used to interpret the conditions under which soil genesis occurred.

BIBLIOGRAPHY

- Abdel-Kader, F. H., M. L. Jackson, and G. B. Lee, 1978, Soil kaolinite, vermiculite, and chlorite identification by an improved lithium DMSO x-ray diffraction test: Soil Science Society of America Journal, v. 42, p. 163-167.
- Bachman, G. O., and M. N. Machette, 1977, Calcic soils and calcretes in the southwestern United States: U. S. Geological Survey, Open-File Report 77-794, 163 p.
- Baker, V., 1971, Paleohydrology and sedimentology of Lake Missoula flooding in eastern Washington: Unpublished Ph.D. dissertation, University of Colorado, Boulder, 152 p.
- Baker, V. R., 1978, Quaternary geology of the Channeled Scablands and adjacent areas, in Baker, V. R., and D. Nummedal, eds., The Channeled Scabland: Washington, D. C., National Aeronautics and Space Administration, p. 17-35.
- Barshad, I., 1966, The effect of a variation in precipitation on the nature of clay mineral formation in soils from acid and basic igneous rocks: Proceedings of the International Clay Conference, Jerusalem, v. 1, p. 167-173.
- Benedict, E. T., 1943, A method of determination of the direction of the magnetic field of the earth in geological epochs: American Journal of Science, v. 241, p. 124-129.
- Birkeland, P. W., 1974, Pedology, Weathering, and Geomorphological Research: New York, Oxford University Press, 285 p.
- Birkeland, P. W., and R. R. Shroba, 1974, The status of the concept of Quaternary soil-forming intervals in the western United States, in Mahaney, W. C., ed., Quaternary Environments: Proceedings of a Symposium, Geographical Monographs, no. 5, p. 241-276.

- Bray, R. H., 1937, Chemical and physical changes in soil colloids with advancing development in Illinois soils: *Soil Science*, v. 43, p. 1-14.
- Bretz, J. H., 1923, The Channeled Scabland of the Columbia Plateau: *Journal of Geology*, v. 31, p. 617-649.
- _____, 1969, The Lake Missoula floods and the Channeled Scablands: *Journal of Geology*, v. 77, p. 505-543.
- Bucha, V., A. Koci, and V. Sibrava, 1978, Paleomagnetic correlation of Quaternary sequences in glaciated and nonglaciated areas, *in* Quaternary Glaciations in the Northern Hemisphere: International Geological Correlation Program, Report no. 5, p. 63-70.
- Bucha, V., V. Sibrava, and V. Lozek, 1975, Paleomagnetic correlations of Pleistocene sediments in central Europe, *in* Quaternary Glaciations in the Northern Hemisphere: International Geological Correlation Program, Report no. 2, p. 9-36.
- Calkins, F. C., 1905, Geology and water resources of a part of east central Washington: U. S. Geological Survey Water Supply Paper 118, 96 p.
- Colman, S. M., and K. L. Pierce, 1981, Weathering rinds on andesite and basaltic stones as a Quaternary age indicator, western United States: U. S. Geological Survey, Professional Paper 1210, 56 p.
- Cox, A., 1969, Geomagnetic reversals: *Science*, v. 163, p. 237-245.
- Cox, A., R. R. Doell, and G. B. Dalrymple, 1968, Radiometric time-scale for geomagnetic reversals: *Quaternary Journal*, Geological Society of London, v. 124, p. 53-66.
- Cunningham, R. L., 1964, Genesis of the soils along a traverse in Asotin County, Washington: Unpublished Ph.D. dissertation, Washington

- State University, Pullman, 158 p.
- Daubenmire, R., 1970, Steppe vegetation of Washington: Washington Agricultural Experiment Station, College of Agriculture, Washington State University, Technical Bulletin No. 62.
- Douglass, L. A., 1977, Vermiculites, in Dixon, J. B., and S. B. Weed, eds., Minerals in Soil Environments: Madison, Wisc., Soil Science Society of America, p. 259-292.
- Droste, J. B., and J. C. Tharin, 1958, Alteration and clay minerals in Illinoian till by weathering: Geological Society of America Bulletin, v. 69, p. 61-68.
- Easterbrook, D. J., 1973, Paleomagnetic events recorded in late Pleistocene sediments (abst.): Geological Society of America, Rocky Mountain Section Annual Meeting, Abstracts with Program, v. 5, p. 36-37.
- _____, 1974, Late Pleistocene glacial and paleomagnetic events (abst): Geological Society of America, Cordilleran Section Annual Meeting, Abstracts with Program, v. 6, p. 170-171.
- _____, 1976a, Quaternary Geology of the Pacific Northwest, in Mahaney, W. C., ed., Quaternary Stratigraphy of North America: Stroudsburg, Penn., Dowden, Hutchinson and Ross, Inc., p. 441-462.
- _____, 1976b, Quaternary history of Washington (abst.): Geological Society of America, Abstracts with Program, v. 8, p. 370.
- _____, 1977a, Paleomagnetic chronology and correlation of Pleistocene deposits (abst.): Geological Society of America, Abstracts with Program, v. 9, p. 961-962.
- _____, 1977b, The Okanogan lobe of the Vashon continental glacier, Part I, Glaciation and catastrophic flooding of the Columbia Plateau, Washington, in Brown, E. H., and R. C. Ellis, eds., Geological

- Excursions in the Pacific Northwest: Geological Society of America, Annual Meeting Field Guidebook, p. 390-414.
- Easterbrook, D. J., and N. Briggs, 1979, Age of the Auburn reversal and the Salmon Springs and Vashon glaciations in Washington (abst.): Geological Society of America, Abstracts with Programs, v. 11, p. 76.
- Easterbrook, D. J., N. D. Briggs, and J. A. Westgate, 1981, Tephrochronology, paleomagnetism, and amino-acid dating of pre-Vashon deposits in northwest Washington (abst.): Geological Society of America, Abstracts with Programs, v. 13, p. 53.
- Easterbrook, D. J., and K. L. Othberg, 1973, Paleomagnetism of Late Pleistocene sediments, Puget Lowland, Washington (abst.): Geological Society of America, Cordilleran Section Annual Meeting, Abstracts with Program, v. 5, p. 36.
- Fanning, D. S., and Keramidas, V. Z., 1977, Micas, in Dixon, J. B., and S. B. Week, eds., Minerals in Soil Environments: Madison, Wisc., Soil Science Society of America, p. 195-292.
- Fink, J., A. Koci, H. Kohl, and M. A. Pevzner, 1978, Paleomagnetic research in the northern foothills of the Alps and the question of correlation of terraces in the upper reach of the Danube, in Quaternary Glaciations in the Northern Hemisphere: International Geologic Correlation Program, Report No. 5, p. 108-116.
- Fink, J., and G. J. Kukla, 1977, Pleistocene climates in central Europe at least 17 interglacials after the Olduvai event: Quaternary Research, v. 7, p. 363-371.
- Flint, R. F., 1938, Origin of the Cheney-Palouse scabland tract: Geological Society of America Bulletin, v. 49, p. 461-524.

- Fryxell, R., 1965, Mazama and Glacier Peak volcanic ash layers:
Relative ages: *Science*, v. 147, p. 1288-1290.
- Fryxell, R., T. Bielicki, R. D. Daugherty, C. E. Gustafson, H. T. Irwin,
and B. C. Keel, 1968, A human skeleton of mid-Pinedale age in south-
eastern Washington: *American Antiquity*, v. 33, p. 511-515.
- Fryxell, R. H., and E. F. Cook, 1964, A field guide to the loess deposits
and channeled scablands of the Palouse area, eastern Washington:
Laboratory of Anthropology, Report of Investigations No. 27,
Washington State University, Pullman, 32 p.
- Gentry, H. R., 1974, Geomorphology of some selected soil landscapes in
Whitman County, Washington: Unpublished M.S. thesis, Washington
State University, Pullman, 99 p.
- Gile, L. H., F. F. Peterson, and R. B. Grossman, 1965, The K horizon:
A master soil horizon of carbonate accumulation: *Soil Science*,
v. 99, p. 74-82.
- Gile, L. H., F. F. Peterson, and R. B. Grossman, 1966, Morphological and
genetic sequences of carbonate accumulation in desert soils: *Soil
Science*, v. 101, p. 347-360.
- Gilkeson, R. A., 1965, Ritzville series: Benchmark soils of Washington:
Washington Agricultural Experiment Station Bulletin 665, 18 p.
- Gustafson, E., 1976, A revised chronology for vertebrate fossil faunas
in eastern Washington (abst.): Geological Society of America,
Cordilleran Section Annual Meeting, Abstracts with Programs, v.
8, p. 377-378.
- Hammatt, H. H., 1976, Late Quaternary stratigraphy and archaeological
chronology in the lower Snake River, Washington: Unpublished Ph.D.
dissertation, Washington State University, Pullman, 272 p.

- Hammatt, H. H., L. L. Foley, and F. C. Leonhardy, 1976, Late Quaternary stratigraphy in the lower Snake River Canyon, toward a chronology of slack water sediments (abst.): Geological Society of America, Abstracts with Programs, v. 8, p. 379.
- Hansen, H. P., 1947, Postglacial forest succession, climate and chronology in the Pacific Northwest: Transactions of the American Phil. Soc., v. 37, p. 1-130.
- Harrison, C. G. A., 1980, Spreading rates and heat flow: Geophysical Research Letters, v. 7, p. 1041-1044.
- Henshaw, P. C., and R. T. Merrill, 1979, Characteristics of drying remanent magnetization in sediments: Earth and Planetary Science Letters, v. 43, p. 315-320.
- Hobbs, W. H., 1947, The Glacial History of the Scabland and Okanogan Lobes, Cordilleran Continental Glacier: Ann Arbor, Mich., J. W. Edwards, 40 p.
- Hus, J., R. Paepe, R. Geeraerts, J. Somme, and R. Vanhoorne, 1976, Paleomagnetic investigations of sediments, in Quaternary Glaciations in the Northern Hemisphere: International Geological Correlation Program, Report No. 3, p. 99-128.
- Hyde, J. H., 1975, Upper Pleistocene pyroclastic-flow deposits and lahars south of Mount St. Helens volcano, Washington: U. S. Geological Survey Bulletin 1383-B, 20 p.
- International Union of Geological Sciences, International Subcommittee on Stratigraphic Classification and IUGS/IAGA Subcommittee on a Magnetic Polarity Time Scale, 1979, Magnetostratigraphic polarity units—a supplementary chapter of the ISSC International Stratigraphic Code: Geology, v. 7, p. 578-583.

- Irving, E., and A. Major, 1964, Post-depositional remanent magnetization in a synthetic sediment: *Sedimentology*, v. 3, p. 135-143.
- Ismail, F. T., 1969, Role of ferrous iron oxidation in the alteration of biotite and its effect on the type of clay minerals formed in soils of arid and humid regions: *American Mineralogist*, v. 54, p. 1460-1466.
- _____, 1970, Biotite weathering and clay formation in arid and humid regions, California: *Soil Science*, v. 109, p. 357-261.
- Izett, G. A., 1981, Volcanic ash beds: Recorders of upper Cenozoic silicic pyroclastic volcanism in the western United States: *Journal of Geophysical Research*, v. 86, p. 10200-10222.
- Jackson, M. L., 1965, Clay transformation in soil genesis during the Quaternary: *Soil Science*, v. 99, p. 15-22.
- _____, 1974, Soil chemical analysis—advanced course: Published by the author, Madison, Wisc., Dept. of Soil Sciences, University of Wisconsin, 895 p.
- Jackson, M. L., Y. Hseung, R. B. Corey, E. J. Evans, and R. C. Vanden Heuvel, 1952, Weathering sequence of clay-size minerals in soils and sediments, II, chemical weathering of layer silicates: *Proceedings of the Soil Science Society of America*, v. 16, p. 3.
- Johnson, L. J., 1964, Occurrence of regularly interstratified chlorite-vermiculite as a weathering product in a soil: *American Mineralogist*, v. 49, p. 556-572.
- Johnson, R. G., 1982, Brunhes-Matuyama magnetic reversal dated at 790,000 yr. B.P. by marine-astronomical correlations: *Quaternary Research*, v. 17, p. 135-149.

- Keroher, G. C., 1966, Lexicon of geologic names of the United States, 1936-1960: U. S. Geological Survey Bulletin 1200, 4341 p.
- King, R. F., and A. I. Rees, 1966, Detrital magnetism in sediments: An examination of some theoretical models: *Journal of Geophysical Research*, v. 71, p. 561-571.
- Kittleman, L. R., 1973, Mineralogy, correlation, and grain size distributions of Mazama tephra and other postglacial pyroclastic layers, Pacific Northwest: *Geological Society of America Bulletin*, v. 84, p. 2957-2980.
- Koci, A., 1974, Paleomagnetic investigation of sediments, in *Quaternary Glaciations in the Northern Hemisphere*, International Geological Correlation Program, Report No. 1, p. 110-122.
- Koci, A., and V. Sibrava, 1976, The Brunhes-Matuyama boundary at central European localities, in *Quaternary Glaciations in the Northern Hemisphere*: International Geological Correlation Program, Report No. 3, p. 135-141.
- Krapf, R. W., 1978, Characterization of loess deposits and paleosols of the Palouse Formation in Idaho and Washington: Unpublished Ph.D. dissertation, University of Idaho, Moscow, 134 p.
- Kukla, G. J., 1975, Loess stratigraphy of central Europe, in Butzer, K. W., and G. L. Isaac, eds., *After the Australopithecines: The Hague, Moulton*, p. 99-188.
- Kukla, G. J., and A. Koci, 1972, End of the last interglacial in the loess record: *Quaternary Research*, v. 2, p. 374-383.
- Kukla, G. J., and Opdyke, N. D., 1980, Matuyama loess at Columbia Plateau, Washington (abst.): *American Quaternary Association, Abstracts with Programs*, no. 6, p. 122.

- Lemke, R. W., M. R. Mudge, R. E. Wilcox, and H. A. Powers, 1975, Geologic setting of the Glacier Peak and Mazama ash-bed markers in west-central Montana: U. S. Geological Survey Bulletin 1395-H, p. 1-31.
- Lenfesty, C. D., 1967, Soil Survey of Adams County, Washington: U. S. Department of Agriculture, Soil Conservation Service, in cooperation with the Washington Agricultural Experiment Station, 110 p.
- Lewis, P. F., 1960, Linear topography in the southwestern Palouse, Washington-Oregon: Association of American Geographers Annals, v. 50, p. 98-111.
- Lotspeich, F. B., and H. W. Smith, 1953, Soils of the Palouse loess, pt. I, The Palouse Catena: Soil Science, v. 76, p. 467-485.
- MacEwan, D. M. C., and M. J. Wilson, 1980, Interlayer and intercalation complexes of clay minerals, in Brindley, G. W., and G. Brown, eds., Crustal Structures of Clay Minerals and Their X-ray Identification: Mineral Society of London Monograph, p. 197-248.
- Mackin, J. H., 1961, A stratigraphic section in the Yakima Basalt and the Ellensburg Formation in south-central Washington: Washington Department of Conservation, Division of Mines and Geology Report of Investigation 19, 45 p.
- Mahaney, W. C., 1981, Paleoclimate reconstructed from paleosols: Evidence from the Rocky Mountains and East Africa, in Mahaney, W. C., ed., Quaternary Paleoclimate, GeoAbstracts, Norwich, England, p. 227-247.
- Mankinen, E. A., and G. B. Dalrymple, 1979, Revised geomagnetic polarity time scale for the interval 0-5 m.y.B.P.: Journal of Geophysical Research, v. 84, p. 615-626.
- McCreery, R., 1954, Mineralogy of Palouse and related series: Unpublished Ph.D. dissertation, Washington State University, Pullman, 120 p.

- McElhinny, M. W., 1973, *Paleomagnetism and Plate Tectonics*: Cambridge, England, Cambridge University Press, 358 p.
- Mehring, P. J., E. Blinman, and K. L. Petersen, 1977, Pollen influx and volcanic ash: *Science*, v. 198, p. 257-261.
- Merriam, J. C., and J. P. Buwalda, 1917, Age of the strata referred to the Ellensburg Formation in the White Bluffs of the Columbia River: *University of California Publications in Geological Sciences*, v. 10, p. 255-266.
- Moodie, C. C., R. Okazaki, H. W. Smith, and J. A. Kittrick, 1966, A note on the clay mineralogy of four samples from the Ringold Formation: *Northwest Science*, v. 40, p. 43-45.
- Moody, U. L., 1977, Correlation of flood deposits containing St. Helens set S ashes and the stratigraphic position of St. Helens set J and Glacier Peak ashes, central Washington (abst.): *Geological Society of America, Abstracts with Programs*, v. 9, p. 1098-1099.
- _____, 1978, *Microstratigraphy, paleoecology, and tephrochronology of the Lind Coulee site, central Washington*: Unpublished Ph.D. dissertation, Washington State University, Pullman, 260 p.
- Morrison, R. B., 1978, Quaternary soil stratigraphy—concepts, methods and problems, *in* Mahaney, W. C., ed., *Quaternary Soils*, *GeoAbstracts*, Norwich, England, p. 72-108.
- Mullineaux, D. R., R. E. Wilcox, W. F. Ebaugh, R. Fryxell, and M. Rubin, 1977, Age of the last major scabland flood of eastern Washington as inferred from associated ash beds of Mount St. Helens set S (abst.): *Geological Society of America, Abstracts with Programs*, v. 9, p. 1105.

- _____, 1978, Age of the last major scabland flood of eastern Washington: *Quaternary Research*, v. 10, p. 171-180.
- Nagata, T., 1962, Notes on detrital remanent magnetization of sediments: *Journal of Geomagnetism and Geoelectricity*, v. 14, p. 99-106.
- Newcomb, R. C., 1958, Ringold Formation of Pleistocene age in type locality, the White Bluffs, Washington: *American Journal of Sciences*, v. 256, p. 328-340.
- _____, 1970, Tectonic structure of the main part of the basalt of the Columbia River group, Washington, Oregon, and Idaho: U. S. Geological Survey, *Miscellaneous Geological Investigations Map I-587*.
- Newcomb, R. C., J. R. Strang, and F. J. Frank, 1972, Geology and groundwater characteristics of the Hanford Reservation of the U. S. Atomic Energy Commission, Washington: U. S. Geological Survey Professional Paper 717, 78 p.
- Packer, D. R., 1979, Paleomagnetism and age dating of the Ringold Formation and loess deposits in State of Washington: *Oregon Geology*, v. 41, no. 8, p. 119-132.
- Pardee, J. T., 1942, Unusual currents in glacial Lake Missoula, Montana: *Geological Society of America Bulletin*, v. 53, p. 1569-1600.
- Patton, P. C., and V. R. Baker, 1978, New evidence for pre-Wisconsinian flooding in the channeled scabland of eastern Washington: *Geology*, v. 6, p. 567-571.
- Pevear, D. R., D. P. Dethier, and D. Frank, 1982, Clay minerals in the 1980 deposits from Mount St. Helens: *Clay and Clay Minerals*, v. 30, in press.

- Phillips, E. L., 1970, Washington Climate: Pullman, Cooperative Extension Service, Washington State University, 46 p.
- Pierce, K. L., 1979, History and dynamics of glaciation in the northern Yellowstone National Park area: U. S. Geological Survey Professional Paper 729-F, 90 p.
- Pierce, K. L., M. A. Fosberg, W. E. Scott, G. C. Lewis, and S. M. Coleman, 1982, Loess deposits of southeastern Idaho, part II: Age and correlation of the upper two loess units: In Cenozoic Geology of Idaho, G. C. Lewis and M. A. Fosberg, eds., Idaho Bur. of Mines and Geol.
- Porter, S. C., 1976, Pleistocene glaciation in the southern part of the North Cascade Range, Washington: Geological Society of America Bulletin, v. 87, p. 61-75.
- _____, 1978, Glacier Peak tephra in the North Cascade Range, Washington: Stratigraphy, distribution, and relationship to late glacial events: Quaternary Research, v. 10, p. 30-41.
- Rees, A. I., 1961, The effect of water currents on the magnetic remanence and anisotropy of susceptibility of some sediments: Geophys. Jour., London, v. 5, no. 3, p. 235-251.
- Richmond, G. M., 1965, Glaciation of the Rocky Mountains, in Wright, H. E., and D. G. Frey, eds., The Quaternary of the United States: Princeton, N.J., International Association for Quaternary Research, Princeton University Press, p. 217-230.
- Richmond, G. M., R. Fryxell, G. E. Neff, and P. L. Weis, 1965, The Cordilleran ice sheet of the northern Rocky Mountains and related Quaternary history of the Columbia Plateau, in Wright, H. E., and D. G. Frey, eds., The Quaternary of the United States: Princeton, N.J., International Association of Quaternary Research, Princeton

- University Press, p. 231-242.
- Rieger, S., 1952, Development of the A2 horizon in soils of the Palouse area: Unpublished Ph.D. dissertation, Washington State University, Pullman, 86 p.
- Rieger, S., and H. W. Smith, 1955, Soils of the Palouse loess: II. Development of the A2 horizon: *Soil Science*, v. 79, p. 301-319.
- Rigby, J. G., and K. Othberg, 1979, Reconnaissance surficial geologic mapping of the late Cenozoic sediments of the Columbia Basin, Washington: State of Washington, Department of Natural Resources, Division of Geology and Earth Resources, Open-File reports 79-7 to 79-15, 88 p.
- Ringe, D., 1970, Sub-loess basalt topography in the Palouse Hills, southeastern Washington: *Geological Society of America Bulletin*, v. 81, p. 3049-3060.
- Russell, I. C., 1897, A reconnaissance in southeastern Washington: U. S. Geological Survey Water Supply Paper 4, 96 p.
- _____, 1901, Geology and water resources of Nez Perce County, Idaho: U. S. Geological Survey Water Supply Paper 53, 28 p.
- Salisbury, R. D., 1901, Glacial work in the western mountains in 1901: *Journal of Geology*, v. 9, p. 718-731.
- Senkayi, A. L., J. B. Dixon, and L. R. Hossner, 1981, Transformation of chlorite to smectite through regularly interstratified intermediates: *Soil Science Society of America Journal*, v. 45, p. 650-656.
- Smith, H. W., R. Okazaki, and C. R. Knowles, 1975, Electron microprobe analysis as a test of the correlation of West Blacktail ash with Mount St. Helens pyroclastic layer T: *Northwest Science*, v. 49, p. 209-215.

- _____, 1977a, Electron microprobe data for tephra attributed to Glacier Peak, Washington: Quaternary Research, v. 7, p. 197-206.
- _____, 1977b, Electron microprobe analysis of glass shards from tephra assigned to set W, Mount St. Helens, Washington: Quaternary Research, v. 7, p. 207-217.
- Smith, W. W., 1962, Weathering of some Scottish basic igneous rocks with reference to soil formation: Journal of Soil Science, v. 13, p. 202-215.
- Soil Survey Staff, 1951, Soil Survey Manual: Washington, D. C., U. S. Department of Agriculture Handbook no. 18, 503 p.
- _____, 1975, Soil Taxonomy: Washington, D. C., Soil Conservation Service, U. S. Department of Agriculture Handbook No. 436, 754 p.
- _____, 1981, Soil Survey Manual: Soil Conservation Service, U. S. Department of Agriculture, in review.
- Steele, W. K., 1981, Remanent magnetization of ash from the 18 May 1980 eruption of Mount St. Helens: Geophysical Research Letters, v. 8, p. 213-216.
- Swanson, D. A., and T. L. Wright, 1978, Bedrock geology of the northern Columbia Plateau and adjacent areas, in Baker, V. R., and D. Nummedal, eds., The Channeled Scabland: Washington, D. C., National Aeronautics and Space Administration, p. 37-57.
- Treasher, R. C., 1925, Origin of the loess of the Palouse region, Washington: Science, v. 61, p. 469.
- Tucholka, P., 1976, Remanent magnetization of loess: Publications of the Institute of Geophysics, Polish Academy of Science, v. C-1, p. 127-141.

- Verosub, K. L., 1977, Depositional and post-depositional processes in the magnetization of sediments: Review of Geophysics and Space Physics, v. 14, p. 129-143.
- Waters, A. C., 1962, Basalt magma types and their tectonic association—Pacific Northwest of the United States: American Geophysical Union, Monograph 5, p. 158-170.
- Westgate, J. A., and R. J. Fulton, 1975, Tephrostratigraphy of Olympia interglacial sediments in south-central British Columbia, Canada: Canadian Journal of Earth Sciences, v. 12, p. 489-502.
- Wilcox, R. E., 1965, Volcanic ash chronology, in Wright, H. E., and D. G. Frey, eds., The Quaternary of the United States: International Association of Quaternary Research, Princeton University Press, Princeton, N. J., p. 231-242.
- Wilson, R. L., and M. W. McElhinny, 1974, Investigation of large scale paleomagnetic field over the past 25 million years: Eastward shift of the Icelandic spreading ridge: Geophysical Journal of the Royal Astr. Society, v. 39, p. 370-586.
- Zijderveld, J. D. A., 1967, Demagnetization of rocks: Analysis of results, in Collinson, D. W., K. M. Creer, and S. K. Runcorn, eds., Methods in Paleomagnetism: Proceedings NATO Advanced Study Institute on Paleomagnetic Methods, Newcastle upon Tyne, U. K., April 1-10, 1964.

APPENDIX: SOIL DESCRIPTIONS

The soils at Washtucna do not readily lend themselves to characterization by the means prescribed by the Soil Survey Manual (1951, 1981). Therefore, a system of description needed to be constructed with which to deal with them. The description follows the Soil Survey Manual (1951) with additional phrases to describe the morphology of the calcareous horizons (plates, nodules) and designation of the carbonate stage of development (Gile et al., 1966).

The soil horizon designation is a compilation of soil horizons from the Soil Survey Manual (1981) with the addition of the K master soil horizon of Gile et al. (1965) for horizons that have stage III and IV carbonate. Horizons that have stage I and II carbonate are called Ck horizons. The term buried soil, and hence the use of the subscript b, is different from that of the Soil Survey Manual (1981). In this study at Washtucna, a buried soil is a horizon or sequence of horizons (either B, C, or K) that have characteristics formed by pedogenic processes on a past land surface and that are now buried by younger sediments. The buried soils are numbered from top (youngest) to bottom (oldest), and this number is in parentheses at the end of the horizon designation.

Colors are for dry soil and follow the Munsell Color Chart.

ROADCUT #3 - 3.2 km west of Washtucna on State Highway #26; SW $\frac{1}{4}$ SE $\frac{1}{4}$ Sec. 19-T15N-R36E, Adams County, Washington. Exposure is on the north side of the highway. Measured section at 90 m west of datum (Figures 3 and 9).

<u>Depth (m)</u>	<u>Soil Horizon</u>	<u>Description</u>
0-.08	Ap	Brown, 10YR5/3, silt loam; moderate fine and medium granular structure; weakly coherent, very friable, nonsticky, slightly plastic; common fine and very fine roots; no effervescence; abrupt wavy boundary:
.08-.24	A	Yellowish brown, 10YR5.5/4, silt loam; weak fine granular structure; weakly coherent, very friable, nonsticky, slightly plastic; common fine and very fine roots; no effervescence; clear smooth boundary:
.24-.56	Bw	Pale brown, 10YR6/3, silt loam; weak medium subangular blocky structure; weakly coherent, very friable, nonsticky, slightly plastic; plentiful very fine roots, no effervescence; gradual smooth boundary:
First buried soil:		
.56-.86	Ckb1(1)	Light gray, 10YR7/2, silt loam; weak medium subangular blocky structure; slightly hard, friable, nonsticky, nonplastic; very few very fine roots; many very fine and fine tubular pores (many filled with CaCO ₃); strongly effervescent with stage I carbonate; fine gravel size particles of carbonate scattered throughout; gradual smooth boundary:
.86-1.18	Ckb2(1)	Pale brown, 10YR6/3, silt loam; massive; weakly coherent, very friable, nonsticky, slightly plastic; few fine carbonate pebbles and filaments; slightly effervescent with stage I carbonate; clear wavy boundary:
Second buried soil:		
1.18-1.43	Kmb(2)	Pale brown, 10YR6/3, silt loam; moderately cemented nodules with stage III carbonate, hard, very firm, nonsticky, slightly plastic; pink, 5YR8/3, stage IV carbonate forms horizontal plates 1 cm thick at top of horizon and fills vertical cracks; common fine, few very fine tubular pores; violently effervescent but carbonate does not dissolve in 1N HCl due to SiO ₂ cement, strongly cemented; gradual irregular boundary:

- 1.43-2.19 Ckb(2) Pale brown, 10YR6/3, silt loam; massive, weakly coherent, nonsticky, slightly plastic; weakly cemented calcareous silt nodules randomly distributed with some fragments of K horizon material; strongly effervescent with stage III carbonate; abrupt irregular boundary:

Third buried soil:

- 2.19-3.46 Kmb(3) Pale brown, 10YR6/3, silt loam; forms moderately cemented nodules with stage III carbonate; very hard, nonsticky, nonplastic; pink, 10R8/3, stage IV carbonate forms horizontal plates 1-2 cm thick at top of horizon and fills vertical cracks; many very fine and medium, common fine tubular pores; violently effervescent but carbonate does not dissolve in 1NHCl due to SiO₂ cement; strongly cemented; forms prominent vertical face at east side of exposure; gradual irregular boundary:

- 3.46-4.73 Ckb(3) Pale brown, 10YR6/3, silt loam; massive, weakly coherent, nonsticky, slightly plastic; weakly cemented silt nodules of stage II carbonate randomly distributed with fragments of K horizon; strongly effervescent; gradual irregular boundary:

Fourth buried soil:

- 4.73-5.58 Kb(4) Pale brown, 10YR6/3, silt loam in strongly cemented nodules with stage III carbonate; hard, firm, nonsticky, slightly plastic; many medium, few coarse tubular pores; violently effervescent; forms vertical face; abrupt wavy boundary:
- 5.58-7.00 Ckb(4) Pale brown, 10YR6/4, loam; massive, loose, nonsticky, slightly plastic; upper 50 cm has randomly distributed calcareous silt nodules and fragments of K horizon; stage II carbonate; strongly effervescent; diffuse smooth boundary:

Fifth buried soil:

- 7.00-7.40 Kmb(5) Light yellowish brown, 10YR6/4, silt loam; forms strongly cemented silt nodules with stage III carbonate; very hard, very firm, nonsticky, slightly plastic; pink, 7.5R8/6, stage IV carbonate fills vertical cracks; few fine tubular pores; strongly effervescent but stage IV carbonate does not dissolve in 1NHCl due to SiO₂ cement; indurated; clear irregular boundary:

7.40-7.56 Ckb(5) Pale brown, 10YR6/3, loam; massive, loose, nonsticky, slightly plastic; contains randomly distributed fragments of K horizon; strongly effervescent with stage I carbonate; abrupt smooth boundary:

Sixth buried soil:

7.56-9.20 Kmb(6) Very pale brown, 10YR7/3, loam; forms moderately cemented nodules with stage III carbonate; slightly hard, firm, nonsticky, nonplastic; stage IV carbonate fills vertical cracks; very few fine, few very fine medium and coarse tubular pores lined with CaCO₃; strongly cemented; strongly effervescent; this soil is the most strongly developed and visually prominent in the roadcut; gradual smooth boundary:

9.20-9.55 Ckb1(6) Pale brown, 10YR6/3, loam; forms weakly cemented nodules with stage II carbonate; weakly coherent, friable, nonsticky, nonplastic; strongly effervescent; abrupt smooth boundary:

9.55-9.70 Ckb2(6) Light yellowish brown, 10YR6/4, silt loam; moderately cemented nodules with stage II carbonate; weakly coherent, friable, nonsticky, nonplastic; strongly effervescent; clear smooth boundary:

Seventh buried soil:

9.70-9.80 Ckb(7) Pale brown, 10YR5/3, loam; massive, weakly coherent, very friable; strongly effervescent with stage I carbonate; stage IV carbonate fills vertical cracks; common medium and fine tubular pores; clear smooth boundary:

9.80-10.95 Kmb(7) Very pale brown, 10YR7/3, loam; forms strongly cemented nodules with stage III carbonate; hard, firm, nonsticky, nonplastic; stage IV carbonate with some pink stains forms horizontal plates between 9.90 and 10.30 m; few coarse, common medium, many fine and very fine tubular pores; strongly effervescent; gradual smooth boundary:

10.95-12.42 Ckb1 Pale brown, 10YR6/3, fine sandy loam; massive, loose, nonsticky, nonplastic; common fine tubular pores; slightly effervescent; diffuse smooth boundary:

Eighth buried soil:

12.42-12.64 Kmb(8) Light gray, 10YR5/2, silt loam; forms moderately cemented silt nodules with stage III carbonate; slightly hard, firm, nonsticky, nonplastic; white, 10YR8/2, stage IV carbonate forms plates 1.0-1.2 cm thick at the top of the horizon and fills vertical

cracks; strongly effervescent, but stage IV carbonate does not dissolve in 1NHC1 due to SiO₂ cement; indurated; abrupt smooth boundary:

12.64- Kb(8) Light brownish gray, 10YR6/2, loam; forms moderately
13.48 cemented silt nodules with stage III carbonate; slightly hard, nonsticky, nonplastic; few fine, common medium and coarse tubular pores filled with carbonate; krotovinas (<1 cm wide) filled with carbonate and tephra; tephra layer 3B at 12.97 to 13.02 m deep; vertically stable face beneath tephra; strongly effervescent; abrupt smooth boundary:

13.48- Ckb2 Pale brown, 10YR6/3, loam; massive, loose, nonsticky,
14.79 nonplastic; few fine tubular pores; slightly effervescent; clear smooth boundary:

Ninth buried soil:

14.79- Ckb1(9) Very pale brown, 10YR7/3, silt loam; forms moderately
15.50 cemented nodules with stage II carbonate; weakly coherent, very friable, nonsticky, nonplastic; few fine and very fine tubular pores filled with carbonate; weakly cemented; strongly effervescent; gradual smooth boundary:

15.50- Kmb(9) Pinkish white, 7.5YR8/2; stage IV carbonate forms
15.65 horizontal plates interlayered with pale brown, 10YR6/3 loam; indurated; violently effervescent; gradual irregular boundary:

15.65- Ckb2(9) Very pale brown, 10YR7/3, loam; forms weakly cemented
16.95 nodules with stage II carbonate; weakly coherent, friable, nonsticky, nonplastic; few fine and very fine tubular pores filled with carbonate; strongly effervescent; clear smooth boundary:

Tenth buried soil:

16.95- Ckb1(10) Very pale brown, 10YR7/3, silt loam; forms moderately
17.05 cemented nodules with stage II carbonate; hard, firm, nonsticky, slightly plastic; strongly effervescent; clear irregular boundary:

17.05- Ckb2(10) Light gray, 10YR7/2, silt loam; forms weakly cemented
19.25 calcareous nodules with stage I carbonate; slightly hard, nonsticky, nonplastic; many micro and very fine tubular pores filled with carbonate; tephra layer 3C at 17.50-17.55 m and 3D at 17.70-17.75 m; slightly effervescent; very abrupt irregular boundary:

Eleventh buried soil:

- 19.25-
20.45 Kbl(11) Light yellowish brown, 10YR6/4, silt loam; forms strongly cemented calcareous nodules with stage III carbonate; hard, friable, nonsticky, slightly plastic; few fine and very fine tubular pores; strongly effervescent; iron oxide stains; gradual smooth boundary:
- 20.45-
20.95 Kb2(11) Pale brown, 10YR6/3, silt loam; forms strongly cemented nodules with stage III carbonate; hard, friable, nonsticky, slightly plastic; very few fine and very fine tubular pores; veins of carbonate visible throughout; strongly effervescent; clear smooth boundary:
- 20.95-
21.45 Ckb(11) Pale brown, 10YR6/3, silt loam; forms moderately cemented nodules with stage II carbonate; hard, friable, nonsticky, slightly plastic; very few very fine tubular pores; strongly effervescent.

ROADCUT #4 - 3.2 km west of Washtucna on State Highway #26; NW $\frac{1}{4}$ SW $\frac{1}{4}$ Sec. 19-T15N-R36E, Adams County, Washington. Exposure is on the north side of the road. Measured section is at 48 m east datum (Figures 4 and 10).

<u>Depth (cm)</u>	<u>Soil Horizon</u>	<u>Description</u>
0-.15	Ap	Pale brown, 10YR6/3, dry, silt loam; moderate coarse granular structure; weakly coherent, very friable, nonsticky, slightly plastic; few very fine and fine roots, common very fine and fine tubular pores; slightly effervescent; abrupt wavy boundary:
.15-.38	Bw	Pale brown, 10YR6/3 dry, silt loam; weak medium subangular blocky structure, sometimes massive, weakly coherent, very friable, nonsticky, slightly plastic; abundant fine roots on ped surfaces, few fine tubular pores in peds, common on ped surfaces; no effervescence; gradual wavy boundary:
.38-.68	Ck1	Very pale brown, 10YR7/3 dry, silt loam; massive (but breaks into medium subangular blocks), weakly coherent, very friable, nonsticky, slightly plastic, few fine roots, many fine and very fine vertical tubular pores, strongly effervescent with stage I carbonate; clear wavy boundary:
.68-1.13	Ck2	Very pale brown, 10YR7/3 dry, silt loam; massive, weakly coherent (easier to penetrate with knife than Ck1), very friable, nonsticky, nonplastic; few fine roots, few fine and very fine tubular pores; slightly effervescent; clear wavy boundary:
First buried soil:		
1.13-1.47	Ckb(1)	Very pale brown, 10YR7/2 dry, silt loam; massive, slightly hard (difficult to penetrate with knife), friable, nonsticky, slightly plastic, few very fine roots, very few fine tubular pores filled with CaCO ₃ ; slightly effervescent with stage I carbonate; clear smooth boundary:
1.47-2.10	Ck3	Pale brown, 10YR6/3 dry, silt loam; massive, loose, very friable, nonsticky, nonplastic, very few very fine roots, few fine tubular and vesicular pores, slightly effervescent, clear smooth lower boundary:
Second buried soil:		
2.10-3.75	Ckb1(2)	Pale brown, 10YR6.5/3 dry, silt loam; slightly hard, friable, slightly sticky, slightly plastic; slight evidence of medium subangular blocky peds with silt film on surface less than 1 mm thick; nodules 2 cm

diameter effervescent on surface, but not interior; very few very fine roots, few fine and common, very fine tubular pores filled with CaCO_3 , strongly effervescent with stage II carbonate; gradual irregular lower boundary:

- 3.75-4.90 Ck4 Very pale brown, 10YR7/2.5 dry, silt loam; massive, loose, nonsticky, nonplastic; many very fine tubular pores filled with stage I carbonate; tephra layer 4B at 448 cm depth; gradual wavy lower boundary:
- 4.90-5.40 Ck5 Very pale brown, 10YR7/3 dry, silt loam; massive, loose, nonsticky, nonplastic; many very fine tubular pores filled with stage I carbonate; strongly effervescent; gradual smooth boundary:
- 5.40-5.80 Ck6 Same as Ck5, with no evident pores; clear smooth boundary:
- Third buried soil:
- 5.80-6.60 Kb(3) Pale brown, 10YR6/3 dry, silt loam nodules in 10YR7/3 matrix, moderate nodule development, slightly hard, slightly sticky, nonplastic; very few fine and very fine roots, few very fine tubular pores; strongly effervescent on interior and exterior of nodules with stage III carbonate; gradual wavy lower boundary:
- 6.60-7.66 Ckb(3) Light yellowish brown, 10YR6/4 dry, silt loam; weak nodule development; weakly coherent, very friable, nonsticky, nonplastic; no evident pores; strongly effervescent with stage II carbonate; tephra 4C is at 736 cm depth.

ROADCUT #5 - 3.3 km west of Washtucna on State Highway #26; NW $\frac{1}{4}$ SW $\frac{1}{4}$ Sec. 19-T15N-R36E, Adams County, Washington. Exposure is on the north side of road. Measured section is at 122 m west of datum (Figures 5 and 11).

<u>Depth (cm)</u>	<u>Soil Horizon</u>	<u>Description</u>
0-.13	Ap	Brown, 10YR5/3 dry, silt loam; moderate fine to medium granular structure; weakly coherent, very friable, nonsticky, nonplastic; common fine and very fine roots; abrupt irregular boundary:
.13-.63	Bw	Pale brown, 10YR6/3 dry, silt loam; weak medium subangular blocky structure, thin (<1 mm) silt film on ped surfaces; weakly coherent, very friable, nonsticky, slightly plastic; common very fine and fine roots; few very fine and fine tubular pores; gradual wavy boundary:
.63-.90	Ck1	Pale brown, 10YR6/3 dry, loam; massive, loose, nonsticky, slightly plastic; few very fine roots; few very fine tubular pores; slightly effervescent; clear wavy boundary:
First buried soil:		
.90-2.30	Ckb(1)	Pale brown, 10YR6/3 dry, silt loam; massive with few weak medium subangular blocky peds; slightly hard, friable, nonsticky, slightly plastic; common very fine and micro tubular pores; common very coarse tubular pores may be krotovinas; pores are filled with stage I carbonate; gradual smooth boundary:
Second buried soil:		
2.30-3.33	Ckb1(2)	Pale brown, 10YR6/3 dry, silt loam; moderate nodule development; slightly hard, friable, nonsticky, slightly plastic; common micro and few very fine and fine tubular pores lined with stage II carbonate; matrix slightly effervescent, but no effervescence within nodules; gradual smooth boundary:
3.33-4.90	Ckb2(2)	Pale brown, 10YR6/3 dry, silt loam; massive; loose, very friable, nonsticky, slightly plastic; very few fine tubular pores filled with stage I carbonate; tephra layer 5B is at a depth of 420 cm; clear wavy boundary:

Third buried soil:

- 4.90-5.67 Kb1(3) Light yellowish brown, 10YR6/4 dry, loam; moderate nodule development; slightly hard, friable, nonsticky, slightly plastic; few very fine and fine tubular pores; strongly effervescent with stage III carbonate; clear smooth boundary:
- 5.67-5.90 Kb2(3) Very pale brown, 10YR7/3 dry, loam; moderate nodule development; slightly hard, friable, nonsticky, slightly plastic; very few very fine tubular pores; strongly effervescent with stage III carbonate; gradual smooth boundary:
- 5.90-7.08 Ckb(3) Very pale brown, 10YR7/3 dry, loam; weak to moderate nodule development; weakly coherent, friable, nonsticky, slightly plastic; few very fine and fine tubular pores; visible iron oxide stains; slightly effervescent with stage II carbonate; gradual smooth boundary:

Fourth buried soil:

- 7.08-7.80 Kb(4) Light yellowish brown, 10YR6/4 dry, silt loam; moderate nodule development; slightly hard, friable, slightly sticky, slightly plastic; common fine tubular pores filled with stage III carbonate; visible iron oxide stains; strongly effervescent; gradual smooth boundary:
- 7.80-8.90 Ckb1(4) Light yellowish brown, 10YR6/4 dry, silt loam; massive; weakly coherent, very friable, nonsticky, slightly plastic; very few fine tubular pores; slightly effervescent with stage I carbonate; gradual smooth lower boundary:
- 8.90-10.25 Ckb2(4) Light gray, 10YR7/2 dry, fine sandy loam; massive; loose, nonsticky, nonplastic; slightly effervescent with stage I carbonate.

ROADCUT #9 - 2.52 km. west of Washtucna on State Highway #26; SE $\frac{1}{4}$ SE $\frac{1}{2}$ Sec. 14-T15N-R36E, Adams County, Washington. Measured section is from exposure on the north side of the road (Figure 7).

<u>Depth (cm)</u>	<u>Soil Horizon</u>	<u>Description</u>
.45	Ck1	Very pale brown, 10YR7/3 dry, fine sandy loam; massive, loose, nonsticky, nonplastic; common very fine roots; slightly effervescent; gradual smooth boundary:
First buried soil:		
1.50	Bwb(1)	Pale brown, 10YR6/3 dry, silt loam; massive with vertical drying cracks (large prisms), weak sub-angular blocky structure; weakly coherent, very friable, nonsticky, slightly plastic; very slightly effervescent with stage I carbonate; forms a vertically stable face; gradual smooth boundary:
Second buried soil:		
.50	Ckb1(2)	Pale brown 10YR6/3 dry, silt loam; moderate nodule development, sparse near top becoming more numerous downward; slightly hard, friable, nonsticky, slightly plastic; slightly effervescent with stage II carbonate; abrupt wavy boundary:
1.75	Kmb(2)	Pale brown 10YR6/3 dry, silt loam; moderate to strong nodule development; very hard, friable, nonsticky, slightly plastic; thin (.5 cm) petrocalcic horizon with stage IV carbonate at top of unit and in vertical cracks, some pink carbonate evident; few very fine, common micro tubular pores filled or lined with CaCO ₃ ; slightly effervescent with stage III carbonate; forms vertically stable face in top 50 cm; clear wavy boundary:
Third buried soil:		
.25	Kmb(3)	White, 10YR8/2 dry, petrocalcic horizon with stage IV carbonate; strongly cemented; violently effervescent; plates are 0.5 to 1.0 cm thick; abrupt wavy boundary:
1.50	Kb(3)	Light yellowish brown, 10YR6/4 dry, silt loam; strong nodule development; hard, very friable, nonsticky, slightly plastic; common micro and very fine, few fine tubular pores; strongly effervescent on nodule surfaces with stage III carbonate; not effervescent in interiors; gradual smooth boundary:

.50 Ckb(3) Pale brown, 10YR6/3 dry, loam; massive; weakly coherent, very friable, nonsticky, nonplastic; slightly effervescent with stage I carbonate; clear wavy boundary:

Fourth buried soil:

1.00 Kb(4) Light yellowish brown, 10YR6/4 dry, silt loam; strong nodule development; hard, friable, nonsticky, slightly plastic; common micro and very fine, few fine tubular pores lined with carbonate; strongly effervescent with stage III carbonate; clear smooth boundary:

1.50-2.00 Ckb(4) Pale brown, 10YR 6/3 dry, fine sandy loam; massive; loose, nonsticky, nonplastic; strongly effervescent with stage I carbonate; clear wavy boundary:

Fifth buried soil:

1.00 Ckb1(5) Light gray, 10YR7/2 dry, loam; massive, some weak nodule development; slightly hard, very friable nonsticky, nonplastic; common fine tubular pores; strongly effervescent with stage II carbonate; in places this unit forms a vertically stable face with common medium tubular pores lined with CaCO_3 ; clear smooth boundary:

1.00-1.50 Ckb2(5) Very pale brown, 10YR6.5/3 dry, fine sandy loam; massive, some weak nodule development; weakly coherent very friable, nonsticky, slightly plastic; few micro and very fine, common fine tubular pores lined with carbonate and accentuated by wind erosion; very slightly effervescent with stage II carbonate; forms vertically stable face; tephra 9B is at the base of this unit; clear smooth boundary:

1.00 Ckb3(5) Pale brown, 10YR6/3 dry, fine sandy loam; massive, some weak nodule development; this unit may be the same paleosol as Ckb2(5), this is the part underneath tephra 9B; slightly effervescent; common fine and medium tubular pores filled with stage II carbonate; abrupt smooth boundary:

3.00-3.50 Ckb Very pale brown, 10YR7/3 dry, sandy loam; massive; loose, nonsticky, nonplastic; slightly effervescent; abrupt smooth boundary:

Sixth buried soil:

2.00 Kb(6) Light yellowish brown, 10YR6/4, dry, fine sandy loam; strong nodule development; hard, firm, nonsticky, slightly plastic; many fine and very fine tubular pores filled with CaCO_3 ; maintains a prominent verti-

cal face with CaCO_3 in vertical cracks; slightly effervescent; stage III carbonate in top 20 cm of unit; gradual wavy boundary:

- 2.50-3.25 Cb1 Pale brown, 10YR6/3 dry, loamy fine sand; single grain; loose, nonsticky, nonplastic; gradual smooth boundary:
- 3.50-3.75 Ckb3 Very pale brown, 10YR7/3 dry, fine sandy loam; massive; weakly coherent, friable, nonsticky, nonplastic; common medium pores filled with CaCO_3 (these protrude from the exposure due to wind erosion of surrounding sediment); krotovinas are filled with CaCO_3 ; rodent bones and long bone fragments; tephra layers 9C, 9D, and 9E are in this unit; the unit fills a channel cut into horizontal weathering zones IX through XII; abrupt smooth boundary:

Seventh buried soil:

- .75-1.05 Kb(7) Very pale brown, 10YR7/3 dry, silt loam; strong nodule development; hard, friable, nonsticky, slightly plastic; few micro and very fine tubular pores; CaCO_3 in vertical cracks; forms semivertical face (45°); violently effervescent with stage III carbonate; diffuse smooth boundary:

Eighth buried soil:

- 3.00 Kb(8) Very pale brown, 10YR7/3 dry, silt loam; strong nodule development; hard, friable, nonsticky, slightly plastic; common micro, few very fine tubular pores; violently effervescent with stage III carbonate; gradual smooth boundary:
- 1.75 Ckb(8) Pale gray, 10YR7/2 dry, silt loam; massive; a few random nodules evident; hard, firm, nonsticky, slightly plastic; violently effervescent with stage II carbonate; clear smooth boundary:

Ninth buried soil:

- 1.08 Kb(9) Pale brown, 10YR6/3 dry, silt loam; strong nodule development; hard, friable, nonsticky, slightly plastic; common very fine tubular pores; violently effervescent with stage III carbonate; nodules decrease in number downward through profile; clear smooth boundary:

Tenth buried soil:

.95 Kb(10) Pale brown, 10YR6/3 dry, fine sandy loam; strong nodule development; hard, friable, nonsticky, slightly plastic; very few very fine tubular pores; violently effervescent with stage III carbonate; clear smooth boundary:

.75-.90 Ckb(10) Very pale brown, 10YR7/3 dry, fine sandy loam; massive with a few scattered nodules; slightly hard, friable, nonsticky, slightly plastic; violently effervescent with stage III carbonates; abrupt smooth boundary:

Eleventh buried soil:

1.00 Kb(11) Light yellowish brown, 10YR6/4 dry, fine sandy loam; strong nodule development; slightly hard, friable, nonsticky, nonplastic; violently effervescent with stage III carbonate.